Electrification of the Eastern Docklands

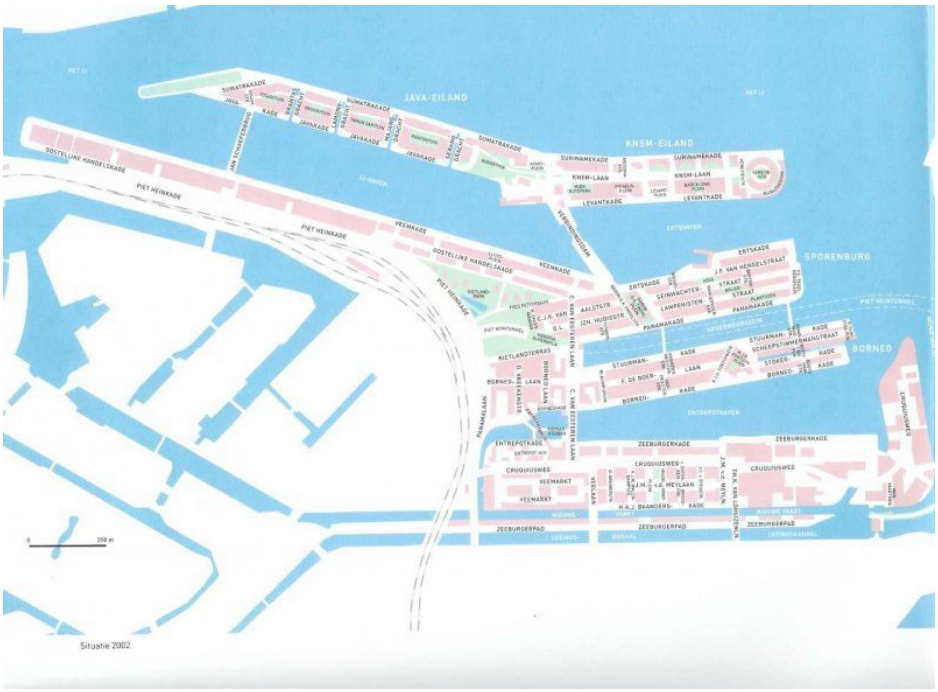

Analyzing the impact of electrification in heating and mobility on the grid in an Amsterdam neighourhood

Dirk Warmerdam
October 30, 2020

Contents

1 Introduction

In a bid to battle global warming the Dutch government has set ambitious targets to cut CO2 emissions in the Dutch Climate Agreement [1]. Aside from this state-driven initiative in line with the Paris agreement, several Dutch cities have presented their own climate initiatives. The city of Amsterdam has pledged to reduce its CO2 emissions by 55% in 2030 compared to 1990 levels which surpasses the national goal by 5% [2]. The capital has laid out a detailed plan to achieve these goals and it is clear that the electrification of mobility and heating, along with the roll-out of solar energy across the city, will play an important role in the future. Amsterdam is planning to install 1 million solar panels by 2022, aims to ban non-electric cars from the city by 2030 [3] and wants all buildings to be heated gas-free by 2040. While all of these steps are very helpful regarding the reduction of greenhouse gasses, they pose a big challenge to local grid operator Liander to ensure sufficient grid capacity [4]. The spokesperson of Alliander (parent of Liander) estimates that in 2050, peak power demand in Amsterdam could be 2.5 to 6 times higher than now. From the 25 substations in the city, which transform high-voltage electricity to middle-voltage, a minimum of 11 will not have sufficient capacity by 2030. The problem lies with an increase in both electricity supply and demand.

On the supply side, as more and more Renewable Energy Sources (RES) have entered the Dutch energy mix in the past decade the strain on the electricity grid has increased. While wind turbines have largely been built offshore and feed into the high voltage grid, on-land turbines and especially large scale solar generation are mainly connected to the middle-voltage (MV) grid which is primarily designed to distribute electricity, not to accept it. On a sub-level, solar panels installed on private roofs deliver their electricity to the low-voltage (LV) grid. The capacities of cables and transformers in residential areas are sized to deliver electricity from generator to consumer, and not the other way around. Liander has indicated that capacity is sufficient to deal with privately owned solar for now, but that the significant increase envisioned by the city of Amsterdam will pose a problem in the future.

On the demand side, electric mobility and heating will create a sharp increase in electricity use. The sale of (battery) electric vehicles ((B)EV's) has markedly increased in the last years, with the share of BEV's in total car sales increasing from less than 1% in 2015 to 14% in 2019 and predicted to grow [5]. The impact this will have on electricity demand can be illustrated by the fact that the average energy charged per day by an electric car equals the electricity demand for one average Dutch household for one day. In other words, if every household has an electric car, residential electricity demand will double. Even more important from a grid perspective is the power required to charge an EV. Modern electric cars charge at discrete power levels which have increased with newer models. Whereas now 7.3 kW is the standard, models set to be released in the next two years indicate a shift to 11 kW charging. This will cause larger power spikes during the periods that owners usually plug in their cars; in the morning at work or in the evening at home.

Electric heat pumps are expected to take over a large part of the heating demand now fulfilled by gas fired boilers. These pumps extract heat from the air, ground or water and use this to heat a heating-agent (fluid) which is then compressed electrically. This compression increases the thermal energy in the fluid which can then be used to heat water or air inside a building. Heat pumps operate at power levels around 1 kW, meaning that continuous operation on a cold winter day could easily double the normal electricity use of a household [6].

The mismatch between the time of energy generation and consumption, along with the large increase in electricity demand straining the grid are two puzzles that need to be solved to allow larger quantities of RES into the energy mix. These RES are essential to electrify our mobility and heating in a sustainable way. Several solutions exist in order to reduce the stress that these factors induce on the LV-grid and previous studies have focused on isolated aspects of the issues posed above. Naturally, the reinforcement of substations, cables and transformers is an option but this necessitates building operations that require huge investments, will inevitably disrupt traffic flows in important parts of the city, and negatively impact the regular lifestyles of residents.

Several studies point to 'smart' solutions as an essential route to decrease power peaks and increase the fraction of solar energy used. At the core of these solutions lies shifting demand from peak times to downtimes. Demand response - or flexibility - is conceptually easy to implement on an end-user scale by giving them the option to pre-heat their house [7], start charging their car at a later time or do the laundry at night. Practical implementation has been proven to be harder as commercial technology has struggled to make it to market. Flexibility can even be aggregated by the energy supplier to achieve a larger effect on peak power demand [8]. While a certain degree of demand shifting is certainly achievable, especially when considering EV-charging at the office, where the rate of adopting smart charging points will be higher, users that charge their EV at home will still want to plug-in their cars when they arrive after work in order to leave with a full battery the next morning. Therefore, smart charging will only have a large effect on peak demand if affordable and easy-to-use technology is introduced and the rate of consumer uptake is high. This can be compared to the heat pump situation which exhibits a morning and evening peak. Demand shifting can be done when using a (well-isolated) house as a heat buffer and heating during the day when PV-production is maximal. While this could work in the winter, in summer a large part of PV production will go back into the grid as PV production is high and heating demand low (or zero).

There is also plenty of research on grid-capacity which deals with the dynamic between TSO and DSO [9, 10, 11, 12]. Traditionally these two links in the electricity chain have been able to operate individually and responsibilities were clearly divided, as long as there was system balance. The role of DSOs is changing due to more intermittent and distributed energy sources in the distribution grid. At the same time TSOs are using flexibility services connected to the distribution grid to balance the system and ensure security of supply, making the need for coordination clear. Other studies look into grid congestion from an end-user perspective and focus on EVs (vehicle-to-grid) as an energy sink and source [10]. While one could view battery electric vehicles (BEVs) as batteries on wheels, the fact that lots of different owners will need to be compensated for their grid services complicates matters greatly. Another approach is to implement home-batteries at every household and aggegrate the resulting capacity [13]. This could be done by the energy company providing power, or a micro-grid (solar and battery system) installer, and spreads investment across a lot of actors. This approach lowers the financial barrier but does not profit from the economies of scale that a MW/MWh scale battery provides. It also causes added complexity and potentially conflicting interests in a system that consists of individual units that need to respond to very different energy demands between households, while still being available for grid services on a larger scale.

A correctly sized neighbourhood battery system can store surplus solar-energy during the day and provide this to end-users in the evening. This increases the fraction of PV-energy that is used by the end-users and decreases the amount that the grid needs to provide during peak hours. Looking at it from a grid-capacity perspective, both peak supply and demand of power decrease which decreases the fraction of capacity used. Such a system usually has a MW/MWh scale when supporting thousands of households and businesses [14] and can provide a number of services to the electricity grid.

This thesis aims to contribute to existing research by approaching the problem of intermittent solar production and peak electricity demand in a holistic way, testing the added value of a neighbourhood battery solution both technically and financially in a real-world situation. It was written as a graduate intern for environmental consultancy Resourcefully who manage several projects aimed at accelerating the energy transition in urban areas. They are involved in EU funded projects focusing on clean electric mobility and increasing the self-use of renewable energy [15]. Via the B-DER project in the Eastern Docklands in Amsterdam, funded by the Dutch government's TKI initiative, Resourcefully monitors the year-round energy consumption and production patterns of 24 households [16]. A blockchain trading platform is now being developed to allow residents to trade surplus power. The Eastern Docklands (ED) was chosen as the use-case in this thesis for a central battery system providing grid-services and functioning as the primary energy storage device for all rooftop solar in the area. It is a combined residential and commercial area with an above average income level, above average EV-ownership and a high potential for PV [17, 18]. The income level is a driver for the adoption of PV and, building on existing EV ownership, a catalyst for high EV adoption in the near future. This creates the potential for a large increase in bidirectional electricity flows and possible grid congestion problems. A high PV potential also makes the ED a prime location for implementing grid storage.

The thesis is structured as follows. The research design - containing an outline, the research question and sub questions - will be outlined in the next chapter. This chapter also explains the research approach, or methodology, taken to answer the research questions. Following this is a data chapter which outlines which data was used, in which form and from which source. It continues with a chapter on model implementation. After this the results from the model simulations will be presented and analysed. Lastly, the discussion and conclusion will assess the strengths, weaknesses and impact of the research, and gives suggestions for future research.

This report provides the reader with a clear insight into the impact of electrification on a real urban neighbourhood. It illustrates the possibilities of a neighbourhood battery system and the effect it can have on maintaining a stable grid in the future. Lastly, it presents a business case calculation of this system based on a novel neighbourhood balancing method and existing grid-services.

2 Research Design

2.1 Research Questions

To achieve all of the goals mentioned in the introduction, the following research questions should be answered.

Main questions

What is the impact of electrification on demand peaks in the distributed electricity grid of the Eastern Docklands, Amsterdam? And how can demand flexibility and a neighbourhood battery system decrease peak demand, increase solar energy usage, and aid in the CO2 reduction plans for Amsterdam?

Sub-questions

1. How does the increase in electrification of heating and mobility translate to a higher electricity demand in 2025 and 2030?
2. How does the realisation of solar potential in the ED translate to a higher local electricity production in 2025 and 2030?
3. How can demand flexibility aid in reducing demand peaks?
4. How can a neighbourhood battery system (along with demand flexibility) aid in decreasing demand peaks, increasing local self-consumption of solar energy and autarky, and thereby decreasing CO2 emissions?
5. Can a viable business case be made for a neighbourhood battery system in 2025-2030 with neighbourhood balancing?

2.2 Research Methodology

To make a prediction on the future energy demand and local supply, this thesis adopts a scenario-based approach. For each type of electric technology, three scenarios corresponding to three years (2020, 2025 and 2030) will be assessed, predicting different rates of PV, heat pump and BEV adoption. The scenarios generate different electricity demands for the relevant technology. These demand profiles feed into an energy system model programmed in Matlab designed to test the operation of a neighbourhood-scale battery system. To see if the neighbourhood battery system can be economically viable, a simple business case calculation is done incorporating possible value streams from performing grid services. The research structure used to answer the main questions and sub-questions is explained in this section. For the benefit of clarity, it is divided in different parts corresponding to the various research steps. The section will paint broad strokes, subsequent chapters will go into more detail.

2.2.1 Literature Support

This subsection will substantiate the research methodology with relevant examples from literature.

The hypothesis posed in this thesis warns for the potential grid-congesting impact of EV's, heatpumps and local solar energy. Several studies have looked at the individual impact of these technologies in the grid of the future. The Dutch energy grid is structured with a Transmission Service Operator (TSO) at the top of the hierarchy, responsible for the high-voltage transmission grid and a Distribution Service Operator (DSO) below it, responsible for the middle- and low-voltage distribution grid. The authors of [11] have looked at the increasingly overlapping challenges for both, caused by penetration

of renewable energy, and the consequent need to cooperate. The paper distinguishes between grid operating issues and market operating issues. The first are related to *determining* the grid capacity to be offered to the different market stages (day-ahead, intraday, real-time) and procuring balancing, congestion and curtailment services when the grid is strained. Cooperation involves a common grid model, calculation method for capacity and unitary input data. The second is related to the *allocation* of said capacity to these market stages. Cooperation involves coupling wholesale markets to use the remaining capacity for congestion mitigation. In this light the authors recommend further regulatory freedom for DSOs to experiment with new concepts such as local energy trading, to solve these issues. The recommendation is taken to heart in this thesis, where neighbourhood balancing is explored as a form of local energy market.

One way grid problems can occur is due to uncertain renewable energy sources (RES). A large influx of solar energy when demand is low can cause grid-imbalances that have to be solved by the DSO. Flexible demand, or demand response (DR) could be utilized to combat these imbalances. In [8], the possibility of aggregating flexible demand from residential and service sector customers and making it available for the DSO is investigated in the context of a realistic use-case. The reason for aggregating demand is that individual consumers do not provide the capacity needed to solve the MW-scale imbalances caused by RES. A Model Predictive Control (MPC) model is used to compute the optimal DR strategy with the objective to minimize supply/demand imbalances, subject to time-constraints imposed by the end-users. This model constantly updates the forecasted imbalances based on the solar production and demand profiles. Aggregating is done by middle-parties, positioned in between DR-offering consumers and DR-seeking electricity market participants. The paper assumes that the aggregator has perfect knowledge of the load demands of the consumers when assessing the available flexible demand, available to shift in time. It also assumes a 50% penetration of electric heatpumps and solar panels among residential consumers. The first assumption is also made in this research, substance is added to the second by including the realistic heat pump potential and suitability of all roofs in the use-case area. Another difference is that flexibility of other appliances such as washing machines is left out, and that EV-flexibility is added. The decision for leaving this out is based on the dominating influence of heatpumps on total demand and the capricious nature of appliance usage. Another advantage of heatpumps is that demand can be shifted over a longer period using the house as a heat buffer. This decreases the time-limitation on load shifting and increases the impact of DR. Household profiles come from the Dutch DSO Alliander, like in this research, and commercial demand is modelled using the same US models as in [13].

Results show that imbalances are highest when solar production is highest, in June, owning to a larger absolute forecast error. Imbalances are conversely lowest when production and errors are lowest, in December. Demand Response reduces imbalances in June for the residential sector by 8.7% on average. The largest effect is observed with the lowest forecast errors and the largest flexible load demand by heatpumps - DR reduces imbalances by 15-16% on average in December. However, the forecast errors have a large influence on results. Days are identified when the forecast error has the same sign for the entire day, for instance when solar production is underestimated for each timestep. These are called single-direction forecast days and can occur for instance on very sunny days in June. There are also days when the sign of the error switches constantly. These are called switching forecast error days. Demand Response can only work when surplus demand can be time-shifted to surplus production, and will therefore have no effect on days when the imbalance has a singular sign. This shows that DR alone cannot solve imbalances completely and fortifies the case for battery storage to exist alongside it. Financially, the study found that there is not an incentive for the aggregator to adopt DR. This is because the objective of the model is to minimize all imbalances, bot positive (making money) and negative (costing money). The incentive to implement DR lies with the TSO who needs to reduce imbalances to prevent grid outages or expensive improvements, and should therefore be the one to financially incentive the aggregator. Battery storage could also provide the necessary revenue to aggregators, if one assumes that they both operate the system and implement DR, an idea explored in this thesis.

In [9], coordination strategies between the EV-user, Fleet Operator (FO) and DSO are investigated to achieve congestion mitigation. The strategies look at the deferral or curtailment of EV-demand without inconveniencing users. Three distinct approaches are mentioned. The first explores a possible distribution grid capacity market. In this market, FO's submit aggregated charging schedules for their fleet to the Market Operator (MO). The latter quotes a price for these schedules based on the difference between the sum of the scheduled charging and the grid capacity limits. The FO then submits a new schedule based on these prices. Another new new price is calculated based on the latest schedules. This process is iterated until price convergence happens. The problem with this idea lies in the complexity of devising and operating a new capacity market with the associated information flows between FO, DSO and MO. However, the research is from 2012 and since then the GOPACS capacity market has been launched [19] which has some similarities with mentioned approach. The FO can be seen as the flex-provider offering their fleet of EV's as aggregated flexibility capacity to the TSO/DSO to solve local grid congestion. GOPACS is explored in this thesis as a possible revenue stream for the battery system, more on this in the Results chapter. The second strategy in the article is advance capacity allocation. In this simple strategy, grid capacity is allocated to EV-users (represented by FO's) based on predicted demand. If any surplus capacity occurs due to deviations from the forecasts, FO's can trade this capacity over the counter. The strong point of this strategy is its simplicity, which requires the DSO only to communicate one (capacity) value to the FO, and then removing the DSO from the equation until the settlement phase. Relying on the FO's to trade capacity does pose a risk because it places on them the cost-burden to develop a reliable system for trading. Lastly, the article introduces a method using a dynamic grid tariff set by the DSO. This price anticipates grid congestion at grid nodes and expects the FO to alter their charging schedules to minimize costs, thus (in theory) automatically mitigating congestion. The complexity in this idea lies with the DSO as they have to model prices and potentially intervene in the charging operation when the pricing scheme does not generate the expected charging demand. FO's and EV-users could thus be severely impacted in their desired operation of the cars.

The research in [10] also focuses on EV's and proposes a multi-level, multi-agent hierarchical market structure in which the DSO uses market mechanisms to influence the decision making of the FO, and the FO uses the same mechanisms on a different market to influence the end-user. Their results are promising and show that the demands of individual users can be met while allocating grid capacity efficiently and not burdening the DSO with very complex computational tasks. Because a holistic real-world use-case is considered in this thesis, on a large scale and comprising of more energy streams than only EV-charging, flexibility is not analysed on an individual actor level. That is why EV-flexibility is implemented by aggregating and centrally coordinating the demand. This takes the form of a pre-calculated charging schedule based on a perfect charging forecast. However, parallels can be drawn with the literature examples. When imagining flexible charging in the real world, user-behaviour can never be predicted with 100% accuracy but it can be steered by sending price signals to the end-user. This resembles the market-based user influencing in [10]. One could imagine that an EV-driver inputs their desired SOC and expected parking time when connecting to a charger. The FO could aggregate all requests and schedule an optimal charging pattern based on grid capacity, similar to the last method in [9]. The end-user pays a dynamic price based on the charging demand of the total EV-fleet. A system like this is assumed to facilitate the practical execution of EV-flexibility in this thesis.

Heatpumps are expected to have a major influence on household electricity use. How large this influence will be is investigated in [6] for the British energy grid. It identifies two problems with connecting a large amount of heatpumps to the grid. Firstly, a substantial voltage drop can be expected when the heatpumps turn on at the same time, which has to do with demand overcoming supply. Secondly, thermal capacity of transformers can become insufficient, leading to overheating unless they are reinforced. Aside from the impact on peak demand the influence on the grid ramp rate is investigated. The grid ramp rate signifies the required rate of power build-up to match demand. The research uses a unique dataset which records the electrical demand of 700 domestic heatpump installations for every two minutes. The authors use a half-hour aggregated version of this dataset to scale demand to countrywide levels, in order to estimate the peak grid demand with varying levels of heatpump penetration. They also state the shortcomings of this method. For instance, it is unknown what the technical characteristics of future heatpumps will be and how many different types of pumps

there will exist. The technology can become more efficient and better integrated with storage and smart grids. In addition, houses can become more thermally efficient like they have become in past years. Therefore, it is stated that the scaling exercise is not done for an exact prediction of demand with mass heatpump uptake, but rather to observe the approximate size of heatpump demand and its relation to total demand and if there is any simultaneity with total demand peaks. The article continues by comparing heatpumps with gas boilers, not in terms of energy consumption but the shape of their demand profiles using normalized versions. These are predominantly the same for the two heating variants and exhibit two peaks during the day at the same time, but the ramp rate is higher for boilers. Boilers also show a more 'peaky' behaviour during the day, which is confirmed by a higher ratio of peak to mean than for heatpumps. At night, boilers fall to 16% of their peak output compared to 41% for heatpumps. The method of gathering of real heatpump data and scaling to a known population at different penetration levels is also used in this thesis.

Results show that heatpumps exhibit a daily morning and evening peak, coinciding with the grid peak. The morning peak is the highest which implies that houses cool down the most during the night and that a base load exists overnight. This is the same for the demand in this thesis. When the data is aggregated and added to the total electricity demand for the UK, at a penetration of 20%, a small morning peak starts to occur. This effect is not very strong yet and the overall profile mainly follows the existing profile with a slightly varying increased total load throughout the day. Peak demand is defined as After Diversity Maximum Demand (ADMD), which is a fancy name for the maximum of aggregated demand. ADMD increases with 14.3% at 20% heatpump penetration among 25.8 million British households. This peak predictably occurs on a winter day in February. Grid ramp rate increases are comparatively small at a 6.1% peak increase in the highest penetration scenario and the daily UK grid profile is not much different from its original shape. When modelling for heatpump demand in this thesis, and adding on the UK example, an even higher penetration is assumed following gas-free policies, and the effect of heatpump demand response on grid peaks is studied.

An urban microgrid with renewable energy production and battery storage was modeled in [13]. The paper compares individual to coordinated storage to see the effect on local renewable energy utilisation. With individual storage, each PV/storage-owner only uses the capacity of their own installation. Coordinated storage pools all available storage and exchanges residual surpluses or shortages with the grid. The paper also tests two algorithms in a modelled environment, one only focused on the current timestep, called 'greedy', and one incorporating the forecasted mismatch 5 hours in the future, called 'peak shaving' to see their influence on peak grid power flows. The greedy algorithm stores any positive mismatch in the battery and meets any negative mismatch until all stored energy is used. By looking a few timesteps ahead, the peak-shaving algorithm can prepare for a peak in demand by holding onto stored energy, enabling it to better meet demand and decrease peaks. Like in this thesis, the authors have had to combine different data sources to paint a complete picture of the energy flows in the area. Dutch statistics data provides the information on the number of households and businesses. Household consumption data is measured from 61 households elsewhere in the Netherlands. Commercial consumption profiles are modelled using adapted US Department of Energy reference models. Solar insolation data is converted to power generation using an existing Matlab model and the specifications of a commercially available solar panel. Where the articles' approach differs from this thesis' research is in the distribution and scaling of production and batteries. A 50% penetration of panels and batteries is assumed and distributed randomly among the prosumers. The installed solar and battery power is scaled according to the energy consumption of the household or business. By running the model 25 times, each time with a different distribution, a statistically significant set of results is obtained. While this last point adds flesh to the uncertain bone of future solar penetration, there is no supporting argument for choosing a 50% adoption rate, and no scenarios are sketched out based on historical growth or future policy.

The results show that coordinated storage causes a relative increase of 39% for self-consumption, rising from 62% to 86%. Almost three times less energy is transferred to the grid. Furthermore, autarky shows a relative increase of 21%, with 69% of local microgrid demand being satisfied with coordinated storage compared to 57% for individual storage. To assess peak-shaving, the authors look at the day with the maximum power peak (demand + generation), equal to 43 MW at 12 in the afternoon. The greedy algorithm does not manage to decrease this peak with either of the storage strategies. The peak-shaving algorithm shows the best results with coordinated storage, which more than halves the peak to a value of 18 MW, compared to 23 MW for the individual storage scenario. This is partly due to the desired peak-shaving behaviour where it waits for the onset of the predicted peak before any energy is delivered from the battery system, thus having the highest amount of energy available to feed into the grid for critical moments of demand. The algorithm cannot always decrease demand peaks, it depends on the amount of local generation that occurs before and during the demand peak. For instance, the highest demand peak in the year is 22 MW and occurs on the 6th of January and is preceded by a period of low solar generation. These issues will occur less frequently when solar generation capacity is increased and, equally importantly, storage capacity is increased so generation can actually be stored and used for high demand periods. A mismatch comparison for each hour of the year between the greedy and peak-shaving algorithm shows statistically significantly better results for the latter, for both coordination strategies. For this thesis, a peak-shaving algorithm is developed that bases the load forecast on historical demand data. It incorporates the principle of holding battery energy delivery until a certain grid-load threshold is reached, in order to have the maximum amount of energy available for the peak.

2.2.2 Area Choice and Data Gathering

The Eastern Docklands is chosen as a use-case for a number of reasons. It is an area which has seen rapid development in the past 30 years, transforming from a dedicated harbour area to a residential area. This gives it a housing type mix weighed towards post 1990 buildings [20]. These fairly new buildings are more suitable for heatpumps than the historical real-estate in the centre of Amsterdam because of a higher degree of insulation. The demographic of the ED has an above average income and is therefore more likely to invest in (still expensive) electric cars, solar panels and heatpumps [17].

These reasons were also the motivation of Resourcefully to start monitoring the energy consumption and production for a selection of ED households. In the separate Flexpower project, public EV-charging at flexible-power charging points in the same area was investigated [21]. A product from this project is the charging session data used to synthesize ED-wide EV-charging profiles in this thesis. Summarizing, the make-up of housing types, demographic of the area, historical expertise of Resourcefully and access to real charging data were the main drivers in choosing the ED.

Five different data-streams are needed to model the electricity flows in the area, namely: household demand, commercial building demand (from now on, commercial demand), EV-charging demand, heatpump demand and solar production. A household demand profile is needed to represent the baseload from lighting, appliances and electric cooking. Distribution System Operator Liander has published a dataset representing the electricity demand of 10.000 households [22]. This set is based on the real aggregated demand of 10.000 Liander customers in 2014. There is no specification of the types of houses contained in the set. It is assumed that with 10.000 houses, there is a fairly good spread in the types of houses. CBS data indicates that there are currently 9362 households living in the ED [20], which is fairly close to the customer base in the dataset. The set is scaled to the total household energy demand in the ED, as published by Liander in the 'kleinverbruiksdata' dataset [22].

While the ED is a mainly residential area, it also contains a substantial number of commercial buildings. The BAG Kadaster mentions 1492 locations of which 85.8% is built in the period 1990-2019. A majority of these businesses is active in the business services and culture/recreation sector (total 63%). The Energy research Centre of the Netherlands (ECN) researched the electricity and gas demands of different kinds of offices, active in different sectors. The demand profiles this has generated are further differentiated by office size and building period. Based on the building period

and industry of the majority of offices in the ED, a demand profile was chosen. This profile is scaled to the total electricity use of businessess and institutions in the ED, as published by CBS [20].

Heatpump data is also derived from ECN profiles. These differentiate between air-air, ground-air heatpumps in various types of houses with different insulation grades. As the ED is made up of 92% apartments, an apartment-profile accounts for the majority of housing demand profiles. About two-thirds of the houses is built after 2000 when insulation grades were improved by law [23]. Later the mandatory insulation level increased even further. Therefore, a fraction of the flats is assigned a 'medium' insulation grade and another fraction is assigned a 'high' insulation grade. Exact values are given in the Data chapter. Ground-air heatpumps require major building work and thus are usually installed during the building process while air-air pumps can be easily installed afterwards. So, a large fraction of heatpump growth will likely come from air-air heatpumps by converting existing homes. To reflect this, the largest part of the apartments is assigned a air-heatpump profile. The remaining 8% of non-apartments are assigned a 'tussenwoning' (terraced house) profile with an air-air heatpump, as this is the prevailing house-type after apartments. Because the Liander household data does not contain electric heating, adding heatpump profiles will not cause the problem of 'double-counting' demand.

Resourcefully was involved in another project in which charging data of public chargers in the ED was analysed. Several charging profiles were identified relating to the connection times and charging duration of users. These profiles were subsequently approximated and normalized to a per session level. This allows for great freedom in scaling and fine-tuning for charging behaviour. The charging profile division is based on the observed behaviour in real local data and the sessions are scaled according to estimated current and future EV-ownership. Also taken into account is a move towards charging at higher power and the ratio between public and private chargers.

There are several sources offering solar insulation data for specific coordinates, with some also offering a solar power production calculation when installed power is given. For this research PV-GIS is used, which uses satellite imagery to estimate the solar insolation at a specific location and height maps to compute the horizon at this location. PV-GIS is developed by the Joint Research Center of the European Commission and made available for public use. The reason for choosing PV-GIS is that it is an reliable data-source that offers energy calculations, but more importantly does not smoothen data by taking an average over several years. The raw data that it outputs is impacted by cloud cover from hour to hour, which is, while less visually attractive, a more realistic representation of the real output of a PV system. For simplicity's sake, a central location in the ED was chosen for a PV system. The total solar potential of the roofs in the area was assessed in 2018 [18]. This potential is used in this research as the maximum size of the system. It is assumed that an increasing fraction of this potential is installed in the years 2020, 2025 up to 100% in 2030.

2.2.3 Scenarios

The state of the energy demand and generation in the ED is assessed in three years, 2020, 2025 and 2030. A horizon of ten years is chosen because 2030 is often mentioned in climate plans as the year in which a certain CO2 reduction or renewable energy goal must be reached [2]. A combination of historical growth, announced future policy changes, sustainability goals from the government and predictions from expert sources allow for the scaling of current electricity demand to scenarios for the three years mentioned above. This is done by increasing the quantity of heatpumps, EV's and solar power in each year, which influences the demand, supply and mismatch at each moment, and thus changes the grid peaks for each scenario. Exact figures are given in the data chapter.

Flexibility of demand is implemented for the EV and heatpump data. This generates new, time-shifted, demand profiles which can be added to the rest of demand to end up with 'Flex' total load profiles for the year, producing two sub-scenarios per year. The peaks in these Flex profiles are compared to Business As Usual (BAU) - non-Flex - peaks. 2020 is used as a base and does not have the solar production required to charge and utilise a neighbourhood battery. Therefore, it is assumed that there is no battery system yet 2020 and peak shaving, PV-utilisation and the CO2 reducing

capacities of the battery system are only assessed in 2025 and 2030. The effect of varying battery capacity on these metrics is studied to end up with a desired, 'ideal', battery size which offers a good mix between utility and cost.

To summarize, a prediction of grid demand and local pv production is made for three years, of which 2020 functions as a base year. For the benefit of clarity the choice has been made to limit the analysis to one level of technology penetration per year. The addition of flexibility and varying levels of storage adds a good level of depth to account for various different situations. The goal of this research is therefore not to exactly predict future grid loads, but to model a realistic scenario and assess the potential of a battery system.

2.2.4 Model Development and Implementation

In order to analyse the impact of different scenarios for electricity demand and generation growth, as well as assess the functioning of a neighbourhood battery, a model with a high degree of flexibility is paramount. Therefore, the model built for this thesis has two main functions:

1. To include, evaluate and visualize all the data-streams associated with the energy generation and demand in the ED.
2. To simulate a scalable neighbourhood battery system that stores excess solar energy and delivers this when needed.

The software package used for building the model is Matlab with Simulink. The first step in creating the model is cleaning up and time-step-equalizing all the data. A time-resolution of 15m is chosen because it is equal to the Program Time Unit (PTU) of the balancing market in the Netherlands [24]. It also achieves a good balance between simulation time and accuracy when modelling for a full year. This required the household-, heatpump- and EV-data to be interpolated from a resolution of 1hr. A linear interpolation method is used which adds three intermediate data-points between the hour-timestamps with a random variation of 2% around the hourly value. The random variation is done by using the 'rand-function' from Matlab, which draws pseudorandom values from the standard uniform distribution on the open interval (0, 1).

Once the data is scaled and interpolated, the main model architecture is built in Simulink. A detailed description and mathematical substantiation of all logic in the model is given in the Model Implementation chapter. A short explanation of the workings is given here.

To be clear, the model is not an electrical engineering representation of a local energy grid. Only active power is considered. The total loads, generation and storage and their interaction are evaluated as if it were a standalone energy system. Grid capacity is taken into account on a neighbourhood level. The goal is to make a prediction of the scale of future electricity demands, relate this to an estimation of grid capacity, and assess the usefulness of a battery system in increasing self-consumption of solar power by charging during the day and discharging during the evening peak, thereby also decreasing peak demand.

The Simulink model allows for scaling of the battery system by increasing the number of batteries. This scaling is performed in the Results chapter based on self-consumption and autarky results. When considering the size of the battery, the focus is on *energy* capacity rather than *power* capacity because in the end the self-sufficiency of the system is dependant on how much energy the installed solar can generate. However, power capacity is not forgotten and the maximum charge/discharge power peaks are analysed in the Results and included in the scaling process. The model also allows for a maximum and minimum State Of Charge (SOC) input.

The main part contains the logic to perform the required battery functions. The algorithm is fed with two versions of each total load dataset, one which incorporates aggregated flexibility of demand and one which does not. Flexibility is pre-calculated using the E-flows algorithm which is developed in-house at Resourcefully [25]. The algorithm is applied to the EV and heatpump data. EV-data shows longer connection times than charging times, and heatpumps can use buildings as a thermal storage device. Both characteristics allow for demand to be shifted in time. E-flows assumes a perfect prediction of demand, as its input are full-year load profiles with at a 15m interval. More detail is given in the Data Gathering and Analysis chapter.

The model has an algorithm with two goals: to minimize the grid interaction (by maximizing solar self-consumption) and to maximize peak-shaving in the evening. The interaction algorithm evaluates the amount of energy that is demanded or produced for each time-step and updates the State of Charge (SOC) of the battery, incorporating charging, discharging and self-discharging losses. Only when the battery's capacity is insufficient, grid interaction takes place. The battery system is given constraints by he peak shaving algorithm, which evaluates the mismatch to see if a threshold is reached and energy is required. The threshold for delivering energy is based on the average evening peak (between 17:00 - 21:00) on the same day from the previous week. If this threshold is reached, the battery recognizes that there is an evening peak and supplies energy. If not, energy is drawn from the grid. This ensures that the maximum amount of energy is available for daily evening peak demand.

The third part of the model is where the results of the simulation are outputted from the Simulink simulation environment to the Matlab workspace for further analysis. The most important outputs of the model are the grid-interaction timeseries and the battery-SOC. Grid interaction is the input for most of the analysis. Battery-SOC is used in conjunction with grid-interaction to assess the effect of the battery size. As an example of this output, the results for a full year simulation run are given in Figure 2.1.

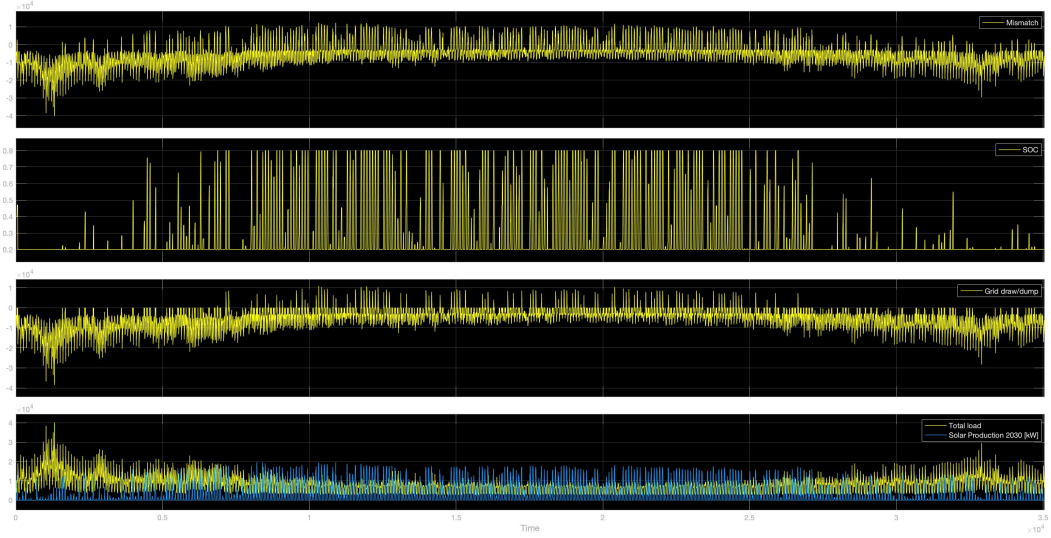

Figure 2.1: The output of the battery model for a full year (2030 scenario).

This figure clearly shows seasonal variation of the loads and solar production, and consequently a varying battery SOC and grid interaction. At the top is the mismatch graph, the difference between total load and production. These are shown in the bottom graph as the yellow and blue traces respectively. The blue production trace is regularly above total load during approximately half the year, from the beginning of spring to the end of summer. Before and after this period loads are higher due to higher heating demand because of colder outside temperatures, and solar production is lower because of lower solar intensity. Because the battery is only charged using solar electricity in this model, this has an influence on the State Of Charge of the battery. Each line in the SOC graph (second from the top) represents a (partial) charge/discharge cycle. It is visible that during spring

and summer, when production is high, the battery is regularly charged up to its maximum SOC and subsequently discharged again to its minimum SOC, representing a full cycle. This depends on the storage capacity of course. Far less cycles take place during the colder months at the beginning and end of the year. The SOC graph in Figure 2.1 shows the equivalent of 160 full cycles.

When the battery is full or empty but there is still a mismatch, grid-interaction occurs where electricity is dumped on or drawn from the grid. The second graph from the bottom shows the grid-interaction, positive when a positive mismatch cannot be stored because the battery is at its maximum SOC (i.e. full), negative when a negative mismatch cannot be supplied because the battery is at its minimum SOC (i.e. empty). The amount of energy that is stored in the battery depends on two things: 1. The amount of solar production. 2. The storage capacity of the battery. In winter the first point is the bottleneck, there is not enough solar production for a surplus to occur, therefore there is no electricity stored in the battery, the SOC stays at minimum level and when a negative mismatch occurs the power needs to be drawn from the grid. During summer the second point can be the bottleneck when there is so much solar production that not all surplus can be stored by the battery. The sizing of the battery is a process that depends on minimizing grid dump to a level that is economically efficient, as will become obvious in Chapter 5.

2.2.5 Results and Analysis

This section presents the results gathered through procedures detailed in the Research Design section and is divided between a technical section and a financial section. The results are analysed and the most important takeaways presented. The technical section starts with an overview of the extreme demand situations occurring over the year and the impact of demand flexibility on these peaks. The peaks are put into perspective by including the estimated grid capacity. It continues with the battery system, specifically how the size of the system influences average evening peaks and midday solar peaks. After this, the impact of flexibility and the neighbourhood battery on CO2 emissions are considered. A link is made with Amsterdam's environmental goals. The financial section evaluates neighbourhood balancing (saldering in Dutch) as an income stream for the battery system and computes the payback time for the battery. A comparison is made to regular existing compensation measures. Other forms of revenue generating grid services are briefly mentioned and their financial impact is evaluated.

3 Data Gathering and Extrapolation

The goal of this research is to model a combined commercial/residential neighbourhood and to predict its bidirectional energy flows in the future. It is therefore important to gather reliable data of the current energy flows. These can be divided between demand flows and generation flows. On the demand side, there is residential and commercial demand forming the base. In addition to this there is demand from EV-charging and heat-pump operation. This section describes how these data-streams were acquired or synthesised. It also outlines how the data was extrapolated to the 2025 and 2030 scenarios. Firstly, it is explained why these years were chosen as a horizon along with an overview for all the evaluated scenarios.

The year 2030 is important in a lot of climate plans. It is the landmark year in which the results of the environmental policies put in place in the past decade will be appraised. Therefore, 2030 is chosen as the horizon in this research. An intermediate year is also needed. Because 2030 is exactly 10 years away, 2025 serves as a neat intermediate date. The penetration of each technology is predicted for these dates based on the current state, a best estimate of the growth rate and the ultimate potential. The current situation is also evaluated. There are thus three main scenarios: current (2020), intermediate (2025) and future (2030). These are expanded further by looking at the situation with and without flexible demand and a neighbourhood battery system. The base year 2020 does not have enough solar installed to make use of a battery system, so only flexibility will be assessed. In total 10 situations are evaluated, summarised in Table 3.1.

Some plots are included at the end to get a feeling for the relative size and shapes of the individual load profiles. These also include a mismatch plot. Mismatch is defined as the difference between all loads and all production at every timestep and is a good way to directly see if there is a surplus or shortage of renewable energy.

Table 3.1: Scenario overview

Scenario	Year	Flexibility	Battery System
1	2020	No	No
2	2020	Yes	No
3	2025	No	No
4	2025	Yes	No
5	2025	No	Yes
6	2025	Yes	Yes
7	2030	No	No
8	2030	Yes	No
9	2030	No	Yes
10	2030	Yes	Yes

3.1 Household demand

Household demand contains all electric device demand from households, including lighting, electric cooking and other appliances, but excluding EV-charging and electric heating. The residential demand profile is based on the aggregated demand data of 10.000 Liander customers in the Netherlands [22]. This dataset was published in 2014 and values are normalized to the average temperature-profile of the last 20 years. Demand is scaled according to the known total electricity demand of residential consumers in the ED (Liander's kleinverbruiksdata per postcode) in 2019, which is published by Liander [26]. The profile had a resolution of one hour which has been interpolated to 15m by adding 2% random noise.

Table 3.2: ED household demand data summary

Variables	Value	Source
Households (2019)	9.362	CBS
Households Liander set	10.000	Liander
Household demand Liander set [kWh]	31.240.940	Liander jaarprofielen
Household demand [kWh]	35.653.638	Liander kleinverbruiksdata
Demand scaling factor	1.14	

Household demand is not scaled to 2025 and 2030. CBS data indicates a small yearly increase in the number of households and a larger decrease in the average yearly household demand, see Table 3.3. It is uncertain if the decrease in average household electricity use can continue at this pace or will be asymptotic. The same thing holds for the number of households. One could imagine that the limited amount of space in the ED will put a brake on its growth. These factors have prompted the decision to refrain from scaling.

Table 3.3: Average yearly household electricity demand.

Year	Households	Average yearly household demand [kWh/year]
2013	9095	2700
2014	8805	2600
2015	9035	2580
2016	9090	2500
2017	9290	2430
2018	9315	2360
2019	9362	2297
Avg. yearly difference	**0.500%**	**-2.65%**

3.2 Commercial demand

The commercial profiles representative for the businesses in the ED are synthesised using normalized (on a scale of 0-1) profiles from ECN, which can be scaled to a desired total energy demand [27]. The ECN profiles are published for different types of businesses, reflected in different yearly operating hours, office sizes and building periods. An estimation is made for a realistic amount of operating hours and size of the average business in the ED. This is based on property registration data detailing the building period distribution of commercial buildings, and the distribution of the types of businesses using SBI-codes. The chosen profile is then scaled to the total energy demand of all commercial users in the ED, as published by CBS via Liander. The resolution of this data is quarterly. A summary is given in Table 3.4.

Table 3.4: ED commercial demand data summary

Variable	Value	Source
Profile	E3A	ECN
Annual operating hours	3.827	ECN
Number of commercial buildings in the ED	1492	BAG Kadaster
Yearly demand offices and institutions [kWh]	47.354.000	CBS

Commercial demand is not scaled for the same reasons as household demand. CBS data indicates a yearly increase (5%) in the number of businesses. No data is available on average yearly electricity demand for different years, for offices. However, one could imagine that the same developments that cause the decreasing household demand - more efficient appliances and better insulation of buildings - would apply to commercial demand. Extrapolating the household figure, this would mean a yearly demand decrease of 2.5% which results in a net increase of 2.5%. This will have a negligible impact when considering for instance the growth in heatpump demand. The space issue also applies, so there is no clear basis here for a growth figure.

3.3 EV demand

EV charging data for the Amsterdam area is not public. However, the Flexpower project mentioned before was conducted in conjunction with the HvA (Hogeschool van Amsterdam) and generated public charging data. This data was analysed by a data analyst to end up with charging profiles representing different charging behaviour. These profiles are based on the connection time and duration of charging sessions. A worktime, short-stay and home profile was identified and synthesised. The worktime profile corresponds to a connection time in the morning and disconnection late-afternoon/early evening. Short-stay corresponds to short connection times all through the day, which are charging sessions from people shopping, eating or meeting. Home profiles correspond to users connecting during the evening and disconnecting the next morning. These profiles allow for individual up- or downscaling to the required amount of charging sessions as well as the observed charging behaviour and are used to generate the EV charging data in this research.

The distribution of the profiles is based on recorded public charging sessions from 2014 to 2018 in the ED, which were classified to the same worktime, short-stay and home category. This distribution is given in Table 3.5. It is clear that the majority of EV users in the ED are either residents charging near their homes, or visitors. The increase in year-on-year-growth from 2017 to 2018 is extrapolated to 2019, and the number of sessions in 2018 is then multiplied with this growth factor to end up with the 2019 public charging sessions. The same process is followed is done for 2020. This results in high growth numbers, visualized in table Table 3.6, but not unrealistically high, as the growth in EV-sales as a fraction of total car sales has been in triple digits since 2018 [28].

Table 3.5: Charging profile fractions in the ED.

Profile	**Fraction**
Worktime	0.11
Short-stay	0.42
Home	0.47

Table 3.6: Extrapolation of ED public charging sessions

Year	**Sessions**	**yoy-growth**	**Δyoy-growth**
2014	8159	/	
2015	9198	12.7%	
2016	10808	17.5%	+37.8%
2017	11933	10.4%	-40.6%
2018	14171	18.8%	+80.8%
2019	18960	33.8%	+79.8%
2020	30503	60.9%	+80.2%

The ED has a relatively large availability for off-street parking (driveway or garage) compared to the rest of Amsterdam, which allows for the installation of private chargers. There is no map for these charging points, like there is for public chargers, but a survey carried out by the author among VVE's in the ED revealed a high penetration of private chargers in the area [29], and a large motivation to

install private charges for future EV purchases. This legitimized the decision to use an estimation by the Rijksdienst voor Ondernemen (RVO) [30] of the number of private chargers in the whole country. Dividing this number by the known amount of public chargers in the country produces a multiplication factor to generate the private charging sessions. One could assume that 'Home' charging will be more prevalent in private charging sessions, but a decision was made to stick to the observed public charging behaviour in the relevant area. Estimation of private charging behaviour would be pure guessing work because no data is available on that subject. In addition, the short-stay charging fraction also captures visitors of businesses who charge their car on private business property, adding to total private charging.

The base number of EV's in the ED in 2020 was derived from the fraction of EV owners in the 'prosumer' group (24 households) from Resourcefully and the before-mentioned survey. Both sources show an EV adoption of 13%. A prediction for EV adoption in the ED was made for 2025 and 2030 based on several EV outlooks from other sources [31, 5, 32, 28]. In 2018, BOVAG, the Dutch automotive industry organisation, made an EV outlook for the next 12 years with conservative, common and progressive scenarios for EV sales ánd the fraction of EV's of total cars in the Netherlands. Time has caught up with this outlook as EV-sales have grown much faster than expected due to favourable fiscal policies, a good charging infrastructure and an increased offering of affordable electric cars, causing their conservative scenario for 2025 to already be reached in 2019. This prompted the decision to update their scenarios, assume the common scenario as conservative and the progressive scenario as common, resulting in 40% BEV of total sales in 2025 under the common scenario. In January 2020 BOVAG published their outlook for the year, which predicted a lower fraction of EV's in total sales (10%, vs. 14% in '19) due to a change to less favourable fiscal rules and a rush in EV-sales at the end of 2019. However, in February 2020 the Dutch government announced a €4000,- buying subsidy for privately used EV's which will partly make up for less business car sales. These developments motivated the choice to assume the 2019 fraction of EV/car sales in 2020 (14%). This needs to be translated to the Eastern Docklands to make an informed prediction. The prosumer pool and ED survey reveal that the % EV/total *sales* in 2019 for the Netherlands, thus copied for 2020, is equal to the % EV/*household* in the ED, indicating that the area is ahead in electric car adoption. The reason for this higher adoption rate is probably due to the well developed charging infrastructure in Amsterdam and high average income [17]. The adoption rate is taken as the base fraction for EV/household in 2020. For '25 and '30, the higher adoption rate is reflected by assuming the EV penetration in sales from the updated BOVAG outlook as the EV penetration in total cars. This is more conservative than continuing the assumption that EV/sales equals EV/household and incorporates the reality that some households do not possess a car.

This results in a predicted EV penetration of 40% in 2025 and 100% in 2030. CBS data gives an average of 0.6 cars/household in 2019, a figure which has been constant for the past years and assumed constant until 2030. One could argue that there is a declining trend in car ownership among young people, meaning cars per household will decrease in the future. This may be true, but the decline could also be countered by the rise in 'share' cars which are almost exclusively electric already. Which trend is overpowering is hard to predict, so a choice is made to stick to the known data. To compute a total amount of EV's in the area for 2020, 2025 and 2030, the fractions EV/cars and cars/household are combined to generate EV/household. Multiplying this with the number of households produces the number of EV's, which is used to scale EV charging demand, based on the amount of current charging sessions with the relevant profiles. The data is summarized in Table 3.7. No vehicle to grid charging was included as this technology is still in a developmental phase, and there are concerns regarding battery life [33].

It is important to include the developments in charging speeds when modelling future EV-charging demand. New EV's are capable of charging at increasingly higher speeds, with 11kW becoming the norm and the more high-end cars also accepting 22kW. Fiscal rules starting to disfavor plugin hybrids in the Netherlands have had a significant negative impact on sales, and thus it can be expected that their 3.7kW charging speed will be represented less in future years. Full electric cars on the other hand are being stimulated with fiscal rules and buying subsidies, so the share of 11 and 22kW charging sessions can be expected to increase. Between these two, 11 kW charging has the best cards to be the dominant charging speed for private chargers, because 22 kW charging requires a bigger

grid connection for consumers which comes with significantly higher costs [34]. Public chargers are regularly used by visiting users who need to charge in a shorter timespan. Historical public charging data from the city of Arnhem, evaluated by Resourcefully in the CleanMobilEnergy project, also points to more 22 kW charging in the public space [35]. The choices regarding charging speeds for the EV-charging data in this research are summarised in Table 3.8.

Table 3.7: Predicted EV-ownership and charging data in the ED

Variable	**2020**	**2025**	**2030**
Households	9.408	9.646	9.890
EV's per prosumer	0.13	/	/
Cars per household (CBS)	0.6	0.6	0.6
EV's per household	0.13	0.238	0.6
Total EV's	1.227	2.292	5.934
Public charging sessions	30.503	56.969	147.496
Private charging sessions	88.220	164.763	426.582
Total charging sessions	118.724	221.732	574.078
Charging sessions/EV/year	96.7	96.7	96.7

Table 3.8: Charging speed fractions in charging session data for the relevant years

Charging speed	**2020**	**2025**	**2030**
3.7	79%	5%	0%
7.3	11%	35%	10%
11	7%	50%	70%
22	3%	10%	20%

3.4 Heatpump demand

For developing the heat pump scenarios, the author looked at the fraction of houses connected to district heating and the distribution of the types of buildings to come to a realistic penetration potential for the whole ED. CBS data indicates that 51% of the ED houses is connected to district heating. District heating heat is generated by burning natural gas, waste or biomass and therefore comes with greenhouse gas emissions. Plans are made to incorporate waste heat from datacenters into this mix but no concrete use case has been established yet. The city of Amsterdam has recently lost a court case against an environmental agency that aims to stop the connection to district heating of the new 'Sluisbuurt', which is yet to be built [36]. This potential legal backlash along with the CO2 footprint makes it unlikely that existing homes in the ED will be connected to traditional district heating in the future. This could change if district heating using datacenter waste heat takes off. Taking the facts mentioned above into account, it is assumed that no new homes will be connected to district heating in the ED in the next 10 years. The fraction of district-heating-connected houses is therefore excluded from heat pump installation, leaving 49% available for heat pumps. Heat pumps are widely being suggested as the new way of heating. The Dutch government have placed heat pumps centrepiece in their plan for gas-free housing. Amsterdam wants to be completely gas-free by 2040. As new homes are already being built without gas-stoves for cooking, heat pumps are the logical next step to completely electrify residential areas. To establish a base 2020 figure, it is estimated that 10% of houses in the ED have a heat pump at this moment. If the city wants to reach its 2040 goals, neighbourhoods with the most suitable houses in terms of insulation must lead the way. That means an aggressive roll-out of heatpump technology is needed in more modern areas like the ED. This is reflected in the scenarios summarized in Table 3.9, where in 2025 the realised fraction of the potential has increased to 50% and in 2030 100% is predicted to be realised.

Heat pumps are only suitable for well isolated houses. Fortunately, the ED is made up of 92% apartments, 60% of which is built between 1990-2000 [20], and 40% is built after 2000. This ensures a fairly high level of insulation which makes it suitable for heat pump adoption [23]. For the older houses insulation works are required. Heat pump consumption profiles were generated from Energy Research Center Netherlands (ECN) profiles for apartments with medium and high insulation [37]. Two different types of heatpumps are included: ground-air and air-air. Because ground-air heat pumps are usually only installed in newly built apartment blocks, it is assigned a 5% fraction of total homes with a high insulation grade (Flat/H/Ground), increasing to 10% by 2030 to account for new building works. The rest of the apartments use air-air heatpumps which can be installed in existing buildings. From these, it is estimated that 55% have 'medium' insulation (Flat/M/Air) and 32% have high insulation (Flat/H/Air) grades corresponding to the building period mix. The rest of the houses in the ED are either house-boats or adjoined homes which have a higher heat demand than apartments. These are modeled using a terraced-house profile with medium insulation (TW/M/Air).

As ground-air heatpump installations increase, the air-air types are expected to be slightly weighed towards higher insulation as some medium-isolated apartments are renovated over the years. The heat pump demand profiles have a resolution of one hour and are interpolated to 15m by adding 2% random noise.

Table 3.9: Predicted heatpump installations per housetype and technology

	2020	**2025**	**2030**
Households	9362	9646	9890
Heatpump potential	0.49	0.49	0.49
Heatpumps installed	10%	50%	100%
of which			
TW/M/Air	8%	8%	8%
Flat/H/Ground	5%	7.5%	10%
Flat/H/Air	32%	31%	30%
Flat/M/Air	55%	53.5%	52%

3.5 Solar production data

To assess the impact of rising electricity demand one must first assess the way in which electrification impacts energy flows. Because Amsterdam is an urban area, lacking the space for large on-land windfarms, rooftop solar energy is the obvious choice to supply the city's renewable electricity. Solar energy is such an important driver because electricity use accounts for 39% of the city's CO2 emissions [2]. The Netherlands's capital has set the goal to install one million solar panels by 2022 and to have 550 MW of installed solar power by 2030, up from 73 MW currently. The 2030 goal is 50% of the potential for the whole city. Previous research into the suitability of ED roofs done by Resourcefully together with the Amsterdam Energy City Lab defines the PV potential as 21.7 MWp [18], or about 4% of the 2030 citywide goal. Currently about 10% of this potential is utilized. Because the ED has a lot of flat roofs, suitable for solar panels, it can act as a catalyst for PV growth in the city. It will be much harder to achieve PV-installations on the old buildings in the city center. Socio-economically, 40% of ED residents are home owners and all residents have an above average income which allows for higher discretionary spending [17], a driving factor for solar panel adoption. In other words, the ED must lead the way in solar installations. Therefore it is assumed that in 2025 75% of the solar potential is built and in 2030 100% is laid out. Table 3.10 summarises this.

Several sources are available offering solar insolation data. These sources usually allow for the input of geographical coordinates. Some sources also offer a solar energy production profile given a certain installed capacity. The data chosen for this thesis is developed by the EU Science Hub and is called PV-GIS [38]. It uses satellite images to compute solar radiation on a certain location. When a location is inputted, the algorithm computes the horizon at this location. The user can then input an installed capacity and PV-GIS outputs the energy production per hour for a defined timeframe.

For the sake of simplicity, the total PV potential in the ED is input as one 21.7 MWp solar system on one latitude/longitude coordinate.

Table 3.10: Solar power installed per scenario

Variables	**2020**	**2025**	**2030**
Potential installed	10%	75%	100%
Nominal power installed [kWp]	2180	16350	21800

3.6 Flexibility implementation

Electric cars and heatpumps allow for a certain degree of flexibility. So called 'smart systems' can control heatpumps to turn on at the beginning of the afternoon to pre-heat a house or instruct electric cars to start charging at a certain time. These flexibility measures can mitigate extreme peaks in demand and, in combination with solar power, can maximize self-consumption of renewable energy. In order to reflect the flexibility potential this technology could unlock, a flexibility algorithm is applied to the EV-charging and heatpump data. This 'e-flows' algorithm, developed at Resourcefully, allows for different flexibility strategies [25].

E-flows accepts datasets containing electricity demand and production profiles, and calculates new supply/demand datasets with flexibility applied forming the input for the battery model. This means that perfect prediction of production and demand is assumed. While this is not completely realistic, very reliable predictions can be made for energy demand and production. Case study research from New South Wales, Australia has shown that very-short term forecasts (5 min intervals) for electricity demand have an absolute error of less than 1% [39]. Day-ahead solar forecasting based on neural network learning can be done with an Normalized Absolute Mean Error between 1-2% on sunny days [40]. E-flows uses a fitting curve to allocate demand which can incorporate a number of variables including demand, production, energy price et cetera. The curves can be equal, opposite or everything in between to the original curves, depending on the weight given to each variable. By assigning these weights, the flexibility strategy can be adapted to suit the situation or goal. For instance, when giving equal weight to peak shaving and solar self-consumption the fitting curve looks like the one in Equation (3.1).

$$fit = (-0.5 * .production) + (0.5 * .demand) \tag{3.1}$$

Note that there is a minus in front of the weight for production. This is because positive weights act as penalty factors inside the fit: the algorithm optimises by shifting demand to wherever the variable that the weight is assigned to is *minimal*. A weight of one for demand tells the algorithm to shift demand to the *lowest* points of demand. A weight of minus one for production therefore tells the algorithm to shift demand to the *highest* points of production, provided there is a surplus is production.

When peak-shaving is considered, the lowest points in the demand fit are identified and load is shifted there, taking into account the flexibility time constraint of the demand. As more demand is shifted to the low points in the fit curve, there are new, lower, points that demand should be shifted to next. The algorithm takes this into account and keeps updating the best locations to shift demand to, generating the typical peak-shaving profile on the right in Figure 3.1. The left portion of this figure shows what would happen if demand is not updated, indicated by 'demand_fixed': demand keeps being shifted to the same initial low-point, causing the formation of a new peak.

A 50/50 weight has been given to peak-shaving and self-consumption in this research. The 'e-flows datasets' are the inputs for the battery model together with the original, non-flexible, datasets. The model simulates the ED energy system for the duration of one year, for each given dataset separately. More on this in the Model Implementation Chapter.

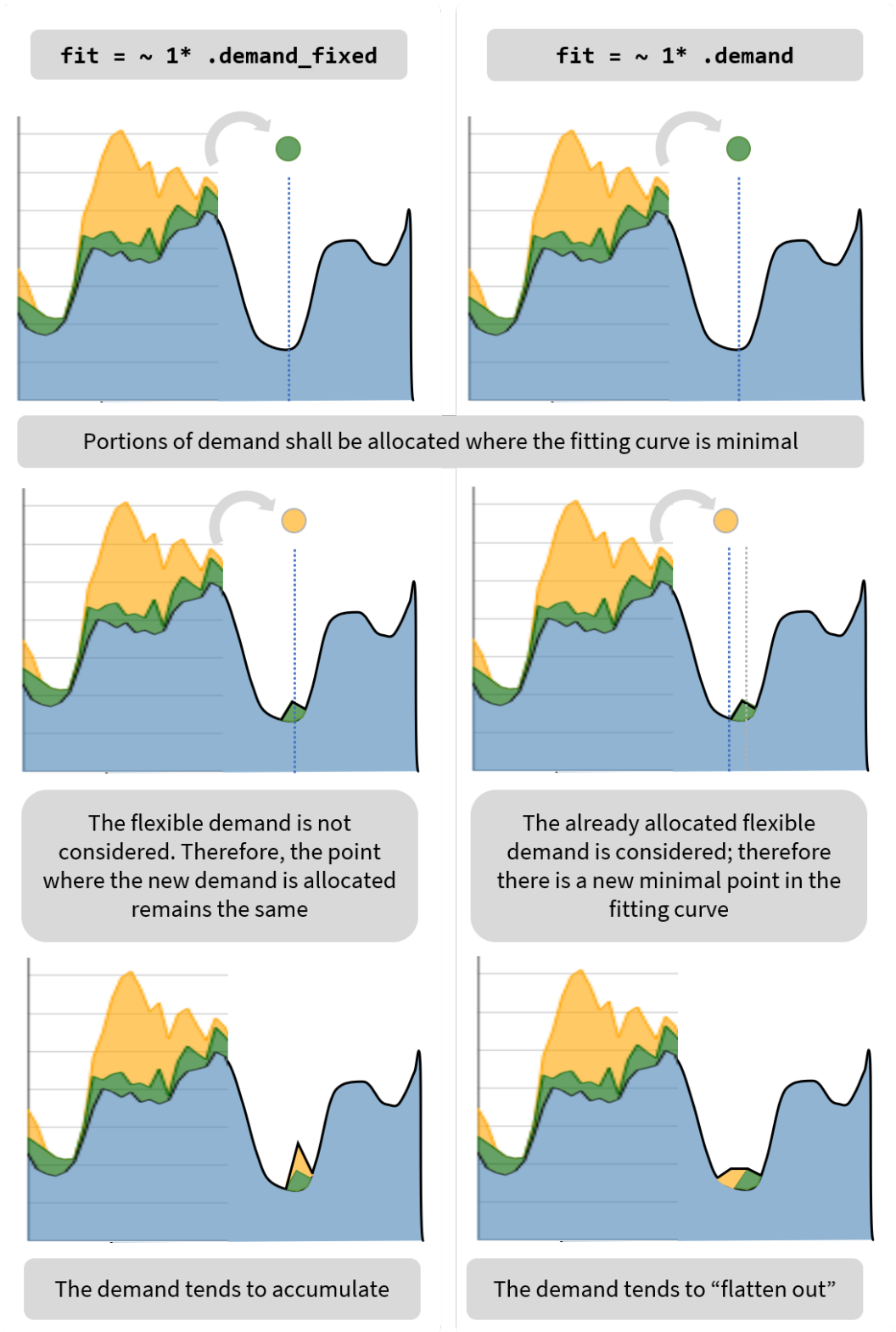

Figure 3.1: The general principle of peak-shaving by e-flows. On the right, the method by which e-flows dynamically transfers load to low demand periods by updating the minimal point. On the left, comparison with a simpler, non-dynamic demand algorithm which shows unwanted behaviour, with a new peak forming. Adapted from [25].

Flexibility in EV-charging is defined by the energy charged, the charging speed and the connection time of the session. When a car is connected for a longer time than is necessary to charge the required amount of energy, the difference between connection time and charging time is the flexibility potential. This potential is then utilized by the algorithm to shift consumption in time. Not all demand is flexible, sometimes a car needs to be fully charged and the connection time only just allows that. In this case charging cannot be delayed. The flexibility strategy can be focussed on maximizing solar self-consumption or maximizing peak-shaving, and everything in between. Because this research has a dual goal; to see how flexibility can decrease demand peaks and increase solar energy use (to decrease CO2 emissions), an intermediate strategy is chosen. This gives equal weight to shifting demand away from maximum values, and shifting demand to maximum solar production values.

E-flows defines how much flexible demand there is by categorizing it into fractions with a different flexibility potential per timestep. A contrived example is given in Figure 3.2. This is a matrix with timesteps as rows, flexibility potentials as columns and charging demand as values. The flexibility potentials are the amount of timesteps demand can be shifted to the future or into the past. For instance, when a car needs to be charged with 10 kWh in the next hour, and it charges at 20 kW, the flexibility potential is equal to half an hour, or two timesteps in the case of the 15m timesteps in this thesis. In the example below, there is no demand with a flexibility equal to 1, variable demand with flexibility 2, a fixed demand of 3 with flexibility 3, no demand with flexibility 4 and one 10 kWh batch of demand with flexibility 5. The fact that demand can be 'backshifted', so advanced in time, means that perfect prediction of demand is assumed.

```
#>       [,1]     [,2] [,3] [,4] [,5]
#>  [1,]    0 2.646572    3    0    0
#>  [2,]    0 8.402889    3    0    0
#>  [3,]    0 7.839502    3    0    0
#>  [4,]    0 9.433603    3    0    0
#>  [5,]    0 2.606275    3    0    0
#>  [6,]    0 3.868473    3    0   10
#>  [7,]    0 9.097361    3    0    0
#>  [8,]    0 8.740563    3    0    0
#>  [9,]    0 7.057992    3    0    0
#> [10,]    0 3.064047    3    0    0
```

Figure 3.2: The e-flows flexibility matrix. Adapted from [25].

For heatpump operation, flexibility can be adapted by changing the 'Time-horizon'. This is equal to the number of hours that the heatpump turn-on time can be advanced or delayed. A certain amount of energy loss is considered to account for imperfect insulation of homes. This is reflected in the 'self-discharge' variable which is set to 1% per hour. A time-horizon of 6 hours is chosen and allows the heatpump to turn on at noon to pre-heat the house of someone arriving home at 18:00. Similarly, the heatpump can turn on at 02:00 to make sure the house is heated by 08:00. A 6 hour is a realistic timeframe to shift demand for households, as it captures the period between 11:00 - 17:00, when the majority of people are at work, and between 00:00 - 06:00, when the majority of people are asleep, and will therfore not cause any inconvenience for the user. Of course, when all heatpumps turn on and off at the same time, the peak-demand issue is worsened. In fact, this behaviour occurs when optimising for solar use. While this is not necessarily bad, because the timing increases self-consumption and helps to balance the grid, if peak-shaving is also required the algorithm tries to prevent peak-forming by 'smearing out' the aggregated demand of the ED over the number of hours defined in the time-horizon. For peak-shaving, the algorithm identifies demand with the highest shifting potential, ideally demand at the top of a peak with a large Time-horizon. So, in the most extreme case of two ED residents with a differing time-horizon, both arriving home at 18:00 to a house regulated at 20 degrees C, one's heatpump could turn on at noon and heat during the day at low power, and the other's at 18:00 at high power. To reiterate, e-flows uses the demand curve for the full year as input, so effectively perfect forecasting is assumed.

In this thesis, Business As Usual (BAU) will designate non-flexible demand and Flex will designate loads where flexibility is applied.

3.7 Grid capacity

While the exact capacity of the electricity grid in the ED is not public knowledge, and the DSO does not disclose this information upon request, research on EU DSO equipment combined with the known household and commercial building figures allows for an estimation. A TSO/DSO observatory document cites an average MV/LV substation (10kV to 400V) power capacity of 4.76 kVA, or 4.76 kW, per LV consumer and a median value of 3.88 kVA [12] for the whole EU. Values for specific countries are not mentioned, so to be conservative the higher mean value of the two is chosen. Because the majority of business in the ED are denominated as "Business Services" (see Research Design chapter), not requiring electricity connections larger than 400V, this capacity per LV-consumer provides the most reliable estimation of grid capacity per consumer. The parameter depends on the typical peak average power of consumers, energy efficiency of the devices and the simultaneity factor.

It is assumed that the grid capacity will grow linearly with the households and commercial buildings in the area. As demographic information is published for the ED by CBS, it is possible to make a forecasted computation of the grid's capacity. Data on the number of households from 2013 to 2019 is used to compute a growth percentage for a prognosis (2.5%). The same growth is applied to commercial buildings, as only a current (2020) figure is published for this by the BAG Kadaster. CBS does publish the number of business registrations in the ED, but these contain a large number of home offices, obvious when comparing this number with the BAG one: 4005 vs. 1492. Including these would cause a large overlap between households and businesses. The resulting number of households and commercial buildings for the three years is multiplied with the mean transformer capacity which generates grid capacities of 51.9 - 56.2 MW, see Table 3.11. Based on this, and because grid capacity does not change in small increments, the middle value from 2025, rounded up to 54 MW is used for later computations.

Table 3.11: Estimated grid capacity in the Eastern Docklands.

Year	**Households**	**Offices**	**MV/LV Substation Capacity per LV Consumer [kW]**	**Estimated Grid Capacity [MW]**
2020	9408	1492	4.76	51.9
2025	9646	1688	4.76	53.9
2030	9890	1910	4.76	56.2
Chosen value	**54 MW**			

3.8 Plots

To give the reader an idea of the individual load profiles, six plots are given here based on data from the 2020, 2025 and 2030 scenarios. The first two are day-plots from 2030 showing the day with the highest solar generation peak of the year (29th of March) and the day with the highest heatpump demand peak of the year (14th of January). The second two show the same days with flexibility applied to the heatpump and EV-demand using the e-flows algorithm. The third two are mismatch plots, using BAU data, which show the weeks where the maximum negative and positive mismatch occurs. Mismatch is defined as the difference between solar generation and the sum of all loads at each timestep. Negative mismatch occurs when total demand is greater than supply, and vice versa for positive mismatch.

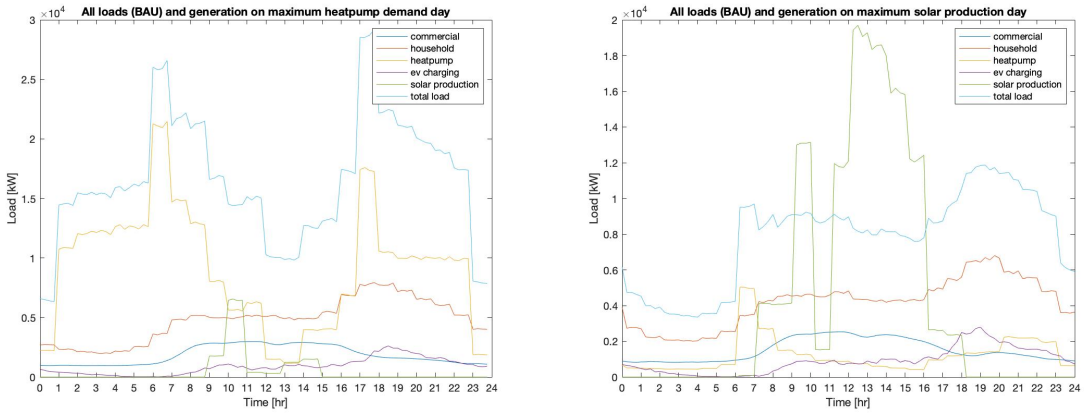

(a) All loads and solar on the 14th of January 2030. (b) All loads and solar on the 29th of March 2030.

Figure 3.3: (a) Shows all loads on the day of highest heatpump demand peak in 2030. (b) Shows the same on the day of the highest solar generation peak in 2030. No flexibility of demand is applied yet to the EV- or heatpump-demand.

The two graphs show very large differences in both heatpump demand and solar generation. Whereas heating demand peaks around 22.5 MW on the January day, it only reaches 5 MW on the 29th of March, an almost five-fold difference. Solar generation variances are relatively smaller with a three-fold difference in peaks between the two days, reaching 6.5 MW on the 14th of January and 19.5 MW on the March day. Both days show a slightly higher heatpump peak in the morning than in the evening. Heatpumps have a very large effect on the peakiness of total load (the sum of all loads without solar generation) on winter days, their peak equalling 82% of the total load peak. This effect is much smaller in March when household demand takes over as the dominant factor.

The commercial and household profiles show similar shapes for the two days, both weekdays, with the commercial profile fairly constant during working hours and the household profile peaking in the evening when lights, tv's, electric furnaces etc. are being turned on. Lighting has a large influence on household demand and causes it to rise much earlier in the day in January due to less sunlight-hours. The primarily residential nature of the Eastern Docklands was already visible in the charging profile fractions in Section 3.3. These fractions have logically translated to the EV-demand profile in Figure 3.3 where the largest peak is in the evening on both days as users plug in their car upon arriving home. Both days exhibit peaks of similar sizes - no seasonal differences are expected of course - with the 7.3% disparity in favour of the March day being attributable to inherent variations in the dataset.

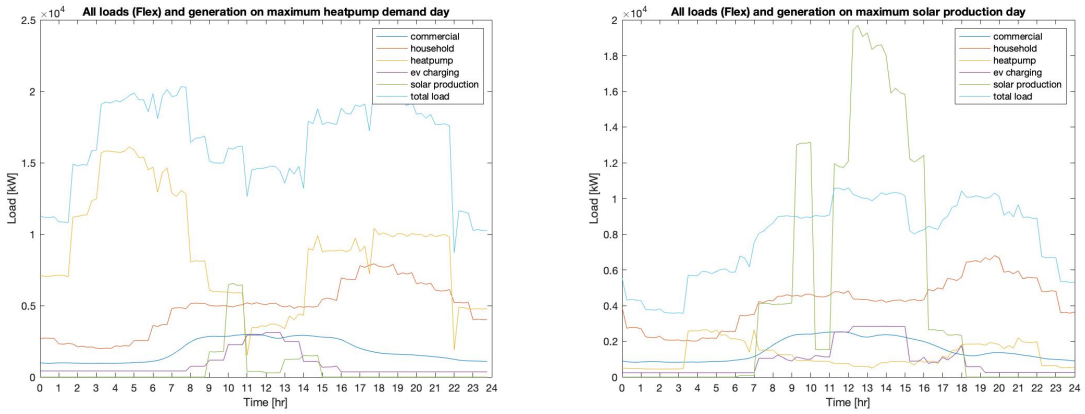

(a) All loads (Flex) and solar on 14/01/2030.

(b) All loads (Flex) and solar on 29/03/2030.

Figure 3.4: (a) Shows all loads on the day of highest heatpump demand peak in 2030. (b) Shows the same on the day of the highest solar generation peak in 2030. Flexibility of demand is applied to the EV- and heatpump-demand.

The graphs in Figure 3.4 serve as an illustration of demand response. While there were huge heatpump peaks in Figure 3.3a, these are decreased by about 30% by the e-flows algorithm in Figure 3.4a. Much of the evening load has now 'filled-in' the through in the middle of the day. The morning peak has lifted the nightly base heat demand to above 5 MW. EV-demand is almost completely shifted to midday and, while there is no solar to match it, this further decreases the evening total load peak. E-flows has less flexible demand to play with in Figure 3.4b. The small morning heating peak that occurs between 6:00 - 7:00 has been carved up and shifted to 3:00 - 6:00. A lot of the 19:00 EV-charging peak is shifted to midday and directly fed by solar, but there is still a large amount of surplus solar which has to be stored by the battery.

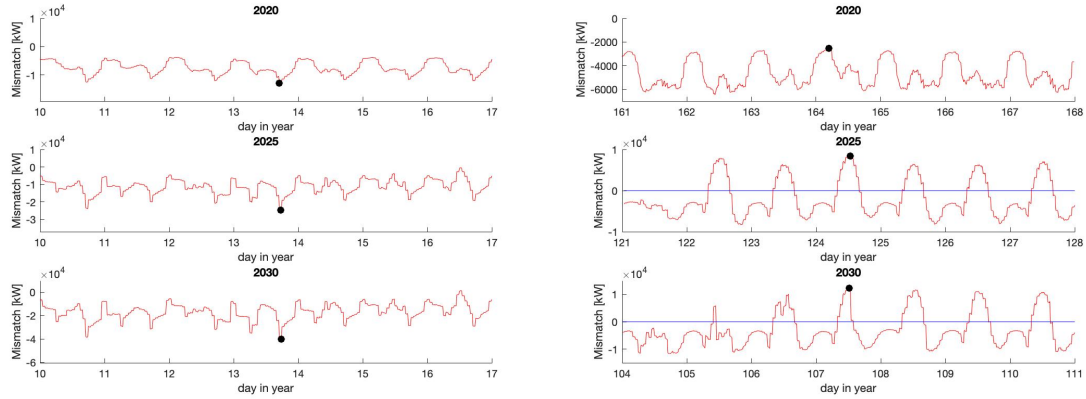

(a) Week containing the largest negative mismatch (black dot) in each scenario year.

(b) Week containing the largest positive mismatch (black dot) in 2030.

Figure 3.5: (a) Shows the mismatch in the week of each year with the largest *negative* mismatch. In this case it is the same week for each year, containing the 14th of January, owning to the heatpump demand peak which occurs on this day. (b) Shows the mismatch in the week of each year with the largest *positive* mismatch. No flexibility of demand is applied yet to the EV-demand or the heatpump demand.

The plots in Figure 3.5 show the two weeks with the largest negative and positive mismatch peak, signified with a black dot, in each year. There is distinct winter and summer behaviour and the daily shapes also differ per year. Looking at Figure 3.5a, it is clear that solar production is not sufficient in any year to sustain the energy load in this cold January week, the same week for each year because of a large heatpump peak on the 13th. Mismatch is negative on all timesteps during the week except for one midday moment on the 16th (2030), indicating that continuous grid interaction is necessary to balance demand. Heatpump loads have such a great impact on overall demand that, on most days, the smallest mismatch occurs just after midnight when heating loads subside (see Figure 3.3a), especially in 2020. Because supply and demand are better balanced in 2025 and 2030, mismatch is also pushed close to zero during the midday solar peak in these years.

Moving on to Figure 3.5b, 2020 does not have a timestep with a positive mismatch, only a least negative one which occurs on day 164 in the middle of the night when electricity loads are smallest. Little midday solar 'lumps' are visible but energy demand remains the dominant factor shaping the profiles. It is a different story for 2025 where large positive mismatches are visible due to solar, peaking at close to 10 MW in the week shown (corresponding to the 28th May - 4th of June). These energy surpluses in the middle of the day often trump the shortages in the evening, emphasizing the need for this energy to be stored. The 2030 week, corresponding to the 14th - 21th of April, starts with three capricious days where not much energy is produced, probably owning to cloudy weather in the solar dataset. However, a maximum surplus of 12.3 MW occurs on the 4th day and there is a positive mismatch on 6/7 days.

Further analysis on the absolute load peaks, their relation to the grid's capacity, the impact of demand response and results of the battery model are given in the dedicated Results chapter.

4 Model Implementation

This chapter explains how the neighbourhood battery simulation is programmed in Matlab and Simulink. First, the choice for this programming language is motivated by explaining which specific characteristics of the software package suit this research. What follows is a short outline of how the data is prepared and fed to the battery algorithm. Next, two flow-charts describe the data flow, and the logic that forms the core of the algorithm. The customizability of the model is shown by outlining all input variables. The chart is accompanied by a section that explicates in detail which calculations are performed in what order, to translate a grid-level energy mismatch into the charge/discharge demand of a neighbourhood battery, its subsequent State of Charge and grid-interaction. It is briefly stated how the Simulink output is used to do subsequent analysis in Matlab and produce the results (graphs).

4.1 The choice for Matlab and Simulink

Regular commercial data software like Excel works well when dealing with a limited amount of datapoints and limited complexity in calculations. Once matrices start to expand beyond a certain dimension size, processing must be performed on the data, and subsequent logic actions are intricate, Excel falls short of the requirements and has the tendency to crash. The load profiles used in this thesis contain data for a full year at an interval of 15m. This results in 35040 datapoints per scenario year (2020, 2025 and 2030) for each demand type (BAU, Flex). While some data preparation could be done in Excel, the calculations needed to generate the results are too complex for Excel. Matlab is a programming language in a numerical computing environment that is designed to manipulate large (matrix) datasets, plotting this data and implementing algorithms. Because building the 35040x3 matrices in this research required combining individual sets and quick visualisations are needed to verify the data, Matlab formed the perfect software tool to perform the actions needed.

After the load profiles are built, they are translated to mismatch and fed to the battery model. Here, mismatch is converted by the algorithm into battery demand. The logic implemented involves boundary conditions for charging/discharging, integration steps, and output commands to generate new 35040-element battery State of Charge and grid-interaction sets. Simulink is the designated modeling and simulation environment for Matlab. It offers a graphical programming interface that allows the user to build a model using blocks that perform certain tasks. The model can then be simulated in short run-times inside the Simulink environment. The potential for visual logic application and the seamless integration with Matlab motivated the choice to program the battery model in this thesis with Simulink.

Several papers dealing with smart grid and battery modelling have used Matlab and/or Simulink ([13, 41, 42]. While the latter two have a more technical focus compared to this thesis, they also model the electrical components of solar cell and wind-turbine, especially [13] is comparable in model complexity with this thesis. These literature examples further solidified the choice for the Matlab/Simulink combination in this research.

4.2 Preparation of model input data

Chapter 3 describes in detail what data is used for the different profiles, how it is scaled and how household, heatpump and solar data was interpolated to 15m time steps. The section on flexibility talks about how normal heatpump and EV-demand was translated into flexible demand using the e-flows algorithm and what settings are used when running the algorithm. This section explains the exact properties of the data feeding into the battery algorithm.

Each scenario (year and BAU/Flex) has one timeseries profile that feeds into its own copy of the battery model. This mismatch profile is the difference between the solar production profile and the total load, which is the sum of all loads. The normal data matrix is made into a timeseries using the

'timeseries' function in Matlab. Timeseries represent the time-evolution of a process and are used by Simulink to identify, model, and forecast patterns and behaviors in data that is sampled over discrete time intervals. The evolution from individual datasets to timeseries is visualised in Figure 4.1.

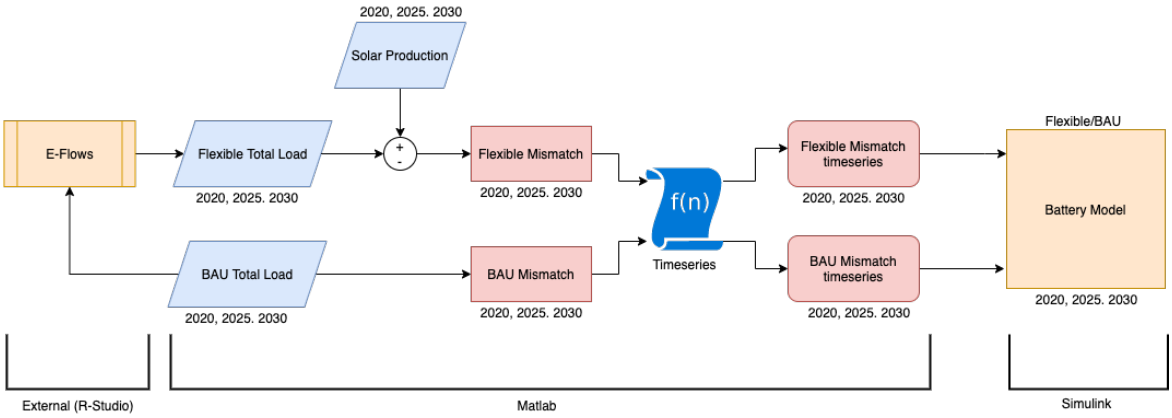

Figure 4.1: The process from data to model. The annotations designate in which programming environment each process takes place.

4.3 Model Flow Chart and Logic

This section talks through the logic in the algorithm using the flowchart in Figure 4.2. Once the mismatch-timeseries is fed into the model, a check is performed if it is positive or negative, designating an energy surplus or shortage. At the same time, another part checks how the battery demand that follows from this mismatch (charge or discharge) relates to the battery's boundary conditions: minimum State of Charge (SOCmin) and Maximum State of Charge (SOCmax). The combination between a positive/negative mismatch and the SOC of the battery creates six different situations, indicated by the yellow boxes. These situations in turn prompt four different actions in the algorithm.

1. **Situation**: Mismatch is positive and the SOC is equal to SOCmin, or between SOCmin and SOCmax. **Action**: The battery is charged.
2. **Situation**: Mismatch is positive and SOC is equal to SOCmax, or *would be* if the mismatch is fed to the battery. **Action**: The surplus energy is dumped on the grid (Grid Dump). This is recorded as grid-interaction.
3. **Situation**: Mismatch is negative and the SOC is equal to SOCmin, or *would be* below it if the mismatch is demanded from the battery. **Action**: The shortage of energy is drawn from the grid (Grid Draw). This is recorded as grid-interaction.
4. **Situation**: Mismatch is negative and the SOC is equal to SOCmax, or between SOCmax and SOCmin. **Action 1**: A second check is made if the mismatch is equal to or smaller (more negative) than the average evening mismatch (see explanation below) on the same day a week earlier. **Action 2**: If the previous check returns TRUE, the shortage of energy is drawn from the battery.

In each case, the prompted action results in an energy delivery to the energy system which resolves the mismatch in the current time step. The Average Evening Mismatch vector mentioned in **Situation** 4. is comprised of the averages of the mismatches between 17:00 - 21:00 of each day in the year. For the first week of the year the values are the same, the second week uses the values from the first week and so on. This tests the algorithm's capacity to delay energy discharge until an evening peak occurs.

When energy is discharged or charged in a real-life battery some losses occur, mostly in the form of heat. A constant loss percentage of 4% for charge/discharge efficiency is included in the model and applied following Equation (4.1).

$$P_{bat}\,[kW] = \begin{cases} Mismatch\,[kW] \;*\; \eta_{charge}\,, for\; Mismatch > 0 \\ Mismatch\,[kW] \;*\; \eta_{discharge}\,, for\; Mismatch < 0 \end{cases} \tag{4.1}$$

$$with: \begin{cases} P_{bat} = Power\; demanded\; from\; battery \\ \eta_{charge},\; \eta_{discharge} = 4\% \end{cases}$$

The percentage is based on the battery losses in [43]. The researchers from this article measured losses from the grid connection to the lithium-ion battery at different SOC's and AC voltages in a vehicle-to-grid EV situation. They distinguish between building electrical losses (charging point losses and cable losses) and EV component losses (battery and power electric unit, or charge controller). The building electrical losses also include transformer losses for the transformation from 480V to 230V which amount to an average of 8%. These transformer losses are also considered in the model in this thesis, before the mismatch timeseries is fed to the battery algorithm, and are applied following Equation (4.2).

$$Mismatch_{inverter}\,[kW] = Mismatch\,[kW] \;*\; \eta_{inverter} \tag{4.2}$$

$$with: \quad \eta_{inverter} = 8\%$$

Self-discharge is another important battery characteristic that describes how much energy a battery loses due to internal chemical processes when there is no energy charged or discharged for an extended period of time. A monthly self-discharge percentage of 5% is included in the model, based on the data for lithium-ion batteries in [44]. The energy lost is computed per 15m time step inside the SOC computation. Once a certain mismatch triggers the battery in a time step, a new SOC (SOC_t) is computed based on the energy demanded from the battery and the SOC from the previous time step (SOC_{t-1}). The new SOC again forms the input for the next SOC computation, but first the self-discharge percentage, scaled for a single time step, is subtracted like expressed in Equation (4.3). The 5% loss is divided over the number of 15m time steps in a month consisting of 30 days, 2880, amounting to a per time step loss of 0.00174%. The use of this 30 day period means that self-discharge is overstated by a negligible 0.00006% for a 31-day month. It is expected that self-discharge will not play a significant role in the total battery losses, as the neighbourhood battery is designed to store energy from midday until the evening, when it will be completely discharged. Table 4.1 summarises all losses included in the battery model, in the order they are applied in the algorithm.

$$SOC_{t-1} = SOC_t \;-\; c_{self-discharge} \tag{4.3}$$

$$with: \quad c_{self-discharge} = \frac{0.05}{2880}$$

Table 4.1: Summarisation of all losses considered in the algorithm.

Type of loss	**Magnitude**	**Is applied on**	**Is applied when**
Inverter	8%	Mismatch	Each timestep
Charge/Discharge	4%	Mismatch	Each timestep
Self-discharge	0.00174% (per timestep) (5% per month)	SOC	Each timestep

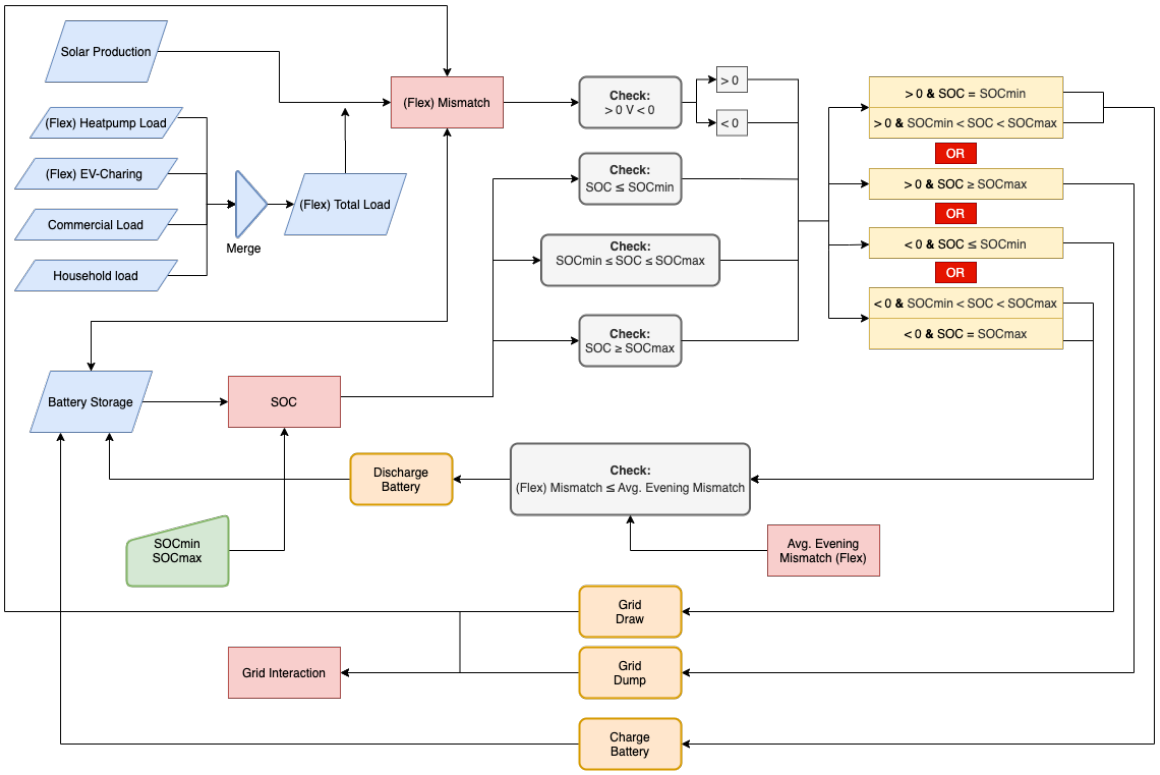

Figure 4.2: The processes in the battery algorithm. The word "Flex" between brackets means that the same process takes place for Flex load and mismatch as for BAU.

4.4 Model output

Running a simulation of the model produces two important outputs: grid-interaction and Battery State of Charge (SOC). These are the input for further analysis in the Matlab environment. This section explains how they are processed to produce the variables that are presented in the results.

Grid-interaction
This variable describes the amount of energy dumped on or drawn from the grid. It can be the result of the two situations described in the Model Flow Chart section: 1. There is a positive mismatch and the battery is full (dump). 2. There is a negative mismatch and the battery is empty (draw). The simulation is run for 50 different battery sizes, running from 0 MWh to 140 MWh, generating 50 different grid-interaction profiles. This allows for analysis of the evolution of other metrics over increasing battery sizes.

In the Matlab model script, grid-interaction is split into draw and dump. These separate datasets are then used to compute the average and peak grid-draw and dump for the full year and for the battery active period. Grid-draw is also input for the CO2 emission calculation. Emissions are calculated by multiplying the interpolated Marginal Emission Profile with the 15m grid-draw data to end up with a 15m CO2 emission profile in kg/kWh. To make the CO2 over Battery size plot, the emissions are summed for the whole year per battery size, generating 50 different profiles for each year and BAU/Flex, or 300 profiles in total. Grid-draw is also used to build the average evening mismatch profile described in the Model Flow Chart section. Lastly, grid draw is used to compute the cost of grid-energy and balancing revenue in the Financial Results section, by multiplying the vector with published day-ahead prices. More on this in the Results chapter.

Grid-dump is used to compute self-consumption by subtracting it from the total solar production, generating total consumption, and dividing the product by total production, see Equation (4.4). Again, 50 grid-dump profiles generates 50 self-consumption profiles. Using self-consumption, the CO2

saved by solar consumption can be computed by using the fact that each kWh of solar consumed is a kWh less that has to come from the grid. The CO2 emission profile from the previous paragraph is used for this effect. The CO2 save profiles are the basis for the CO2 emission section in the Results.

$$Self\text{-}consumption = \frac{Total\ consumed\ production}{Total\ production} \tag{4.4}$$

Autarky is another metric that comes from the grid dump profiles. It is the measure of self-sufficiency of a renewable energy system. So, what fraction of consumption is provided by (solar) production. The definition is expressed in Equation (4.5).

$$Autarky = \frac{Total\ consumed\ production}{Total\ energy\ consumption} \tag{4.5}$$

Battery State of Charge (SOC)
SOC is a measure of the energy content in the battery at each given time step. The change of SOC from one time step to the next expresses the energy going into or out of the battery. By constructing a vector of SOC differences over the 35040 time steps in a year, and relating this to the storage capacity, an battery energy (or power) flow vector can be made. This forms the basis of computing neighbourhood balancing revenue where ingoing energy is multiplied with a certain margin per kWh. More detail is given in the Financial Results section of the Results chapter. The definition of the energy flow vector is given in Equation (4.6).

$$E_{bat}\ [kWh] = \sum_{1}^{35040} (SOC_t - SOC_{t-1})\ *\ C_{bat} \tag{4.6}$$

$$with: \begin{cases} E_{bat} = Energy\ flow\ through\ the\ battery\ per\ time\ step \\ C_{bat} = battery\ capacity\ [kWh] \\ SOC_t = State\ of\ Charge\ in\ the\ current\ time\ step \\ SOC_{t-1} = State\ of\ Charge\ in\ the\ previous\ time\ step \end{cases}$$

SOC is also used to calculate the number of cycles the system goes through, which is a statement of its degradation. One cycle is equal to fully charging and discharging the battery. The amount of yearly cycles is computed by first extracting the positive values (energy charged) from the energy flow vector. Only the positive (or negative) values suffice, because all energy charged is also discharged (the battery is empty on 31/12 00:00) and, as explained above, one battery cycle involves both. The positive values are summed, equalling the total amount of energy that went into the battery for one year. Dividing this total by the battery capacity produces the cycles per year. This calculation is expressed in Equation (4.7).

$$Cycles = \sum_{t=1}^{35040} \frac{E_{bat}(t)}{C_{bat}}, \quad for\ E_{bat}(t) > 0 \tag{4.7}$$

5 Simulation Results and Analysis

This section presents the results gathered through procedures detailed in the Research Design section and is divided between a technical section and a financial section. To answer the four sub-questions and subsequently the main research question, the following analysis steps are followed. Firstly, extreme situations during the year are defined. Extreme situations are times where either demand or supply of electricity show their maximum peaks. These extreme peaks could impact the stability of the grid and necessitate grid improvements. These values are related to the grid capacity, which is estimated by multiplying the number of households with the average grid capacity per low-voltage user. It is also of interest to see how flexibility performs during these situations by making a comparison between the scenarios with and without flexibility. The section continues with results from the battery model, showing specifically how the size of the system influences average evening peaks, midday solar peaks and autarky and self-consumption. Based on these metrics a battery sizing is done.

The second aspect being investigated is the impact that a battery system has on decreasing the overall CO2 emissions of the ED. A Marginal Emission Factor (MEF) [45] is used to compute the CO2 emission of each MWh drawn from the grid. The use of the MEF instead of an average emission factor is fairly new in literature. Using it produces a more reliable estimation of CO2 savings by adding renewable energy. This is because the conventional energy generation which is replaced by renewables in each specific settlement period comes from facilities operating at the (price-setting) margin, and is not evenly distributed over all generation facilities. Typically, these marginal facilities have a higher than average CO2 emission per produced energy unit. Including the MEF in emission calculations therefore produces higher and more realistic CO2 emission savings. This MEF profiles used in this research are based on the energy mix in the Dutch grid at each hour. When more solar energy is used, because the battery can store and supply it at the right times, less energy is needed from the grid and thus CO2 emissions decrease. An assessment is subsequently done how this decrease relates to CO2 reduction goals from the municipality.

Thirdly, the business case surrounding the neighbourhood battery system is evaluated. The Dutch government has compensated people exporting energy to the grid with a price per kWh equal to the electricity price they pay to their energy-suppliers (including taxes) up until now, but will stop doing so after 2030. This so called 'saldering', or balancing, was a major source of income for PV-owners and therefore contributed significantly to the business case for solar panels. When this ends, the compensation for private energy producers will solely come from energy suppliers that have to pay 80% of the variable electricity price to customers feeding electricity into the grid, which is much less than the previous full-price compensation. This means the business case for a neighbourhood battery performing 'neighbourhood balancing' becomes more attractive, especially when the compensation price would be somewhere between the variable energy price and the previous state-funded balancing price. This form of a local energy market has been mentioned in other literature as a very promising future value stream [46]. Neighbourhood balancing would compensate the energy producers in the neighbourhood for the energy they feed into the battery during the day, and charge consumers the commercial price for the electricity they consume at peak hours. This way the households receive a higher price for their electricity, the battery system earns a compensation per transaction and there is certainty that locally produced energy is also used locally. The benefit of neighbourhood balancing at different prices is investigated and compared to current and planned future compensation policies. In addition, an overview is given of other grid services and their potential revenues. Using these figures, the payback periods for the battery system at the previously chosen size and cost are computed.

Table 5.1: Nomenclature in this section. Explains all terms in Table 5.2.

Term	Explanation
Total load	The sum of all energy demand profiles
BAU	Load without flexibility applied to heatpumps and electric vehicles
Flex	Load with flexibility applied to heatpumps and electric vehicles
Commercial	Load from the commercial demand profile
Household	Load from the household demand profile
Heatpump	Load from the heatpump demand profile
EV-charging	Load from the EV-charging demand profile

5.1 Technical Results and Analysis

5.1.1 Peak Loads and Production

Table 5.2: Comparison of BAU and Flex peaks for each type of demand and production.

Type of demand	Year	BAU [MW]	Flex [MW]	Difference	On date and time
Total load	2020	12.81	11.23	-12%	14/01/2020 17:15
	2025	24.60	16.95	-31%	14/01/2025 17:15
	2030	40.54	27.16	-33%	14/01/2030 18:00
Average peak	2020	6.99	6.83	-2.9%	/
	2025	7.30	6.88	-5.8%	/
	2030	9.26	8.06	-13%	/
Commercial	/	3.09	/	/	14/12/2020 11:45
Household	/	8.66	/	/	18/12/2020 18:00
Heatpump	2020	3.02	2.13	-29%	14/01/2020 07:00
	2025	15.11	10.41	-31%	14/01/2025 07:00
	2030	29.72	21.11	-29%	14/01/2030 06:30
EV-charging	2020	0.50	0.05	-90%	11/09/2020 18:30
	2025	1.20	0.77	-36%	24/04/2025 18:00
	2030	3.17	1.64	-48%	15/07/2030 17:45
Solar production	2020	1.975	/	/	27/03/2020 12:30
	2025	14.78	/	/	27/03/2025 13:00
	2030	19.69	/	/	27/03/2030 12:30

Table 5.2 shows all peaks in demand and production on their relevant dates. The BAU column gives the peaks without flexibility in demand. The Flex column shows the same peaks when flexibility of demand is applied, allowing a direct comparison. Additionally the peaks in solar production are given. Starting with solar, all peaks occur on the same day in march around midday. The dates are the same because the original production dataset is based on the installed capacity in 2030 and scaled down to 2025 and 2020 levels. There is a slight variation in the times because of the random interpolation around the original hourly values. All peaks correspond to around 90% of installed capacity. Comparing the peak times of solar with those of the loads, a high degree of simultaneity is not expected as most load peaks occur in the morning or evening, except for the relatively small commercial peak which occurs in winter (see explanation below).

Because the number of heatpumps and charging sessions increases over the years, it is no surprise that the peak demands follow suit as is visible in Table 5.2. What is more interesting however is how flexibility in demand decreases (or increases) these peaks. Starting with the total load peaks, the flexibility algorithm shows a strong capacity to decrease these extreme values by 12 to 33%. Flexibility demonstrates a larger impact in later years because of the increase in heatpump and EV demand. Worth noting is that all peaks occur on the same date and around the same time.

The dates of the heatpump peaks give away the cause; the 14th of January is an especially cold day in the dataset where the heatpump demand is derived from.

The Flex values in Table 5.2 are from the same date and time as the BAU peaks, in order to compare the two, but they are not the absolute maxima for the flexible demand profiles. These are given in Table 5.3 along with the dates of occurance and compared to the BAU values at these moments (not displayed). The decreases are comparable with those on the dates of the BAU peaks. The dates of occurrence are now spread across four days in January because of cold outside temperatures. These peaks prove that the flexibility algorithm shifts demand as desired and does not create higher peaks at other times.

Table 5.3: Peaks of Flex total load, compared to BAU at the moments of occurance.

Type of demand	**Year**	**Max Flex [MW]**	**Difference**	**On date and time**
Total load	2020	11.36	-11%	10/01/2020 17:15
	2025	18.36	-25%	11/01/2025 18:45
	2030	27.36	-33%	14/01/2030 08:00

Moving down in the table to commercial and household demand peaks, their dates and times correspond to lunch and dinner times in winter respectively when a substantial amount of electric cooking stoves are turned on. The peaks probably occur in winter because of the higher lighting demand (darker days). The datasets could also contain an amount of electric heating. Offices typically have electric climate systems which heat during winter. The household dataset is from 2014 when heatpumps were not prevalent in homes, and does not specify heating technology, but the existence of electric heating in a group of 10.000 households cannot be ruled out.

Heatpumps develop as the dominant factor in demand from 2025. The peaks all occur on the same day and around the same time, due to an outside temperature of -15C in the dataset that the demand is based on. Because the data was interpolated from hourly to quarterly by adding intermediate datapoints that differ randomly from the hourly values by 2%, the peak values can differ by a maximum of 3 timestamps from the original hourly peak-value. This is acceptable because it does not detract from the illustrating value of the absolute peaks and the relative impact of flexibility. The e-flows algorithm manages to decrease the heat pump peaks by around 30% for each year.

EV-charging peaks show the highest percentual decrease compared to the BAU scenario. The 2020 scenario grabs the attention with a percentual decrease of 90%. This can be explained by the solar-optimisation/peak-shaving parameter settings of the flexibility algorithm and the relatively low number of EV's in 2020. The algorithm is set to weigh peak-shaving and solar-use equally. This means that if the connection time of the charging session allows it, the session will be moved towards maximum solar production hours i.e. around noon. As more charging is moved there, the algorithm starts to spread the demand more evenly from noon to evening. Because there is still a relatively low amount of demand to move in 2020, there is 'space' for this demand around noon causing it to be transferred away from the evening, and the peak subsequently lowered more than in 2025 and 2030 when there is more demand.

Comparing the EV peaks in 2025 and 2030, one observes a larger peak reduction in the later year which can be explained by recalling the charging speed fractions in Table 3.8. The increase in 11 and 22kW charging mean that cars are charged faster, but connection times predominantly stay the same for all profiles (home, worktime, short-stay). While it could be said that short-stay chargers may base the time of their activities on the charging time of their EV's, sleeping and working hours certainly do not change with faster charging. So, as the time required for charging decreases there is more potential to move the activity in time. The demand is spread out more and peaks decrease, explaining the larger percentage-decrease in 2030 compared to 2025.

However, it is remarkable that the *absolute* peaks of flexible EV demand, given in Table 5.4 are higher than in the BAU scenario. This is a side-effect from the maximisation of self-consumption, when demand is shifted to maximum solar production times (around noon) by e-flows. 2020 shows the

highest increase due to a low absolute demand (easier to shift). To assess if this is worrying behaviour from the flex algorithm, it helps to compare the *total load* peaks at the moments of the Flex and BAU EV-demand peaks, displayed in Table 5.5. If the Flex total load peaks are lower, there is not an adverse effect where demand flexibility is creating higher grid peaks elsewhere in the day/year. In 2020 the Flex total load peak is higher than BAU at the time of the EV charging peak. However, it should be noted that the 2020 EV Flex peak occurs in February, whereas the BAU peak occurs in September when there is less heat pump demand. The possible adverse effects of flexibility should thus be judged with the 2025 and 2030 peaks, which are both lower by 3% and 27% respectively. The 2030 Flex peak even occurs in April, which has a substantially higher heat pump demand than during the BAU peak in July, proving that the flexibility algorithm does not create higher total load peaks in comparable seasonal circumstances.

Table 5.4: Increase in Flex EV-charging peaks compared to BAU

Type of demand	**Year**	**Max Flex [MW]**	**Difference**	**On date and time**
EV-charging	2020	1.55	210%	28/02/2020 12:45
	2025	2.22	85%	21/05/2025 11:30
	2030	3.97	25%	12/04/2030 12:15

Table 5.5: Comparison of total loads on date of maximum EV-charging.

Type of demand	**Year**	**Demand [MW]**	**Flex [MW]**	**Difference**	**Flex date and time**
Total load	2020	6.86	9.71	42%	28/02/2020 12:45
	2025	7.32	7.10	-3%	21/05/2025 11:30
	2030	9.83	7.14	-27%	12/04/2030 12:15

Grid Capacity
Electricity grids in the Netherlands are built with a certain redundancy, typically twice the required capacity based on the combined connections of industrial, commercial and household users. As mentioned in the introduction, new technologies like datacenters and electric cars have been asking more capacity of the grid in the past years. This means the two-fold redundancy has been increasingly let go by DSO's [47]. Comparing the grid capacities with the peak loads and production in relevant years, it is clear that this leniency is also a requirement for the future if costly grid reinforcements are to be avoided.

In terms of production, the solar capacity peaks reach a maximum of 36.5% of grid capacity in 2030, staying within the two-fold redundancy rule. The total load peak in 2020 is still well within the limits at 23.7% of grid capacity for BAU (see Table 3.11) but 2025 shows a BAU load peak coming close to the redundancy limit at 45.6% of capacity. The effectiveness of flexibility is proven by the Flex peak equalling only 31.4% of capacity. The 2030 peaks pose the biggest threat to grid stability at 75.1% of capacity for the BAU scenario which surpasses the historically desired two-fold redundancy. Flexibility has the highest effectiveness here, reducing the peak with 33% and reaching only 50.3% of total capacity.

5.1.2 Battery Operation

This section will present and analyse the results of the battery model. It will go over the most important results for 2025 and 2030 using graphs that show the two years together as much as possible. The effect of time-shifted demand on the workings of the battery is reflected by including both BAU and Flex traces. As mentioned earlier, 2020 is not included because of the low solar penetration in this reference year. To reiterate, the dual goal of the model is to increase solar energy use and decrease evening demand peaks and as mentioned in Chapter 4. A decision was made to

focus on the evening peak because this is typically the highest peak of the day and because decreasing the morning peak requires nightly charging, using (mainly non-renewable) grid energy.

The section starts by showing the results of a battery test. In this test, an artificial demand profile with a block shape is fed to the system to see if it responds as expected. After this is demonstrated, an example day is chosen to compare grid-interaction for Business as Usual, Flex and Flex + Battery output data. This demonstrates if demand flexibility application and the battery system influence energy exchange with the grid as desired; decreasing grid draw and dump. Then, the contrast between winter and summer days is illustrated. Two plots containing State Of Charge (SOC), mismatch and grid interaction traces show the functioning of the storage system for two three-day periods: one in June, falling inside the 'battery active period' and one in November, falling outside this period. The active period runs consecutively from day 78 to day 260 and is equal to the 50% of the year with the highest cumulative positive mismatch. A positive mismatch generates surplus energy that can be stored for later use by the battery and allows it to perform peak shaving. A third plot shows the contrasting impact of demand flexibility in the two periods. After this, peak shaving and CO2 reduction results for the full year, and battery active period, are presented and related to the size of the battery system.

Battery Test
The battery test simulation is performed with the parameters in the table below. A mismatch profile, which forms the input of the model for this test, has been designed to answer two questions: 1. Is the energy balance correct when running the model? I.e. do the mismatch energy amounts carry over to the simulation results. 2. Does Simulink execute the tasks in the model in the correct order, generating the desired battery system behaviour? If both questions are answered positively, it can be assumed that the model also works as designed when given normal demand and production profiles. The profile stays at a constant 9 MW for three hours, or 12 timesteps, and then switches to a constant negative mismatch of -9 MW for the same duration. This is repeated for one year to see if the model performs as predicted for all 35040 timesteps. Because the battery has a minimum SOC of 20% and a maximum SOC of 80%, it can use 60% of its storage capacity, which means that at a total capacity of 45 MWh, the *effective* capacity is 27 MWh. It thus follows that the battery should be fully charged after the three hours of positive mismatch, and fully discharged after three hours of negative mismatch. Consequently, grid-interaction should be zero because mismatch switches to positive in the immediate timestep after the battery is empty. When the model operates on regular demand data, a mismatch threshold is implemented to delay battery discharge until the evening peak. For this test, the threshold is set at 0 MW to see if discharge starts immediately when mismatch switches signs.

Table 5.6: Properties of the data and model for the simulation in Figure 5.1.

Battery algorithm properties		
Battery Storage Capacity	45 MWh	
Transformer efficiency	100%	
Charge efficiency	100%	
Discharge efficiency	100%	
Min/max SOC	0.2/0.8	
Mismatch profile properties	Load	Duration
Positive	9 MW	3 hrs
Negative	-9 MW	3 hrs
Repeated for the duration of one year		

The graph in Figure 5.1 shows the result of the test simulation for eight three-hour periods, or 24 hours. Looking at the SOC trace relative to the mismatch, it is clear that the battery is completely charged (at 0.8 SOC) after three hours of positive mismatch and completely discharged (at 0.2 SOC) after three hours of negative mismatch. The start of the first positive period exactly coincides with a vertical grid-line. At the same line, SOC is at the minimum level and starts to increase to the right of this line. This demonstrates immediate charging at positive mismatch. The end of the third positive period exactly coincides with another vertical grid-line. At the same line, SOC is at a peak and starts to decrease in the next timestep. This indicates that the battery model starts to discharge immediately when mismatch crosses zero towards negative. Lastly, zero grid-interaction for the entire 24 hr period confirms a correct energy balance and indicates that the battery model evaluates mismatch and SOC at the same timestep, ensuring an immediate response of the system. These test results answer both test questions posed above positively, and therefore prove the correct functioning of the battery model.

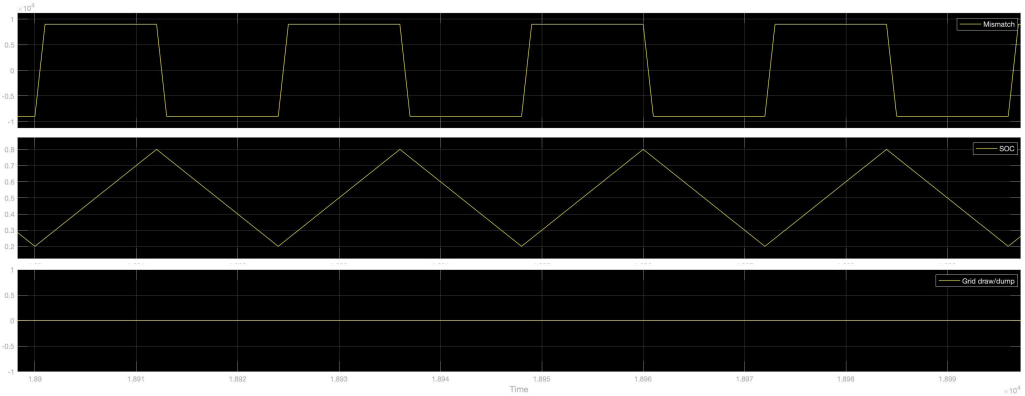

Figure 5.1: Simulink plot showing a Mismatch block-profile, and the resulting SOC and Grid-interaction.

Grid-interaction Comparison

An important question to answer is how the e-flows flexibility algorithm works in conjunction with the battery model. The way they are implemented, e-flows does not take the battery into account, but the battery does in effect take e-flows into account because the demand profiles are 'made flexible' before they are fed into the battery algorithm. However, this research is not an exercise in optimizing a specific combination of flexibility and storage, that is out of its scope. It does aim to show how these two likely additions to our future energy interface influence each other. Depending on the way that demand response and storage will be implemented in the real world, situations will probably occur where a neighbourhood battery has to deal with the flexible heatpump demand of a large apartment building, which does not necessarily base its load-shifting decisions on the solar energy feeding into the battery because it focuses, for instance, on minimizing electricity cost. More on this in the Discussion and Conclusion.

To establish if demand response and the battery system perform as designed and desired, it is useful to see how grid-interaction changes from Business As Usual (BAU) demand, to demand where flexibility is applied, to demand where flexibility ánd the battery algorithm are combined. Grid-interaction occurs when electricity is drawn from the grid (grid-draw) or is supplied to the grid (grid dump). The mismatch between supply and demand determines if grid-draw or dump is needed. If supply (of renewable energy) is greater than demand, mismatch is positive. If vice versa, mismatch is negative. The three traces in Figure 5.2 show the grid interaction on the 31st of March 2030 for BAU-demand, Flex-demand and as output of the battery system. To clarify, BAU demand and Flex demand both represent the total load profile for the Eastern Docklands, but for Flex demand heatpump- and EV-data have gone through the e-flows algorithm where flexibility of demand is applied. Grid-interaction for BAU and Flex is equal to the mismatch, incorporating the inverter efficiency, which is computed by subtracting demand from the solar production profile. The third trace is the result of running the battery algorithm with Flex demand as input. The 31st of March is chosen because it has enough

solar production to fully utilize the battery and also enough heatpump demand to clearly demonstrate its use. The simulation run uses a 45 MWh battery, based on the sizing in Section 5.2.

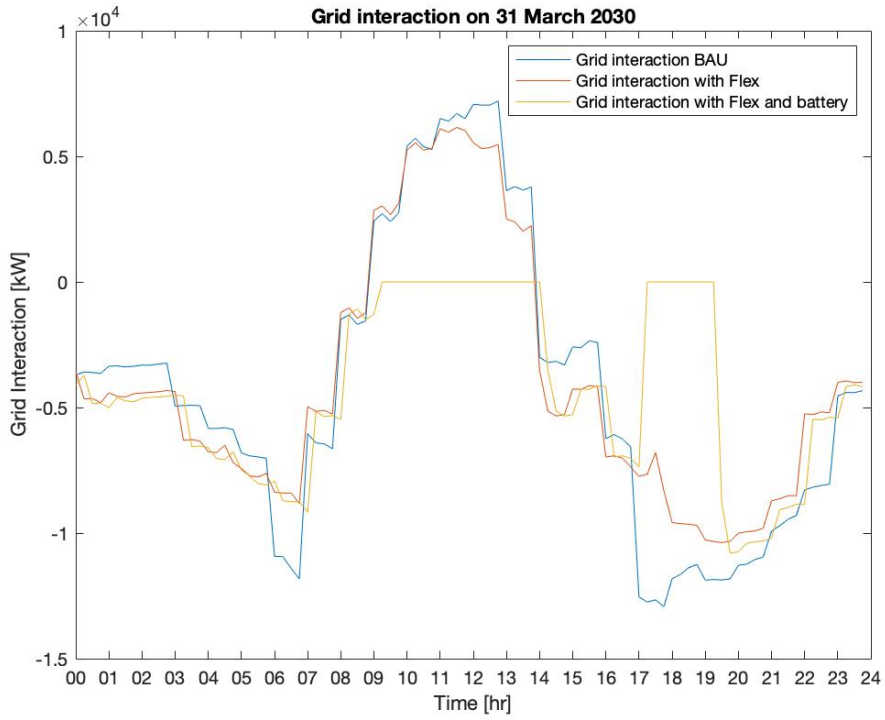

Figure 5.2: Graph showing the grid-interaction on the same day, for three levels of smart energy technology implementation.

Moving through the day, and starting by comparing the BAU and Flex traces, the first obvious difference is a higher Flex load at night: this decreases strain on the grid in the morning. The result is a much lower grid draw peak. At the peak-production hour around noon, demand flexibility manages to decrease grid dump significantly by shifting demand there, providing a higher self-consumption. From 14:00-16:00, flexible load again surpasses non-flexible load to generate a lower grid draw evening peak. To take it out of abstraction, this is electrical heating by heapumps being advanced in time. EV-charging for home-profile consumers is not advanced and therefore not involved in increasing afternoon load, but shaves the evening peak by being *delayed* until the night. The demand of work-chargers (charging during the day) is shifted to midday.

The battery tries to minimize grid-interaction. Grid-dump is prevented by storing solar energy and grid draw peaks are kept to a minimum by discharging this energy at the right time. Peak shaving is made effective by holding energy delivery until the mismatch between supply and demand reaches a certain threshold, equal to the average mismatch between 17:00 - 21:00 on the same day one week earlier. This behaviour is clearly visible in Figure 5.2. The battery trace follows the Flex trace (with a 1-timestep delay, an artefact of outputting from Simulink to the Matlab workspace) until the y-axis zero crossing. Here a positive mismatch occurs - solar production is greater than demand - and while in the BAU and Flex scenarios this electricity is dumped on the grid, the battery trace has zero grid-interaction as all surplus is stored. Once mismatch becomes negative again, the battery trace rejoins the Flex trace until the mismatch threshold is reached and the battery starts to discharge. At this point grid-interaction jumps to zero as all electricity demand is provided by the battery. Once storage is depleted, the grid needs to provide the necessary electricity again and the battery trace rejoins the Flex trace. The battery system has decreased the evening peak from 13 to 11 MW, a difference of 20%.

Seasonal Comparison
Solar production varies a lot throughout the year due to seasonal weather variations. This means that during spring and summer the battery system has more energy to work with and therefore a higher effect on grid-interaction. To illustrate this, two three-day sets of battery output are shown in Figures 5.3 and 8.6. The different traces show the mismatch, SOC, grid-interaction, total load and solar production at each timestep, for a simulation run with a 45 MWh battery. Demand and solar production profiles from the 2030 BAU scenario are used as input for the simulation. The data corresponds to three days in June, with high solar production, and November, with low solar production. A third figure only depicts total load and solar production for the same three-day sets, but with demand flexibility applied and shows the combination of battery and demand response in different seasonal circumstances.

The red vertical lines in Figure 5.3 at the onset of a SOC decrease indeed confirm that energy delivery does not start immediately when mismatch is negative. There already is a clear delta between the total load and solar production lines, mismatch is between 5 MW and 7.5 MW below zero, once SOC reduces. Grid interaction is zero from the red line point while the battery delivers its energy. The last June day might fool the viewer in thinking that SOC decreases at the zero-crossing of mismatch, but the total load trace shows that a sudden decrease in solar production causes mismatch to cross the threshold needed to activate the battery.

The flattening SOC curve at 80% shows that a 45 MWh battery cannot store all available solar energy during peak production times. This surplus energy is 'dumped' on the grid, indicated by a positive grid interaction trace. While this may feel intuitively not right in light of maximizing self-consumption, Figure 5.9 shows that the battery must be 2.5 times larger to completely eliminate grid dump. This would not make economic sense, as will be demonstrated in Section 5.2. One way to decrease the magnitude of dump or draw peaks is to decrease the charging/discharging rate of the battery. Taking charging as an example, slowing this down spreads out charging over the positive mismatch period and thereby 'shaves off' a portion of the *entire* positive mismatch curve. When done right, the energy charged is still the same as with charging at the same power as the mismatch. A disadvantage of slower charging is that in real-life it is unknown if potentially there is a cloud coming that will decrease solar production for a period of time. When the battery has been charging at a lower rate until that point, energy will have been wasted. The same thing holds on days without any cloud cover but with less sun-hours and lower solar intensity. Here you would want to charge at full-speed because the battery will not be full without doing so, and consequently charging at a lower speed would have also wasted energy. Slower discharging spreads out the available energy over the negative mismatch period and thereby shaves off a portion of a broader piece of the curve. The disadvantage of this is that when a large power peak comes the battery is not capable to deliver the required power, because its discharging rate is limited. This shows that the optimal charging and discharging speed depends on the situation and that ideally it could adapt to the (predicted) circumstances. This level of complexity has not been implemented in the model but could be a good avenue to explore for further research.

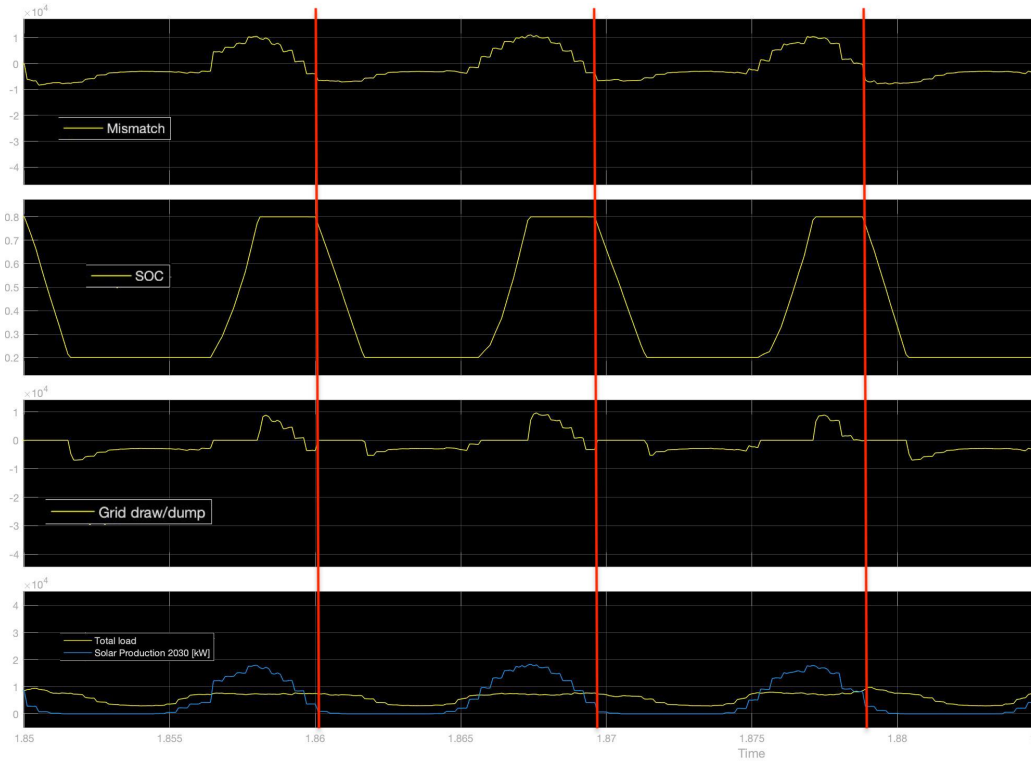

Figure 5.3: Battery operation plot showing how the battery responds (in terms of SOC) to a mismatch in supply and demand during three days in June, falling in the battery active period with high solar production. The red lines indicate the start of energy delivery by the battery once a certain mismatch threshold is reached. Grid interaction is electricity going into or coming from the grid. The x-axis units are the 15m timesteps x 10^4. The y-axis units are in kW.

Much less solar production and more electricity demand can be observed during the three November days in Figure 8.6. Production peaks at just above 10 MW on the first day in the graph, whereas the June peaks approach 20 MW. A difference in peak width also indicates a smaller amount of hours in which energy is produced. The total load trace has two distinct peaks in the morning and evening because heating and lighting are turned on, bringing the evening total load peaks to a value of about 20 MW on each day, compared to a maximum of 10 MW on the third June day. Higher demand usurps supply completely, leaving the battery effectively powerless to perform peak shaving. As a result the SOC only slightly leaves the minimum level of 20%. However, this is an opportunity to put it to work on other grid services like frequency control or congestion services. While solar production is normally less in winter, wind energy with an intermittent character peaks during the colder months. This intermittency causes frequency derivations and endangers grid stability, which is why an Frequency Containment Reserve market is launched where flexibility providers can bid their capacity to accept or deliver energy when needed. While no wind energy is modelled in this thesis research, the battery will be connected to the energy grid and as such could be used for these additional services. More information on FCR and congestion management, and their revenue potential, is given in the Financial Results section.

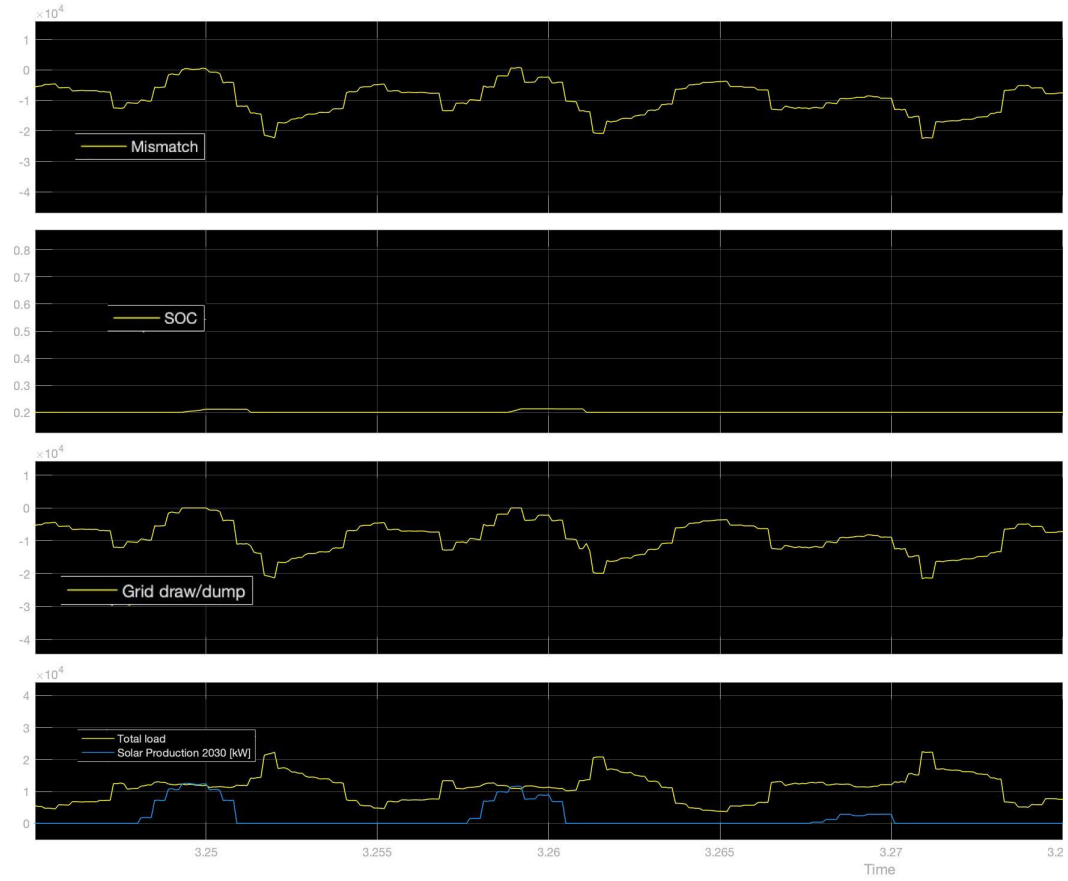

Figure 5.4: Battery operation plot showing how the battery responds (in terms of SOC) to a mismatch in supply and demand during three days in November, falling in the battery inactive period when solar production is low.

To further show the symbiosis of Flex and battery, and to see the shifting of loads from day to day, the total load and production curves from the earlier three-day sets have been combined in Figure 5.5. The upper graph evidently depicts three November days with its relatively low solar production. What stands out compared to Figure 8.6 are the non-existent morning and evening load peaks. The evening heating peak has been back-shifted to the afternoon which results in a load trace that is slightly higher than production, meaning production is completely used up. This removes the very small energy amount that went into the battery without demand flex and means that the complete capacity is available for other grid services. The morning load is back-shifted to the night which has no effect on battery operation, because this peak occurs before any solar production, thus before the battery can come into play. Some fore-shifted evening EV-load joins the back-shifted morning load of the next day in the middle of the night, raising the nightly minimum load.

The bottom graph in Figure 5.5 shows the June days. Almost no difference is visible compared to the BAU trace, there is not enough heatpump demand to shift and the relatively small EV-demand does not have enough impact on the total load. This indicates that flexibility of demand has the most impact on cold days when heatpump demand is high. Conversely, the battery system works best during sunnier (warmer) days when there is solar energy to store. So, when taking a year-round view, demand response and battery storage complement each other nicely with peak-shaving.

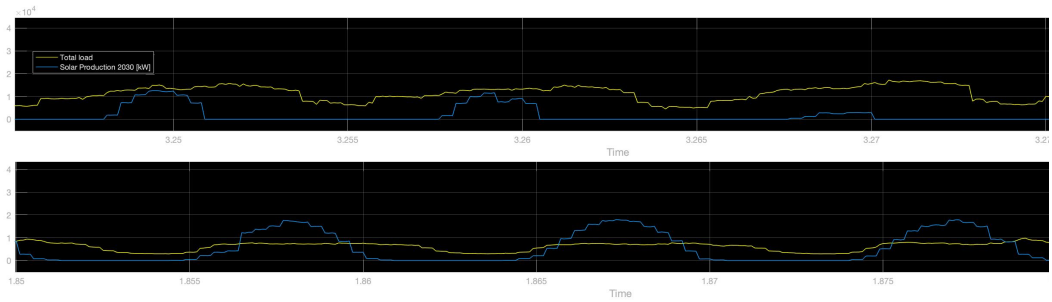

Figure 5.5: Battery operation plot during the same two sets of days, June below November from a simulation run with flexibility of EV- and heatpump-demand applied.

Peak shaving and grid interaction: Full Year

This section starts with an analysis of the peak power exchanges with the battery, before the rest of the results are related to storage capacity. It is important to know these power peaks when sizing the battery because satisfactory operation not only depends on how much energy can be stored in the system, but also *how fast* it can respond to charge/discharge requests. To see the power requirements of a battery the peak battery charge/discharge power at an increasing storage capacity is plotted in Figure 5.6. This is a relevant comparison because as more storage capacity is available, more energy can also be stored or discharged, increasing the likelihood of larger power exchanges.

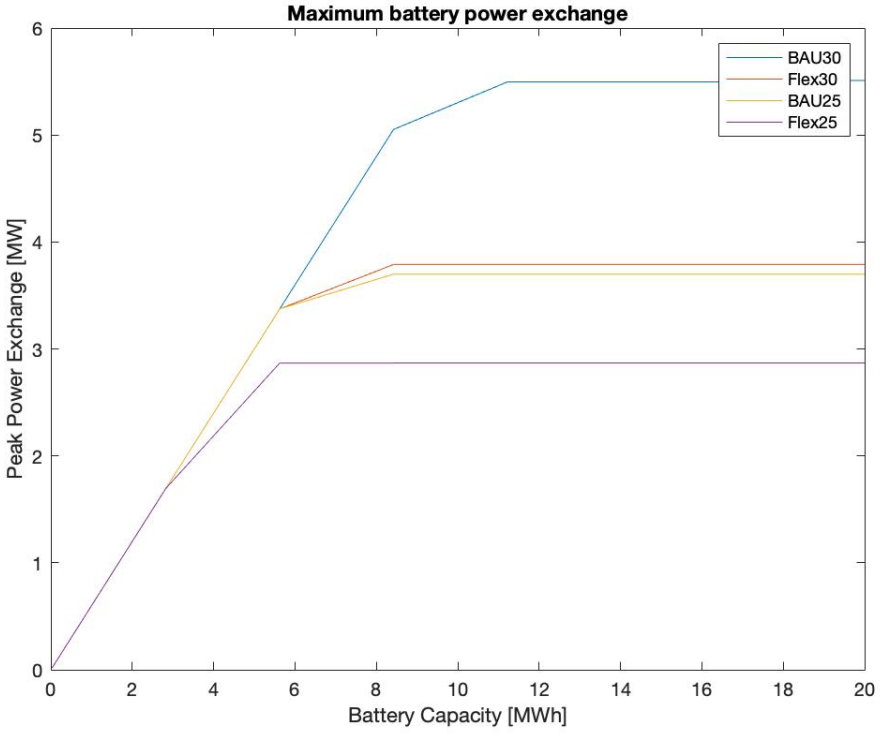

Figure 5.6: Battery charge/discharge power peak at increasing energy storage capacity.

Looking at the graph, this theory holds until a certain amount of storage capacity, depending on the year and scenario, when the peak power exchange remains constant. The point of constant peak exchange increases with increasing solar power and energy demand (2030 vs. 2025) and is higher for BAU than Flex. This makes sense, as higher supply and demand will generate higher power

exchanges with the battery, and demand response aims to match the two to minimize the size of the exchanges. The constant peak power exchange point implies that after this point power capacity is not an issue anymore, and storage capacity is the bottleneck for further utility. See the much higher storage capacities at which traces reach their asymptotes in Figures 5.7 and 5.8 and **??** and beyond. Table 5.7 contains the peak power exchange values for each year and scenario, which can be read as the minimum power capacity of the battery system for each circumstance.

Table 5.7: Peak Power Exchanges with the battery, for each year and scenario. These are the maximum values for each trace in Figure 5.6

	Peak Power Exchange (BAU) [MW]	Peak Power Exchange (Flex) [MW]
2025	3.70	2.87
2030	5.50	3.79

The top graph in Figure 5.7 shows the average evening grid demand (draw) in 2025 and 2030 for battery sizes ranging from 0 to 140 MWh, with and without demand flexibility. As mentioned in Chapter 4, the depth of discharge (DoD) setting in the model is 60%. The battery capacity sizes on the x-axes are the *total capacities*, before DoD is considered. The *effective capacity* is thus 60% of these values. Evening is defined as 16:00 to 20:00, capturing the majority of residents arriving home from work and corresponding to the observed evening heatpump peak in [6]. The 2025 traces have lower absolute values and there is less difference between BAU/Flex traces, owning to the lower absolute total loads and less (flexible) EV and heatpump demand. It is clear that the battery system has a substantial impact on the evening peak. The traces show diminishing returns at increasing battery sizes, with a constant value reached around 50 MWh (shown by the red lines). These points correspond to possible battery sizes. At this size, for 2025 the decrease in the average peak compared to having no battery is 19.8% for the BAU (non-flex) trace and 18.5% for the Flex trace. For 2030 the values equal 29.5% (BAU) and 23.3% (Flex). The peak-shaving difference between BAU/Flex in 2030 exists because there is more more peak-shaving potential for the battery system without demand flexibility, provided there is enough PV load. This last point is important because this is evidently not yet the case in 2025 which has 3/4 of the PV rated power of 2030.

Also notable is how the difference between BAU/Flex traces progresses. The 2030 difference is equal to 14.9% from x = 0 and converges to 9.5% from a battery size of 50 MWh onwards, whereas 2025 starts at a difference of 6.1% and converges to 4.4% at the same battery size. It is worth looking at the relative heatpump, EV and PV penetrations between the two years. 2030 has 2x the amount of heatpumps, 2.5x the amount of EV's and 1.33x the amount of PV. This means that towards 2030 loads increase more than production, increasing the load/production ratio. More 'relative load' in 2030 puts more emphasis on flexibility at small battery sizes. This effect decreases when storage increases and the battery is better suited to handle the evening peak. More 'relative production', or a smaller load/production ratio, in 2025 means there is relatively less potential flexible load to move to midday, and relatively more production that can be used in the evening. So, the effect of Flex is decreased, explaining the smaller difference between BAU and Flex in 2025. This demonstrates that the ratio between production and consumption influences the joint effectiveness of demand flexibility and battery storage.

It is evident from the y-axis in the bottom graph in Figure 5.7 that absolute values are lower for grid dumps than draws. Converging can be observed for the 2030 BAU/Flex traces in an absolute value sense, but the percentual difference diverges, starting at 32.8% and, while absolute dump values decrease as the battery size increases, maximizing at 480% for a battery size of 42 MWh (at this point the Flex trace has almost reached zero while the BAU trace is still firmly positive). Both traces start converging towards zero around the 50 MWh mark. Because a larger battery can store more energy less is dumped on the grid. The Flex algorithm performs essentially the same function, moving load to high solar yield periods so production is usurped. This is why the algorithm has less impact at higher battery sizes when the battery snaps up a larger chunk of production. When storage has a certain size no energy is dumped anymore, annihilating the difference between a system with and

without demand flexibility.

Less relative load in 2025 decreases the flexibility potential. The absolute differences between the BAU/Flex traces are thus smaller. Traces show the same diverging/converging behaviour as 2030 but zero dump is reached at a higher battery size, owning to the higher production/load ratio. This even causes the BAU trace to cross the 2030 Flex trace around 37 MWh.

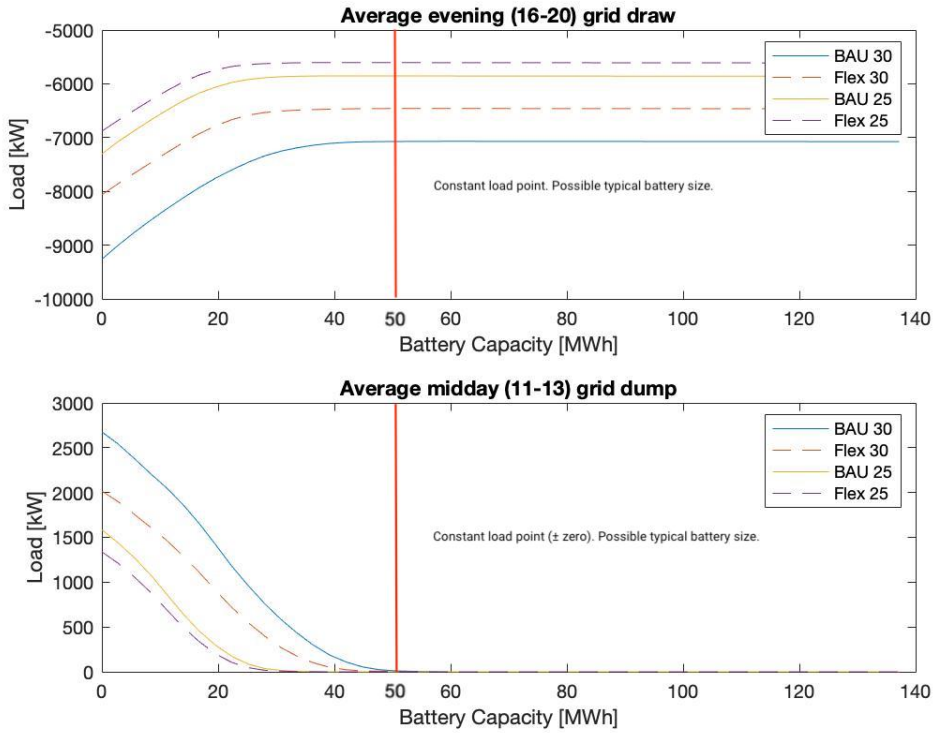

Figure 5.7: Avg. evening grid draw/midday grid dump in 2025/2030.

Peak shaving and grid interaction: Battery Active Period
Figure 5.8 shows the average evening draw and midday dump for the battery active period. During these days temperatures are highest, the weather is sunnier and therefore heatpump demand is lowest while PV-yield peaks. This translates to lower average evening draws and higher average midday dumps for both years. The large drop in evening draws compared to the full year is testament to the large influence of heatpumps on total demand. At 50 MWh, the traces are all between 1600-1700 kW and 2030 BAU draw is 2.34 times lower compared to zero storage, a 67.3% decrease. For Flex the reduction equals a factor 2.24, equalling a 52.7% decrease. 2025 draw is reduced by 51.5% (BAU) and 48.1% (Flex) at 50 MWh. This is due to more installed solar power in 2030, which allows the battery to deliver more energy in the evening to lower peaks. The 2030 BAU/Flex traces converge from a 20.5% to a 10.7% difference at 50 MWh. For 2025 traces converge from 7.11% to 6.59% at 50 MWh.

Grid dump traces look similar to the full year but show a higher battery effect, i.e. a slightly steeper drop at increasing battery sizes, especially for 2030 with its higher PV-yield. Absolute values are higher overall than the draw peaks, but the traces show the same converging behaviour for BAU/Flex at the same battery sizes.

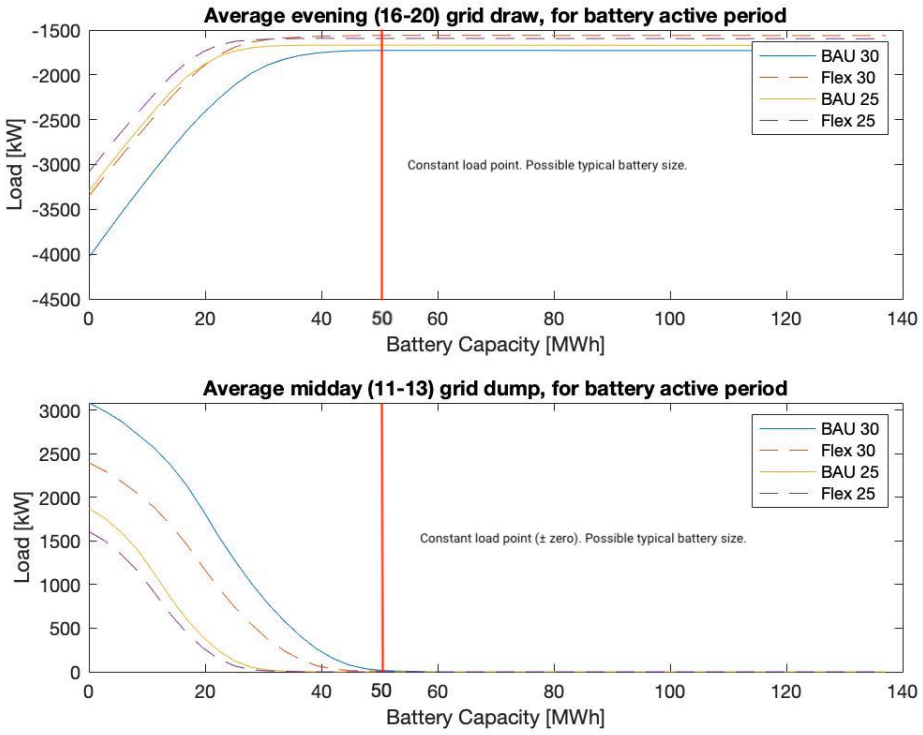

Figure 5.8: Avg. evening grid draw/midday grid dump in 2025/2030, for battery active period.

Figure 5.9 shows the peak dumps for 2025 and 2030. There is no difference between the full year and the battery active period because they all occur during the latter. The 2030 BAU/Flex traces are close together, the difference increasing at larger battery sizes when less production is 'unstored', and it becomes easier for the Flex algorithm to shift load to cover it.

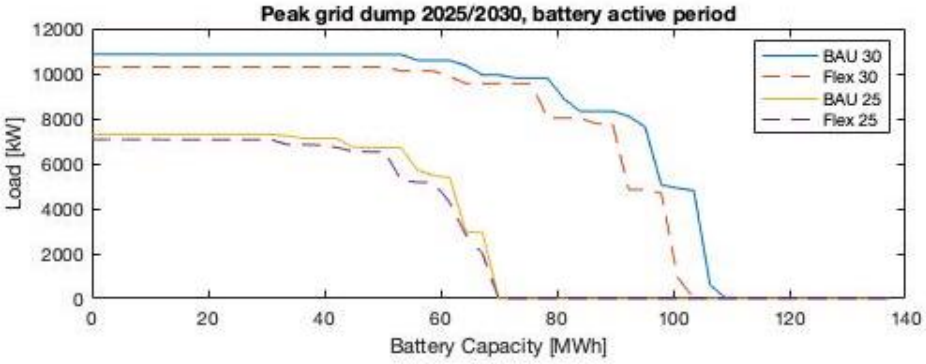

Figure 5.9: Peak midday grid dump in 2025/2030.

The battery system does not manage to decrease the yearly draw peaks from Table 5.2, for either year or scenario, as is reflected by the constant load traces in Figure 5.10. These peaks come from heatpump demand peaks which occur in January when there is not enough solar to counter them, and thus the battery has no effect.

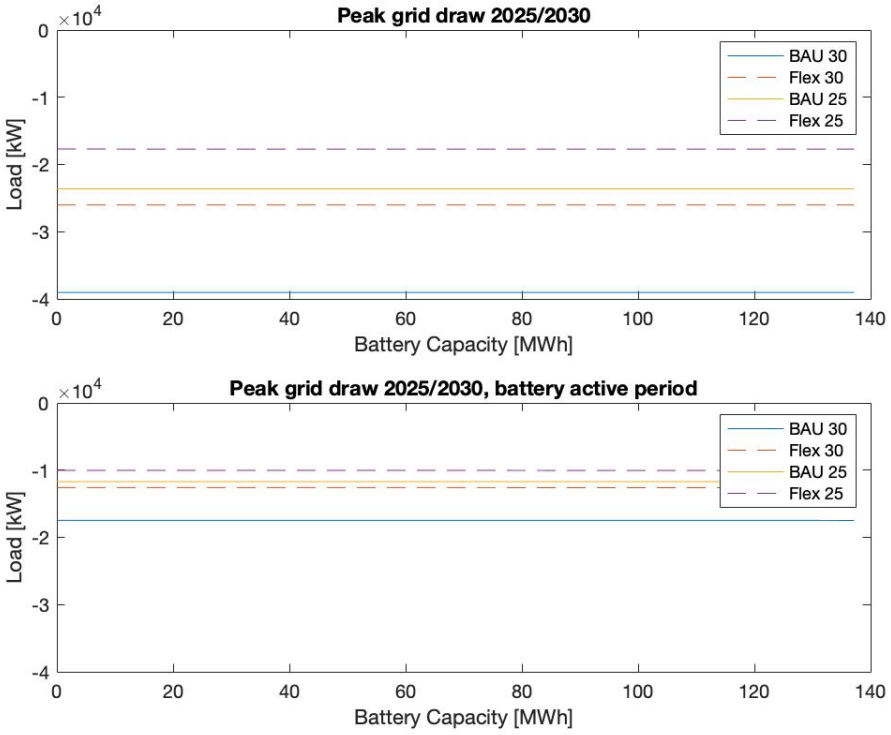

Figure 5.10: Peak midday grid dump in 2025/2030.

CO2 reduction

As mentioned in the introduction, the city of Amsterdam wants to decrease CO2 emissions by 55% compared to current levels, the maximum value of a 21-55% bandwidth set by the local government. This reduction must be achieved by 2030 with a combination of different policies. The pillars of these policies are the electrification of heating, mobility and more renewable energy generation in the city, primarily from solar panels. This section assesses the CO2 reductions achieved with predicted solar power levels in 2025 and 2030, and the impact flexibility in demand and the neighbourhood battery system have on this. Flexibility should move demand to solar production hours, thereby increasing the self-consumption of solar energy. The battery system aims to do the same by storing during the day and supplying in the evening.

Autarky and self-consumption are two important terms here that have been briefly described in Chapter 3. To reiterate: Autarky is the degree in which an electricity user is self-sufficient with renewable energy generation. So: what fraction of demand is provided by renewable generation, see Equation (4.5). Self-consumption is the fraction of generated renewable energy that is used, see Equation (4.4). These fractions can be increased by storage or flexibility. When autarky and self-consumption increase, less energy is dumped on the grid and less is drawn from the grid. Because around 9% of the total amount of energy used in the Netherlands is *currently* from renewable sources (a large fraction coming from carbon-neutral biomass plants), most of the grid-drawn electricity has a CO2 footprint [48]. This means that, at the current energy mix, every kWh that is *not* coming from the grid but is generated by solar and used directly or through the battery, saves CO2. That is the way how CO2 savings are calculated in this results section and means *future* savings are always in relation to textitcurrent emissions, just like the CO2 goals of the Netherlands and Amsterdam are related to 1990 levels.

Figure 5.11 presents the relation between battery size and autarky/self-consumption. The BAU autarky in 2030 starts at 25% and increases towards 33% when it joins the Flex trace. Demand flexibility increases autarky in 2030 by 1.5% at zero capacity. BAU and Flex traces converge when battery capacity increases and the battery can store more solar power, removing the need for Flex to

transfer load. The higher impact of Flex at small capacities is illustrated by a higher Flex autarky in 2025 compared to BAU 2030, at zero battery capacity, while absolute solar production is much higher in the later year. Autarky reaches a maximum of 30.4% in 2025, for which both traces are much closer together due to less Flex potential, around 50 MWh.

There is more solar power in 2030 compared to 2025 but not enough matching load when it is produced, which is visible in the bottom graph of Figure 5.11. While there is more load in 2030, this is mostly heatpump demand that exists in the evenings when there is no solar production. Flex has a big impact here, increasing 2030 self-consumption by 5% at zero battery capacity. All traces naturally converge towards 100% at very high battery capacities. 95% self-consumption is reached at a much lower battery capacity in 2025 than 2030, 25 MWh for Flex compared to 40 MWh in 2030, an almost two-fold difference. This argues for a modular battery structure that can be upgraded to match solar installation.

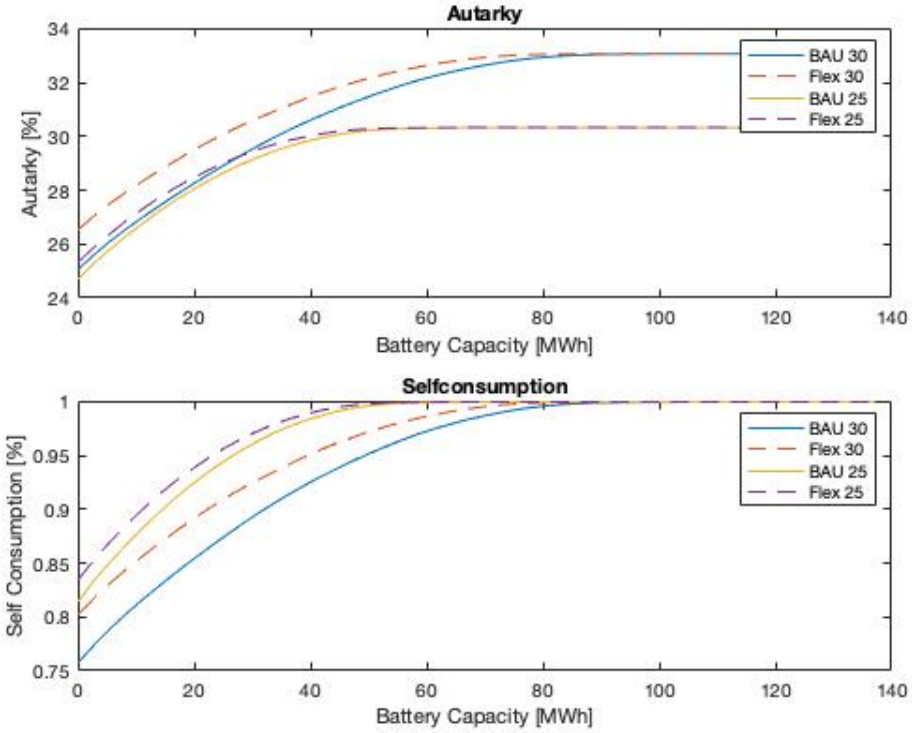

Figure 5.11: Autarky and self-consumption in 2025/2030 for BAU/Flex.

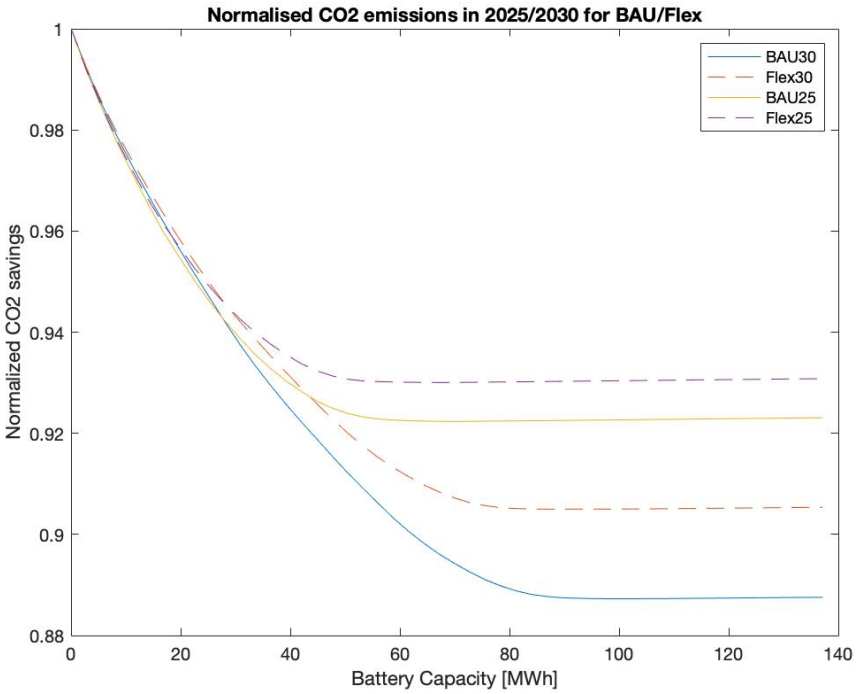

Figure 5.12: Normalised CO2 emissions in 2025/2030, for BAU/Flex.

The result of increased self-consumption at higher battery capacities is visible in Figure 5.12, where normalised CO2 savings are shown at different battery capacities. These values come from calculating the marginal CO2 impact of each kWh electricity drawn from the grid, using the Marginal Emission Factors from [49, 45]. It is noteworthy that all traces overlap until about 20 MWh, after which they start to diverge and the 2030 BAU scenario shows the highest maximum savings of 11.4% compared to no battery. The overlapping occurs because below 20 MWh there are peaks in production in all years that the battery is unable to store, and thus dumps on the grid. This requires grid draw at a later time when this dumped energy is required. Above 20 MWh, the battery is able to store the solar peaks and 2030 BAU shows the largest CO2 emission reduction because its higher production peaks necessitate less grid draw, explaining why the 2030 traces are below 2025. The maximum emission reduction in 2025 is 7.8% for the BAU scenario. The BAU scenarios can make bigger gains in both years than Flex because the battery has a higher influence on self-consumption without flexibility of demand, the difference is 2% in 2030 and 0.8% in 2025. The larger difference between the 2030 traces compared to the 2025 traces, like in the self-consumption graph in Figure 5.11, is due to more flexibility potential in demand and production in 2030.

Relating these CO2 savings to the city goals requires a clear definition of what city emissions are attributable to the ED. Figure 5.14 is useful in this regard and shows the total CO2 equivalent emissions in the city of Amsterdam, per source. The area is mainly residential and does not contain any heavy industry or harbour activity (anymore, despite the name), so this is excluded from the calculation. No highways run through the ED which makes the case for discarding highway emissions from the equation. The rest of the mobility emissions, 'Amsterdamse wegen' (Amsterdam roads) are relevant. They include CO2 emissions of vehicles driving on roads within the city. Also included are the built environment ("Gebouwde Omgeving") and Electricity ("Elektriciteit") emissions (except for industry). These include CO2 emissions from gas heating and the CO2 footprint of grid electricity use. This leaves a total of 72% of emissions that are relevant to living and working activity in the ED. To end up with an emissions number attributable to the ED, this number has to be multiplied with the fraction of Amsterdam residents living in the area. While this discards the number of people working there and also emitting CO2, the fact that it is mainly a residential area still makes it a fair way to attribute emissions. The calculation is given in Equation (5.1), with E_{ED} the emissions that

are attributable to the ED, P_{ED} the population of the ED, P_{Ams} the population of Amsterdam, C_{ED} the fraction of city emissions attributable to the ED and E_{total} the total city emissions in 1990. What this means in terms of total emission values is given in Table 5.8. The 1990 level is used because the 55% reduction percentage in the city's statement is relative to 1990 levels.

$$E_{ED} = \frac{P_{ED}}{P_{Ams}} * C_{ED} * E_{total} \tag{5.1}$$

Table 5.8: CO2 emissions in the ED, calculated using Equation (5.1).

Variable	Value	Unit
ED emissions fraction (C_{ED})	0.72	/
Total Amsterdam emissions in 1990 (E_{Ams})	3810	kilotonnes
ED population (P_{ED})	20564	/
Amsterdam population (P_{Ams})	872779	/
ED emissions	**84.82**	**kilotonnes**

Using these facts, it is possible to compute how much the solar, Flex and battery save as a fraction of total ED emissions. The amount of CO2 saved is equal to the product of the *consumed* solar electricity and the Marginal Emission Factor per timestep. Solar consumption increases with storage capacity and is larger when flexibility of demand is applied, recall Figure 5.11. When the total amount of CO2 saved is divided by the total emissions attributable to the ED, the result is the fraction saved. Comparing this to the city reduction goal will show how much these technologies can help in reaching it. This is visualised in Figure 5.13, which shows that BAU and Flex are very similar at 16.6% and 17.6% saved in 2030 (zero battery capacity) respectively. For 2025 it is even closer at 13.4% and 13.7% respectively. The 2030 traces converge to a maximum of 22.0% and 2025 plateaus at 16.5%. The solar, Flex and battery can thus drive 33% - 40% of the envisioned maximum CO2 emission reduction of 55% in 2030, mentioned at the start of this chapter. It should be noted that this figure is likely negatively influenced by how CO2 emissions are calculated in [2]. Amsterdam quotes the CO2 *equivalent* emissions, which includes other greenhouse gasses besides CO2. However, it does not disclose what percentage of equivalent emissions actually is CO2. It is therefore possible that the total emission value for the city is inflated compared to the CO2-only value, which decreases the emission reduction calculated here using the Marginal Emission Factor. More on this in the discussion.

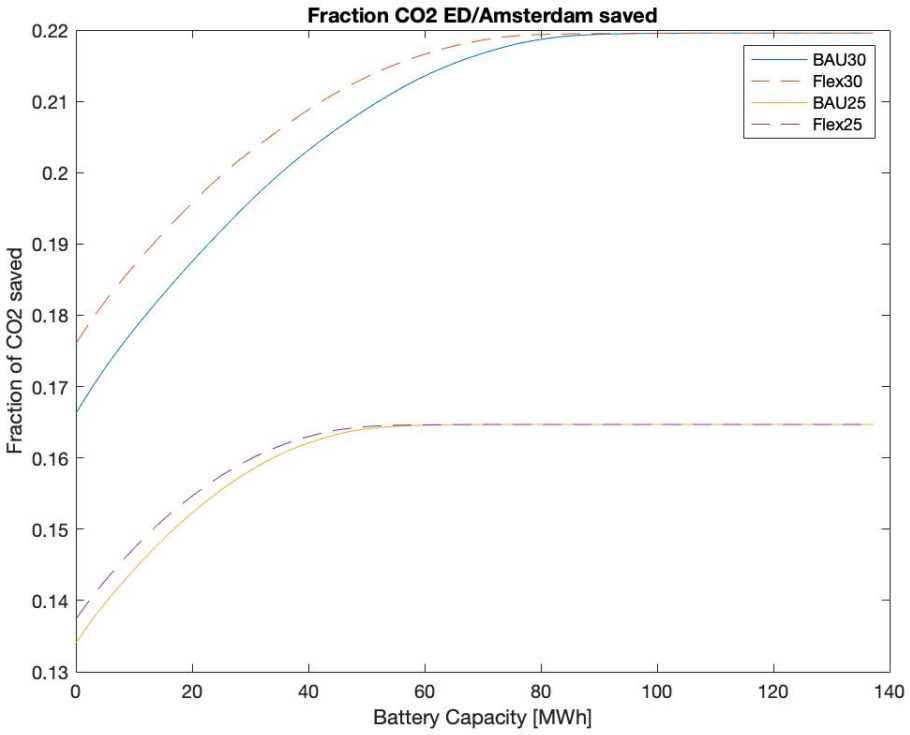

Figure 5.13: Fraction of CO2 attributable to the ED, saved by solar self-consumption in 2025 and 2030.

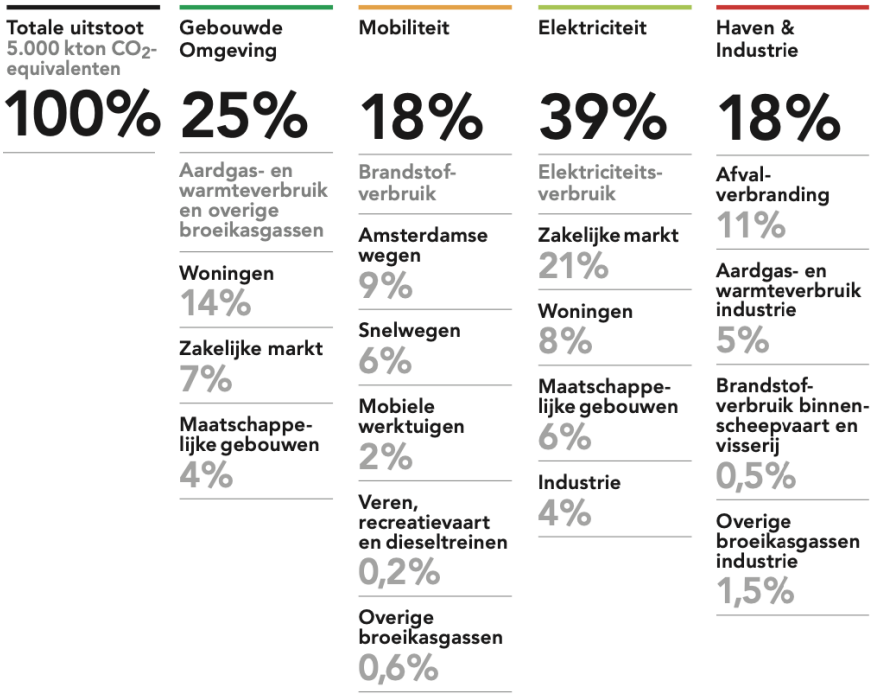

Figure 5.14: CO2 (equivalent) emissions per sector, adapted from [2].

5.2 Financial Results and Analysis

The financial results and analysis section will dive into the costs associated with grid energy, and how solar, Flex and the battery system can save on these costs. It will also present the results of a new idea regarding compensation for home owners' surplus electricity. This will be related to the coming changes in the balancing regulation which has compensated home energy producers until now. A sizing and cost estimation will be done for a battery system. The potential of the battery to generate revenue using the new compensation method, along with performing existing grid services will be assessed. These other grid services will be mentioned and revenues estimated, but they are not implemented in the battery model and as such are not explored in detail.

Cost of grid electricity
Prices for the day ahead market in the Netherlands are published on a transparency platform from ENTSO-E [50]. 2019 data is used in this thesis to compute the costs of grid draw, and how much can be saved by implementing demand flexibility and a battery system. Each consumed kWh of electricity generated by solar, either directly or via the battery system is a kWh less that has to come from the grid. Of course energy prices will change as more renewable will enter the mix in the future. They are predicted to become much more volatile, even reaching zero at peak production times but increasing compared to current levels at times of high demand [51]. This further increases the potential for a battery system to generate revenue. Therefore, the 2019 prices used for the graph below serve only as an illustration for the financial impact of flexibility and storage. The section on neighbourhood balancing shows a realistic way of maximizing the economic worth of solar energy in the future.

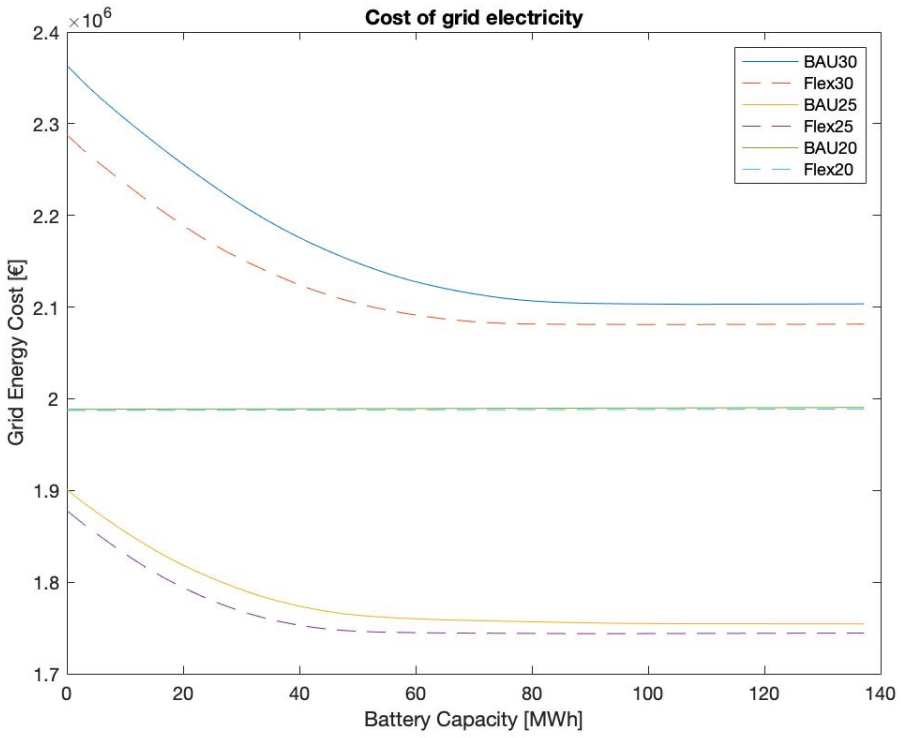

Figure 5.15: The total cost of grid draw for each year.

The almost constant lines for 2020 indicates that Flex and the battery system have a negligible impact on grid draw, the low amount of solar capacity necessitating the majority of electricity to come from the grid. Demand flexibility reduces grid draw costs by €3000,- per year for 2020 by slightly increasing solar self-consumption. It is still included as a reference to the 2025 level. Even though total energy consumption in 2025 is much larger than in 2020, due to more heatpumps and

EV's, the grid draw cost level is more than 20% lower at 50 MWh storage because a larger share of demand is serviced by solar. At this capacity, the battery saves €150.000,- per year on grid electricity. Demand flexibility reduces necessary grid electricity by €29.000,- compared to BAU at 0 MWh storage, the difference decreasing with increasing storage capacity. This is because the battery does the same thing as Flex, increase self-consumption, and the law of diminishing returns applies: at some point so much demand is serviced by stored energy that shifting the remaining demand has less effect. This is why the traces show the typical BAU/Flex convergence for grid draw derived variables at higher battery capacities. In the 2030 scenario a 50 MWh battery saves €216.000,- of grid energy for BAU and €185.000,- for Flex per year. If customers pay a fair price for neighbourhood generated energy, which could even be below retail, there is a margin to be earned by the battery. This will be assessed in the next section on neighbourhood balancing.

Neighbourhood balancing

The Dutch minister of Economic Affairs and Climate has decided to tail off the existing compensation ruling from 2023 by 9% per year until 2030 [52]. From 2031 onwards there is no compensation from the government, the only compensation will come from the energy supplier and is equal to 80% of the quoted variable energy price. This reduces the average price a customer receives for feeding-in energy by around 15 cents per kWh. Table 5.9 shows the impact this has on the total revenue that producers in the ED will receive for their energy. If a neighbourhood battery is implemented to complement growing solar installations, it could facilitate a new way of compensation, dubbed 'neighbourhood balancing' by this author. The idea is that energy producers get a fee for their energy which is above the variable price, to incentivize connections to the battery and solar panel installations, and consumers pay a 'normal' electricity price for energy from the battery. The spread is income for the battery. The different prices are summarised in Table 5.10.

Table 5.9: Impact of changing balancing compensation between 2030/2031.

Scenario	Year	Balancing revenue	Difference
BAU	2030	€705.660,-	
BAU	2031	€349.610,-	-49.5%
Flex	2030	€575.900,-	
Flex	2031	€285.320,-	-49.5%

Table 5.10: Energy prices used for financial calculations.

Variable	Price [€/kWh]
Average variable energy price (Jun-19 - Jun-20)	0.0756
Average Dutch commercial energy price (Jun-19 - Dec-19)	0.22
Neighbourhood balancing bid price	0.125
Neighbourhood balancing ask price	0.22
Neighbourhood battery margin	0.095

Choosing a bid and ask price is of course arbitrary, but two values have been chosen for the purpose of this thesis. The bid price is 5 cents above the state-mandated price payable by the energy suppliers, reducing the drop in balancing income for solar panel owners between 2030 and 2031 by a third. Consumers buying from the battery pay a fee of 22 cents/kWh, equal to the current electricity price. However, it can be expected that energy prices will grow with at least the inflation rate per year in the next 10 years. This means 22 cents will be below the regular commercial electricity price in 2030, again incentivizing consumers to connect to the battery.

With the prices in Table 5.10, one can compute battery income from neighbourhood balancing. The margin per kWh is multiplied with the amount of energy going through the battery to end up with a total yearly trading income. How much energy goes through the battery depends on its capacity (and the solar production) and is thus closely related to the self-consumption. A higher capacity results

in less grid draw and dump. That is why the graph in Figure 5.16 looks very similar to Figure 5.12, but inverted, as it is also dependent on grid dump. The same differences between BAU/Flex exist, with more energy going into the battery without Flex, as Flex tries to prevent this by transferring load. That is why the BAU revenues are higher than Flex. The revenues are used to compute the payback period of the estimated costs associated with a battery system. For this purpose, a scaling is done based on the results in this chapter. Additionally, a brief review will be made of other grid services and their potential revenues for a battery of this scale.

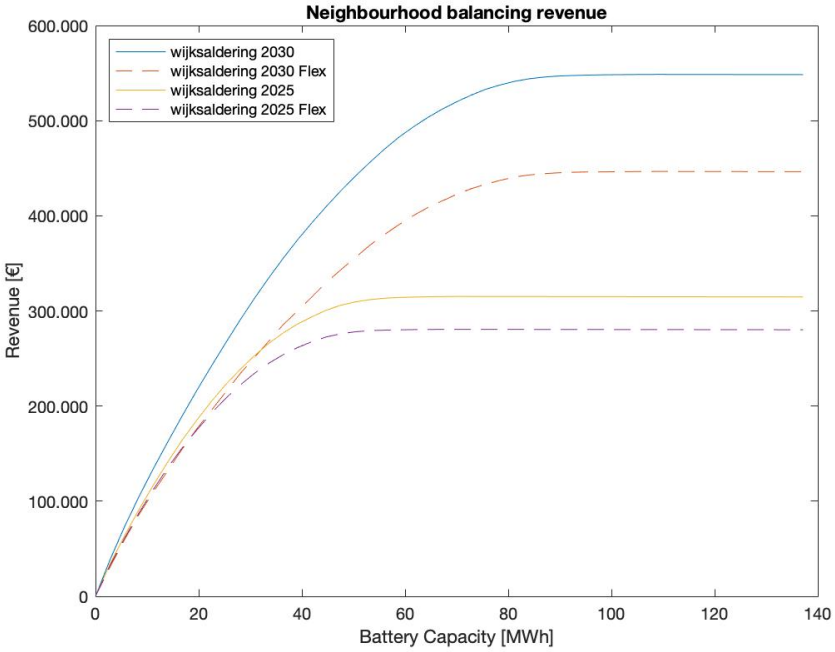

Figure 5.16: Total margin revenue of neighbourhood balancing, for 2025 and 2030.

Sizing, costs and payback period of the battery

Once the problematic impact of foresaid energy scenarios is clear, a battery storage system is identified as a possible solution and a possible revenue stream is suggested, the next step is sizing the system [53]. A battery can be sized based on a variety of desired results, but in the case of the neighbourood battery two focus points are identified: capacity to increase self-consumption and autarky, and generating revenue to improve its business case. Self-consumption and autarky are the basis of all other results. When they increase, by definition (average) grid draw/dump and thus CO2 emissions decrease and revenues increase. A 'huge' battery which could store every last kWh of solar can generate more revenue in the neighbourhood battery scenario, as more energy can be bought and sold, but it would be far too expensive. Conversely, a battery that does not make a substantial impact on the grid because of its relatively small size will perhaps not get the necessary backing from important stakeholders like the municipality and TSO/DSO as it is non-essential. There is a sweet spot to be found, and the fact that grid draw/dump, autarky and self-consumption results show diminishing marginal returns at higher storage capacities is helpful in finding it. However, a neighbourhood battery must first and foremost have a substantial positive impact on grid stability and renewable energy use. This is the pre-requisite for it to be built and generate revenue. 'Positive impact' is still a very vague term which must be defined with hard demands that in the end generate a desired battery size. Then, the financial implications of this size must be assessed with respect to cost, revenue and payback time.

In order to have the positive impact mentioned above the battery needs to be functional in relation to self-consumption and autarky, the two driving Key Points of Interest (KPI's). Functional can be defined by setting a desired value for the KPI's as a fraction of the maximum values, while recognizing their asymptotic nature, and then seeing at which storage capacity this value is reached. After analysing Figure 5.11, a 95% fraction is identified as a good intermediate between performance and size because it falls before the asymptote is reached for both KPI's and is close to maximum performance. To prevent unnecessary complicating the sizing of the system one required capacity per scenario year is determined. As BAU and Flex traces differ and reach this fraction at slightly different battery sizes, a middle point between the two traces is chosen from which the size is derived. The required power capacities come from the BAU scenario in Table 5.7. The desired fraction of 95% results in the battery capacities displayed in Table 5.11.

Table 5.11: Battery capacities at 95% of the maximum KPI values in each year.

Year	**KPI**	**95% value**	**Storage capacity (middle point of BAU/Flex)**	**Required power capacity (from Table 5.7)**
2025	Autarky	28.8%	23.8 MWh	3.70 MW
2025	Self-cons	95%	26.6 MWh	3.70 MW
2030	Autarky	31.4%	44.8 MWh	5.51 MW
2030	Self-cons	95%	44.8 MWh	5.51 MW

Before deciding on a definitive battery sizing, battery degradation must be taken into account. Research on Lithium-ion batteries has shown that degradation depends on a various factors like charge/discharge power, depth-of-discharge (DoD), outside temperature etc [54]. This type of battery is widely used in EV's and other storage devices and its degradation characteristics are used for estimating the degradation of the battery system in this thesis. The DoD implemented in the model is 60%, which is seen as an optimal compromise between battery life and capacity usability. That means that the battery is charged to a maximum state of charge (SOC) of 80%, and discharged to a minimum SOC of 20%. Battery testing results in [54] show that batteries exhibit linear degradation for a certain DoD at an increasing number of cycles. With a 60% DoD, this degradation is 1.4% per 1000 cycles. Table 5.12 shows the number of cycles that the battery system experiences for each year and scenario.

Table 5.12: Cycles per year and degradation of the battery after 25 years.

Year	**Scenario**	**Number of cycles**	**Degradation after 25 years**
2030	BAU	159	5.6%
	Flex	129	4.5%
2025	BAU	146	5.1%
	Flex	149	5.2%

A battery capacity of 95% after 25 years does not require overdimensioning of the battery, as a 60% DoD is still achievable without coming near the maximum capacity of the battery. The sizes in Table 5.11 therefore do not have to be increased, and have only been rounded for calculation purposes; to 25 MWh for 2020 and 45 MWh for 2030. There is a large difference in income between BAU and Flex for 2030 so these will be stated individually, as will the payback periods. The 2025 BAU/Flex traces are very close together at 25 MWh, so one revenue figure will be used for both. This results in a neighbourhood balancing income for the battery of €215.200,-. For 2030 the values are 406.400,- (BAU) and 328.400,- (Flex). The Net Present Value of the investment in the battery system is computed with Equation (5.2) using these revenues [55].

$$NPV = \sum_{t=1}^{n} \frac{R_t}{(1+i)^t} \tag{5.2}$$

In this equation, R_t are the balancing revenues in year t. These are discounted with the denominator using a discount rate i, which is equal to the return that can be achieved with an alternative investment. This discount rate consists of a risk-free rate and a risk-premium, see Equation (5.3). The risk-free rate is usually equal to the rate on a long-maturity state bond. The risk-premium accounts for the additional risk that the investment poses relative to a risk-free bond (assuming that the state has a low default risk). In this case, the investment can be classified as low risk because it is assumed that there is a guaranteed demand for the battery services once the system is implemented. The risk-free rate can be taken zero, corresponding to the 30 year bond yield for the Netherlands. A risk premium of 5% was chosen based on [56, 57]. For this computation the revenues have been scaled with yearly inflation equal to 2%, the average yearly inflation in the Netherlands over the past 25 years [58]. The results are displayed in Table 5.13.

$$i = R_f + R_p \tag{5.3}$$

Table 5.13: NPV of the battery system for 2025 and 2030.

Start year	End year	NPV (Flex NPV)
2025	2050	€3,698,029
2030	2055	€13,017,114 (€10,518,750)

The costs of a battery system are expressed in €/kWh and a cost of €350/kWh is used from a report from the company DNV-GL [59]. This is based on a 25 MWh/10MW system and is a conservative estimation because the 2030 battery size will likely give it an economies of scale advantage. The storage and power capacity of the reference system is scaled for the 2030 scenario. Table 5.14 shows the costs for the battery systems in 2025 and 2030, including all subsystems and associated costs.

Table 5.14: Cost of the battery systems in 2025 and 2030.

Scenario	Storage capacity	Power capacity	Battery costs
2025	25 MWh	10 MW	€8,750,000,-
2030	45 MWh	18 MW	€15,750,000,-

Comparing these costs with the NPV of 2025 and 2030, it is clear that the balancing income is not enough to cover the investment costs. While 2025 is a long way off, the 2030 NPV is only 20% below the costs for BAU. In any case, additional forms of income are needed for both years. A short overview of other services the battery could provide, along with an estimation of the revenue these services could provide is given in the next section.

Other battery services

Two types of battery services are often mentioned in conjunction with peak shaving: Frequency Containment Reserve (FCR) and congestion services on the new GOPACS market. FCR is production capacity made available by Balancing Service Providers (BSP's) for discretionary increasing or reducing of the energy output, in order to balance the energy grid. The capacity must have a minimum size of 1 MW and a fast response time (¡5m) [60]. This function has been historically provided by gas and coal turbines, but as these are being phased out in favor of renewable production capacity, new forms of FCR are being evaluated - for example wind turbines and battery systems [61]. A European auction market has been set up where providers can bid their daily capacity and country TSO's can select the desired capacity/price bid. A separate system then calculates the optimal combination of bids incorporating all TSO submitted bids. A single price is then determined, equal to the highest price in an accepted bid, which is payed to the individual BSP's. The European Network of Transmission System Operators for electricity (ENTSO-E) publish FCR prices in €/MW/week. The average price over a year lies around €2500/MW/week [62].

Because FCR capacity is expressed per MW the power characteristics of the reserve system are important. Again, the costs per kWh storage used in the computations above are based on a 25 MWh/10 MW system. The power capacity in this reference, copied for 2025 and scaled for 2030, is larger than the required power capacities in Table 5.11 but this gives the system redundant capacity in case (a part of) the battery malfunctions or there is further growth in demand and to perform more FCR and congestion services. Using (part of) its power capacity for FCR can generate a lucrative extra value stream for the system. The results of the battery model have shown that the year can be divided between a battery active period and a battery inactive period. During the active period most of the capacity is needed most of the time to store solar power and perform peak shaving. The largest FCR potential lies in the inactive period. This period covers autumn and winter when wind production is typically highest (which is why solar and wind are complementary energy sources) which often causes big production surpluses [63] during the day. At the same time, the highest demand peaks occur during this period because of a much larger heating demand. These surpluses will only become larger as more wind farms go into operation, and threaten the stability of the grid. The battery system can act as a BSP and store excess wind energy when solar production is low, and as such could use up to 100% of its capacity for FCR in the inactive period. To be conservative it is assumed that the system has, on average, 75% of capacity available for FCR on each day during the battery inactive period, and the battery only performs FCR, this would generate the estimated revenues displayed in Table 5.15.

Table 5.15: Estimated yearly revenues for performing FCR-services during the battery inactive period. 75% of max. battery capacity available.

	2025	**2030**
Number of days in battery inactive period	183	183
Estimated battery capacity available for FCR [MW]	7.5	13.5
Average FCR revenue [€/MW/week]	2500	2500
Estimated yearly FCR revenue [€]	487.500,-	877.500,-
NPV of FCR revenue over lifetime [€]	8.377.273,-	28.106.588,-

These yearly revenues are 2-3 times greater than the neighbourhood balancing revenue and the NPV of the FCR revenues in the 2030 is almost two times greater than the cost of the system, given in Table 5.14. This signifies the importance of including FCR in the battery services portfolio to solidify the business case of a neighbourhood battery system and to even make a profit over its lifetime.

Grid congestion can be caused by too much demand as well as too much production. Congestion problems therefore occur in urban area's like Amsterdam, where datacenters and EV's are demanding an ever bigger slice of the energy pie, but also in rural areas where solar farms are being built and the grid is not designed for the associated large energy inflows. These congestion issues can thus be solved by increasing demand or production locally, and must be mitigated to prevent premature and costly grid reinforcements. To do this, a new congestion market called GOPACS has been launched as an initiative of Dutch TSO's and DSO's [19]. GOPACS is coupled to the intraday market platform EPTA and allows flexibility providers to bid their production or demand capacity. When there is a local congestion problem, the TSO/DSO can buy this capacity to solve it. However, there must be an overall grid balance at all times. So, when a party increases consumption or production, an equal but opposite action must be done at another, uncongested, grid location to preserve this balance. In order to guarantee that this counter-action takes place, the TSO/DSO pays the spread between the GOPACS ask price of the first party at the congestion location, and the bid price of the second party at the non-congested location.

Congestion services are estimated to generate around €2850/MW/month [59]. Applying the same assumptions as in the FCR estimation, i.e. 75% of capacity available for congestion services on each day in the battery inactive period, operating on the GOPACS market would generate the estimated revenues presented in Table 5.16.

These estimated revenues equate to 50-60% of the neighbourhood balancing revenues and therefore are a good addition to the battery system. Especially during the otherwise inactive autumn and winter period. The NPV of the revenues in the case of 2030 would amount to about 50% of the cost of the battery system. A combination of FCR and GOPACS services could also be implemented, where FCR can be performed during high wind production periods, mostly during the day, and GOPACS services are mostly performed during the evening peak. The battery could then be charged with wind energy during the day, with a zero CO2 footprint, but it could also accept (partly) non-renewable electricity to cover the windless days during the battery inactive period. As more renewable energy enters the mix, the average CO2 footprint of grid electricity will naturally decrease.

Table 5.16: Estimated yearly revenues for performing congestion services on the GOPACS market during the battery inactive period. 75% of max. battery capacity available.

	2025	**2030**
Number of days in battery inactive period	183	183
Estimated battery capacity available for GOPACS	7.5	13.5
Average GOPACS revenue [€/MW/month]	2850	2850
Estimated yearly GOPACS revenue [€]	128.250,-	230.850,-
NPV of GOPACS revenue over lifetime [€]	2.203.867,-	7.394.195 ,-

6 Discussion

This thesis set out to estimate the impact of electrification on demand peaks in the distributed electricity grid of the Eastern Docklands in Amsterdam. It also explored how demand flexibility and a neighbourhood battery system can decrease demand peaks, increase self-consumption of solar energy and aid in the CO2 reduction plans for the city of Amsterdam. It adds to existing research, which often focuses on one type of load [64], by including all relevant electricity loads that currently exist and predicting how they will progress by making a substantiated prognosis of heatpump and EV penetration. Furthermore, it contributes by proposing a new way of compensating prosumers for their surplus solar energy when existing compensation is abated by the Dutch government, called neighbourhood balancing. This not only incentivizes solar panel installations but increases local consumption of renewable energy and lowers grid dump. It also provides a reliable income stream for the operator of the neighbourhood battery while this storage system provides valuable services to the grid. Lastly, the thesis also contributes by showing how such storage can decrease CO2 emissions by using newly developed Marginal Emission Profiles, and relates the gains to governmental and municipal climate plans. The following sections will answer these questions following the sub-questions posed in section 2.1 of the Research Design chapter.

6.1 Impact on the grid

The electrification of heating and mobility will substantially increase both the average as the peak power demand of the grid. In the 2030 scenario, peak demand will increase more than three-fold compared to 2020. In the 2025 scenario the rise is two-fold. This is mostly because of the large impact that heatpump load has on total demand. On the day of the maximum total demand peak, the heatpump peak equals almost 75% of this total demand peak. This is number is large but not unrealistic when comparing it to findings in a British literature article [6]. In this research on heatpump penetration in Great Britain, a 20% heatpump adoption rate among all households in the country led to a 14% rise in peak grid demand. The adoption rate in this thesis is larger at 49% and the absolute user base is smaller, leading to a less spread out and more peaky demand profile. Also, the outside temperature in the dataset from the article rarely went below zero degrees, whereas the *average* outside temperature in the heatpump dataset (from reference year 1987) in this thesis is -0.44 C in January and February, and the *minimum* temperature is -15 C. The average temperature in the Netherlands in 2019 during the same months was 4.73 C, indicating that the reference temperatures in the dataset are relatively low. This is supported by the fact that the average yearly temperature in the Netherlands has risen by 2 C since 1987 [65]. Because outside temperature is very influential on heatpump demand, adapting the demand profile with more recent temperature data could result in lower load peaks. EV-charging has a much smaller role to play, despite a dramatic rise in the number of charging sessions, the average charging power and the fact that the evening EV-peak coincides with the heatpump peak. The maximum peak in 2025 and 2030 equals about 10% of the heatpump peak. Possible explanations for the small impact of EV's are:

1. EV-charging is not as peaky has heatpump demand and has a better spread throughout the day.
2. EV-charging does not require as much power as a heatpump.
3. The estimated number of sessions in the scenario is too low.

The first explanation is partly true, looking at Figure 3.3. EV-demand has a better spread throughout the day and a less pronounced evening peak than heatpumps, but a peak none the less. The second explanation is not true when looking at individual charging sessions. A modern EV can charge at 11 kW whereas a heatpump will use around 1 kW during normal operation. There are also more EV's than heatpumps predicted in 2030 (5934 vs. 4846). One would therefore expect a larger peak than is present in the data. The most plausible explanation for this is an underestimation of the number of charging sessions.

Average grid demand, computed for the evening peak during the whole year, increases by 32.5% in the 2030 scenario compared to 2020. For 2025 the increase is 4.4%. While a less impressive figure than the three-fold difference in peak demand, this is still a substantial rise considering that it is computed over the whole year and therefore includes summer days where heatpump demand is minimal.

Solar production reaches a peak of 19.7 MW in 2030, almost half of the yearly total load peak, making it an important factor when considering the strain of peak loads on the grid. Its 2025 peak is almost equal to the heatpump peak and both are more than half of the total load peak in that year.

Relating these results to the estimated capacity of the grid, only the 2030 peak threatens the stability of the grid, reaching 75.1% of capacity. This violates the two-fold redunacy rule that the Dutch TSO's have adhered to, but which has been increasingly let go in the past years. It must be said that estimating grid capacity is a difficult exercise because so little information is made available by the TSO. The estimation is based on a capacity value per low-voltage consumer that is mentioned in an EU TSO/DSO observatory document [12], and is an average across all EU countries. The actual grid capacity could therefore be both higher and lower than the estimate made here.

6.2 Effect of demand flexibility

Demand flexibility ("Flex"), also named demand response in literature and this thesis, has a substantial impact on peak power demand. Flex decreases the BAU total load peak by 33% in 2030 and 31% in 2025. This means only 31.4% and 50.3%, respectively, of grid capacity is reached. While demand shifting creates a higher peak for EV-charging, this does not cause the absolute Flex total load peak to increase. In fact they decrease by figures similar to BAU and occur on other dates. Peak shaving gains between 29-31% are made for heatpumps. This is very promising for future implementation given the predictable nature of heatpump demand. While the overall potential of demand response is great, its application requires near-perfect load prediction and control over load generating appliances. Even as the accuracy of predicting solar production and electricity demand has gotten very reliable [39, 40], controlling demand requires the large-scale implementation of a new generation of interconnected technology that employs control strategies that both respond to individual user requirements and the needs of the greater grid [64]. This implementation problem poses a great challenge for the future.

6.3 Effect of neighbourhood battery storage

Literature considers the integration of batteries in a local energy grid along two main lines: as one central MW-scale system, or as connected but smaller distributed units at prosumer level [66, 53, 67]. This thesis models a system of the first kind and investigates how it can work together with flexibility of demand to reduce peak loads on the electricity grid. The model is general in its technical characteristics, it does not incorporate specific properties of the Eastern Docklands. This presents an advantage for further application at other locations where demand and production data is available. The disadvantage is that the exact location where congestion or capacity problems will occur cannot be pinpointed.

Demand response and the battery system work well together on days with enough solar production. The comparison in Figure 5.2 shows that flexibility decreases the morning peak, maximizes self-consumption at noon and displaces some evening demand to the afternoon and night. This leaves the remaining solar surplus for the battery to store and discharge during the evening peak, which is already lowered by Flex. Reducing average grid demand is helpful to the DSO as it deals with peak loads, which dictate grid operation and reinforcement costs. The battery is powerless on cloudy (winter) days when there is no, or little, surplus, which promotes the idea of charging with grid-electricity during cold, sunless periods. This is further made attractive by the increasing penetration of renewables, decreasing the CO2 footprint of grid-electricity and leading to lower electricity prices [51]. The system also has more capacity available in the winter period to perform grid-services like frequency control and congestion management.

The battery algorithm focuses on minimizing evening grid draw by supplying solar electricity. In the 2025 scenario, the average evening grid draw, between 16:00 and 20:00, over a full year is decreased by 19.8% at a typical battery size of 50 MWh compared to no storage. More solar in 2030 empowers the battery to reduce evening draw even more at a 29.5% reduction. Applying flexibility reduces the relative impact of storage by 1-6%, as demand peaks are already lowered, but it does decrease absolute draw values by another 10%. *Average* midday grid dump is almost zero with a 30 MWh battery in 2025 and a 50 MWh one in the 2030 scenario but *peak* dump still exists at these sizes. In the battery active period, the period running from day 78 to 260 with the highest cumulative positive mismatch, the relative effect of the battery is dramatically greater. Here, average evening draw is decreased by a maximum of 67.3% in 2030 and 51.5% in 2025. A potential improvement for the model could be to implement an adaptable charging/discharging-rate. The adaptable charge rate could be increased when a short positive mismatch is foreseen, and decreased when the predicted surplus is large and lasts long. In the latter case, charging is spread-out over the surplus period and the size of grid dump peaks is decreased. The same thing hold for the discharge rate, which could be decreased when a long negative mismatch period is predicted, and increased when the shortage is short-lasting. The peak values for draw and dump are not easily abated. Peak grid dump shows little elasticity at increasing battery capacities and only starts to decrease substantially at very large sizes. The dump loads are not insignificant, reaching 25% of grid capacity at 11 MW in 2030, which could necessitate connect/disconnect control of installed solar power to prevent sudden spikes in grid-voltage and frequency. Peak grid draw cannot be influenced at all by a battery system, similar to what has been found in [13]. This is due to insufficient solar generation when the peaks occur in January. So, curtailing these loads must come from demand response.

Autarky and self-consumption results benefit from the existence of a battery system which is advantageous for local prosumers. Autarky, which is limited by the energy that the installed solar power can produce, can be increased by 8 percentage points, reaching a maximum of 33%. An autarky of 31% is already reached at the typical battery size of 50 MWh, a 20% increase compared to zero storage, and gains after this capacity are therefore minimal. Self-consumption is between 75% and 80% without storage and increases towards 100% at very large battery sizes ($\pm$100 MWh). At a typical battery size of 50 MWh, self-consumption is more than 90% in each scenario. Demand flexibility improves this compared to BAU by 2%, but only for 2030. These results lie in the same bracket as found in [13].

Increasing the self-consumption of solar energy by applying demand response and implementing battery storage lowers the necessity for grid draw. This reduces the CO2 footprint of energy consumption at the current Dutch electricity mix, where on a yearly basis about 9% comes from renewable sources [48]. Battery storage can decrease CO2 emissions with a maximum of 11.4% compared to no battery for the 2030 BAU scenario. Flexibility decreases the impact of the battery by 2% because it takes away some self-consumption potential. In 2025 the battery has less effect as there is less solar generation and the largest emission reduction is for the BAU scenario at 7.8%. The absolute emissions can be related to CO2 emissions in Amsterdam that are attributable to the Eastern Docklands. Making this relation shows that a battery system can save 21% of the total current CO2 emissions in the area in the 2030 scenario at a typical battery size of 50 MWh. Given the city of Amsterdam's emission reduction goal of 55% by 2030, neighbourhood battery storage could thus drive 40% of this goal. It should be noted that this calculation relies on two sources for CO2 emissions. One contains the marginal emission CO2 emission profiles for electricity production in the Netherlands, described in [49], the other is the CO2 equivalent emissions in Amsterdam. While the first *only* considers CO2 in the total emissions of electricity generators, the latter also includes other greenhouse gasses besides CO2, like NOx, in the calculation. It is therefore likely that the fraction of CO2 saved is underestimated in this thesis.

The financial benefit of battery storage is assessed in three ways: how much it reduces grid-electricity costs, how much it can earn by performing neighbourhood balancing and what potential revenues come from other grid-services. First, it was explored how consuming less grid-electricity reduces grid-costs using day-ahead market prices for 2019. The results show that consuming solar energy lowers the yearly cost of consuming grid-electricity by 20% in 2025 compared to 2020, even though demand in the later year is much greater. At a typical battery size of 50 MWh, grid costs in 2025 are €150.000,- lower compared to no battery. Demand flexibility adds another €29.000,- to these savings. The same storage capacity saves €215.000,- in the BAU scenario and €185.000,- for Flex in 2030.

A desired battery size for each year was found by setting a self-consumption and autarky requirement of 95% of their maximum values. This results in a 25 MWh and 45 MWh battery for 2025 and 2030 respectively, at a build cost of €8.75M and €15.75M, excluding maintenance costs. Neighbourhood balancing at a margin of 9.5 cents per kWh generates €3.7M over a 25 year lifetime for the 2025 scenario and €13M for 2030. The difference is due to greater energy exchange in 2030. To achieve a positive business case other grid-services must be added to the functional portfolio of the storage system. Two services were included, one focusing on maintaining a constant grid frequency by bidding capacity on the Frequency Containment Reserve (FCR) market, and one aimed at reducing grid congestion by offering flexibility on the GOPACS market. Performing FCR services using 75% of capacity on each day during the battery inactive period could generate €8.4M over the battery lifetime in 2025 and €28M in 2030, 1-2 times the cost of the system in the respective years. Participating on the GOPACS market for the same hours also generates a healthy income for the battery at €2.2M and €7.4M for 2025 and 2030 respectively. This income provides a robust buffer against potentially higher prices that could occur during the building or operation of the system and could impact its turn-key and lifetime costs.

An optimal combination of FCR and GOPACS can probably increase these revenues even further. The battery inactive period falls in the autumn and winter when wind energy production is typically high [68]. As mentioned earlier, the frequency issues caused by intermittent wind present an opportunity for the battery system to perform FCR during an otherwise inactive period. At the same time the capacity can be used to store wind surplus and solve congestion issues during peak evening demand on the GOPACS market. The intermittency of renewables will also cause more volatile prices, presenting an arbitrage opportunity for a battery system to 'charge low' and 'sell high'. The revenue from neighbourhood balancing could also be improved by using a dynamic pricing scheme, where the ask price depends on energy demand. If a consumer charges their car at midday using solar electricity from their neighbour, stored in the battery system, they pay less than if they charge in the evening when everyone arrives home from work. This increases the margin for the battery system further improving its business case.

So, a battery system has positive effects on the distributed grid and can create a revenue stream which can cover its costs. However, all this depends on how many prosumers and consumers are connected to the storage. The installed solar power modeled in this research utilizes all suitable roofs in the ED, meaning there are households that cannot install solar panels. These people will most likely not acquire generation capacity in the future but will continue to use electricity that could come from the grid or the battery. They will need a (financial) incentive to connect to the battery but at the same time, this incentive cannot lower the margin for the battery system excessively. The selling price for battery energy is taken the same as the current commercial electricity price in this research. This might have to be lowered to spur on non-producing households to connect to the battery. Another solution could be that the DSO or another party operating the battery pays for the connection of the homeowners, like suggested in [69]. The DSO has an overriding interest in maximizing the number of connections, as optimal peak shaving could avoid costly grid reinforcements.

6.4 Limitations of the research

Some limitations have already been mentioned, like the likely underestimation of charging sessions and CO2 savings, and the rough estimation that had to be made for the grid capacity. Regarding the charging sessions, when extrapolating the sessions to private charging the same profile fraction as for public charging was used. One can imagine that private charging would include more nightly charging and less worktime charging. This was not considered when scaling demand and could have had an impact on the aggregated EV-charging profile. The estimation on grid capacity means that it is less obvious how negative the consequences of the foreseen demand increase will be. However, to a stakeholder that does have exact knowledge of grid capacity the results will be very relevant.

The results show that the demand increase will be driven mainly by heatpumps. While detail has been added to the upscaling of the heatpump profiles by differentiating with the type of technology and insulation level, scaling a single profile to several thousand users has some inherent drawbacks. It houses the implicit assumption that the control strategy of one heatpump will be copied to all other users. This means that every peak occuring in the profile remains there and is increased with the scaling factor. In practice, the control strategies of thousands of heatpumps will be slightly different, depending on make, model and user preference, and thus the profiles will have peaks at slightly different times which evens them out when a large number of them is aggregated. A similar note should be added for solar production. The installed solar power is modeled as one big solar field, where in practice the panels will be distributed over several roofs. The panels will have a slightly varying orientation on almost every roof, not all are oriented optimally, and as such real energy generation will be different both in magnitude and profile shape. More or less energy produced can influence the peak-shaving results the battery can achieve positively or negatively. Aggregating the profiles of several thousand solar panels will even out any singular peakiness which could be positive for the battery in terms of the peak power influx that it needs to cope with.

The e-flows flexibility algorithm which is used to apply demand response on the data in this research serves as an illustration of the power of load flexibility to decrease power peaks and increase self-consumption of solar energy. The way it is implemented in the model, assuming perfect prediction of supply and demand, does not make any qualifications on the practical implementation of the technology. Flexibility in EV-charging and heatpump operation must come with advanced levels of control by the user (agreeing with delaying charging or setting a desired temperature for when one arrives home) or by the technology, energy supplier or DSO itself (unilaterally shutting down charging at peak demand or self-learning the temperature requirements of the user and deciding the optimal strategy given the demand of other heatpumps). The best results are achieved when flexibility is coordinated [13] which requires uniform communication protocols and comes with its own legal issues. Many hurdles still have to be taken, although the Flexpower project in Amsterdam, while not demand response in the purest sense, has taken steps in the right direction [21].

The battery system model in the research is a standalone storage facility that allows analysis on power flows and energy quantities given a demand and supply profile. It does not consider technical characteristics of the grid like voltage and frequency or integration on a grid-node level. Therefore, simulating it produces results that are meaningful in view of load peaks, autarky and self-consumption, but they do not say *where* problems will occur or how much the grid balance metrics are impacted. This translates to the explorational nature of FCR and GOPACS income calculations. These were not modelled but only estimated based on battery capacity and time available during inactive periods. Performing these grid services can also decrease the battery lifetime by increasing the number of cycles which needs to be explored further and in more detail. Another thing that could be added to the model is a variable charge/discharge rate. This could improve the peak-shaving performance and decrease grid-dump peaks further. Lastly, the cost of the battery system was based on another use-case and does not consider the local circumstances in the Eastern Docklands or maintenance costs. These could have a large impact on both the turn-key and lifetime costs when such a system is built.

7 Conclusion and Next Steps

Governmental policies are playing a catalysing role in the roll-out of novel heating and mobility technology. The electricity needed to power these innovations must come from renewable sources, in light of the overarching objective to decrease greenhouse gas emissions in an effort to slow down climate change. While the share of wind and solar energy in the Dutch electricity mix has been growing over the last decade, it has become clear that their intermittent characteristics can pose a threat to the stability of the grid by causing large supply peaks. When the simultaneous electrification of mobility and heating takes off as anticipated in the coming years, a similar spike in demand is expected that could render the current grid capacity insufficient. It is therefore of paramount importance that new smart ways to deal with supply and demand peaks are developed, tested and implemented on a nationwide scale. These can prevent expensive grid reinforcements, or worse, power outages.

This thesis has approached the problem of high renewable penetration coupled with electrification in the context of a realistic urban neighbourhood in Amsterdam. It has made a prediction of future aggregated load profiles, based on an estimation of the solar, heatpump and electric vehicle potential in the area, and compared this with current levels. Secondly, it has assessed the potential of demand response to abate excessive demand peaks in the morning and evening. In addition, a comprehensive evaluation of a neighbourhood battery system was done by simulating a modeled battery system, with three objectives in mind. One, to see how storing local solar energy surpluses can be used to perform peak shaving in the evening. Two, to analyze how increasing self-consumption of locally produced electricity can reduce CO2 emissions from grid-electricity. Three, to assess if a healthy business case can be built around local battery storage.

The results show that realising the potential for heatpumps and electric vehicles in the Eastern Docklands can increase peak power demand by a factor of three in 2030. Realising all solar potential can cause power supply peaks equalling 50% of grid capacity. Demand response is very effective in reducing demand peaks year-round, shaving off more than 30% of the maximum aggregated load peak and 10% of the average evening peak. The battery system is only functional during half the year when enough solar energy is produced, and reduces the average evening peak by two-thirds in this period. Taking the average over a full year the reduction equals 30%. At a typical battery size, self-sufficiency of the neighbourhood is increased by 20% to around 30% in the 2030 scenario. Self-consumption can be increased to over 90%. The combination of solar, demand response and storage can help the city of Amsterdam achieve 40% of its CO2 reduction goals. A battery storage system can turn a profit over its lifetime with an optimal combination of neighbourhood balancing, FCR- and congestion-services.

This research contributes to existing literature by taking a holistic view of the problem in a realistic environment, encompassing all demand types encountered in the distributed grid and proposing a new use-case for local storage. Further research can build on this by focusing on the following aspects. The Eastern Docklands are surrounded by water which could provide a source of heat for a, less conventional, water-water heatpump. Exploring the suitability of this technology to provide heat to the area could broaden the scope of electric heating possibilities. A collaborating investigation with DSO Liander can shed light on the exact grid capacity situation in the neighbourhood. Important things to assess would be where they see congestion happening based on observable trends and technical grid characteristics, and if storage could be a practical solution. This should incorporate a more detailed estimation of costs, evaluate legal hurdles and specify the location-specific potential of grid-services, including charging the battery with grid-electricity.

These recommendations call for more theoretical research on a practical subject. Above all it is time to put theory into practise. Existing experiments on local smart grids that have taken place in the Eastern Docklands profit from the forward-looking mentality of its residents. The municipality and grid-operator should take advantage of this mindset by putting their weight behind the upscaling of these trials and initiating new ones. There is a need for more funding and less constrictive rules when communities want to install solar panels, participate in demand response or experiment with energy storage. This is the fastest way to assess what works and what does not work in the real world. Only then the city of Amsterdam can truly move towards a sustainable future and reach its climate goals.

8 Appendix

The Matlab script, raw data and Simulink model are available digitally upon request. The Appendix contains extra figures that are output from the script.

8.1 Extra figures

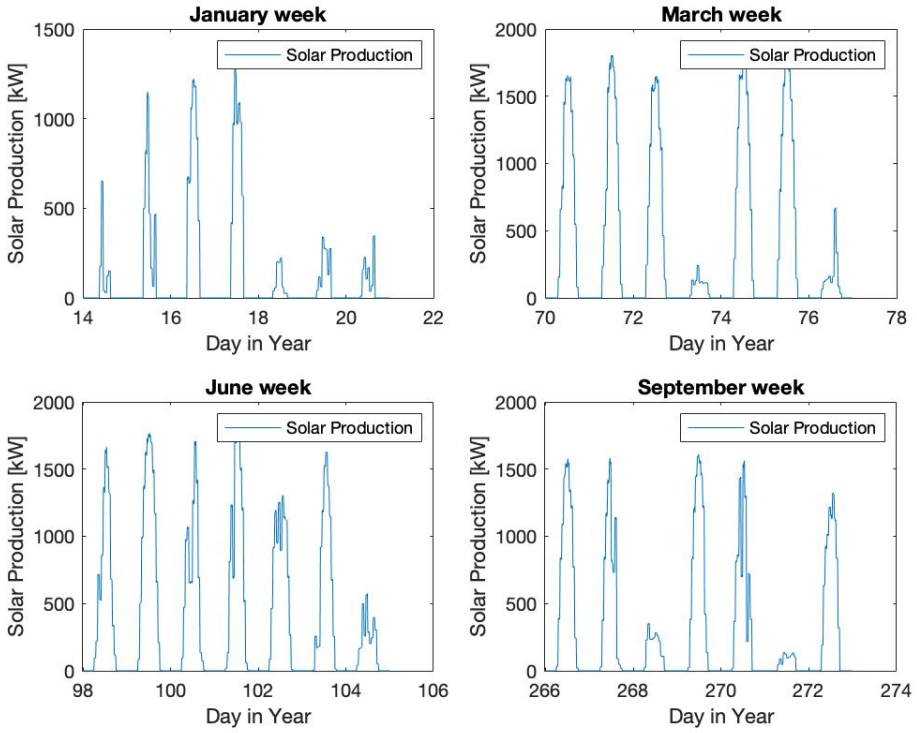

Figure 8.1: One week of solar production data for four different months.

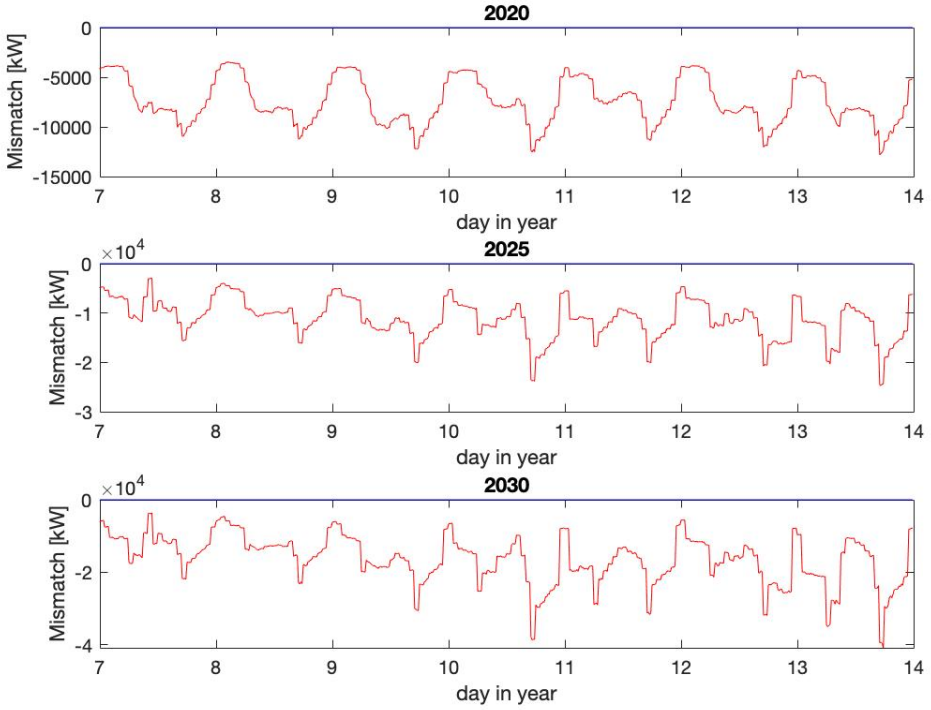

Figure 8.2: Mismatch during one week in January, for the three scenarios.

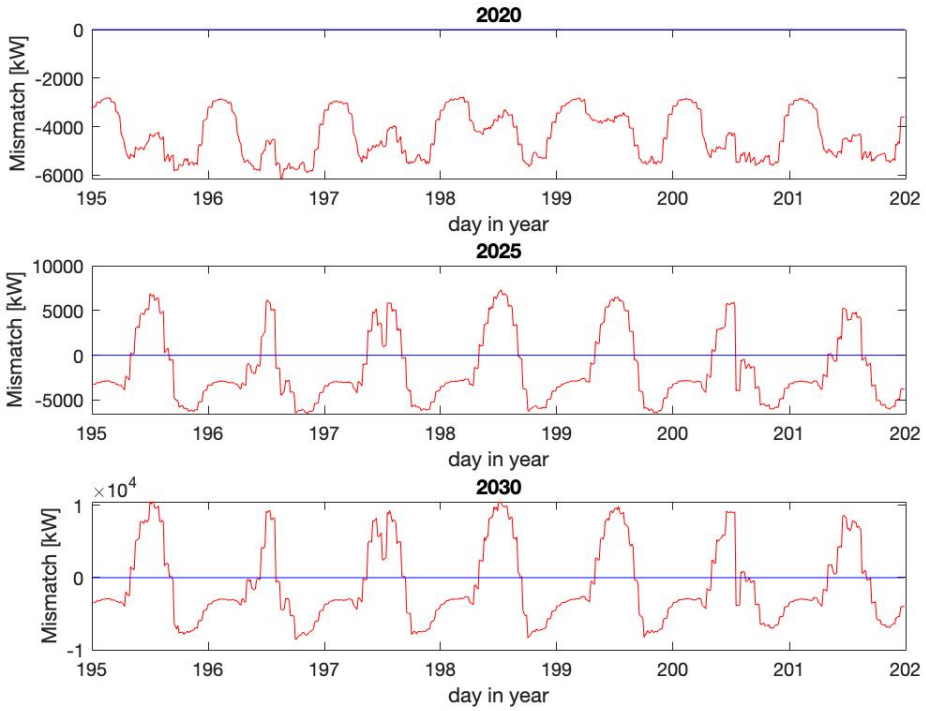

Figure 8.3: Mismatch during one week in June, for the three scenarios.

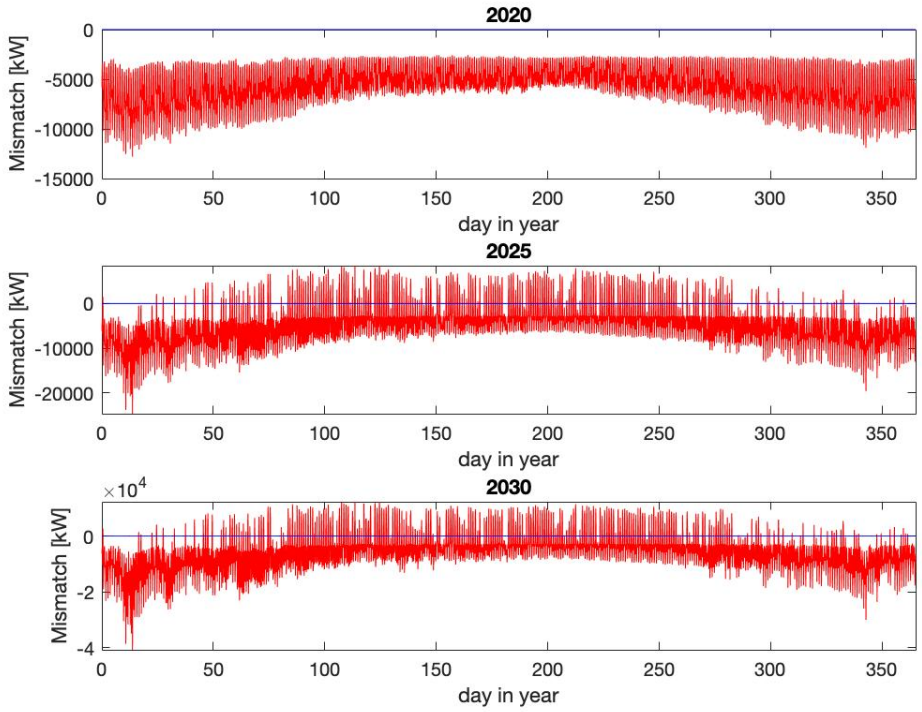

Figure 8.4: Mismatch during a full year, for the three scenarios.

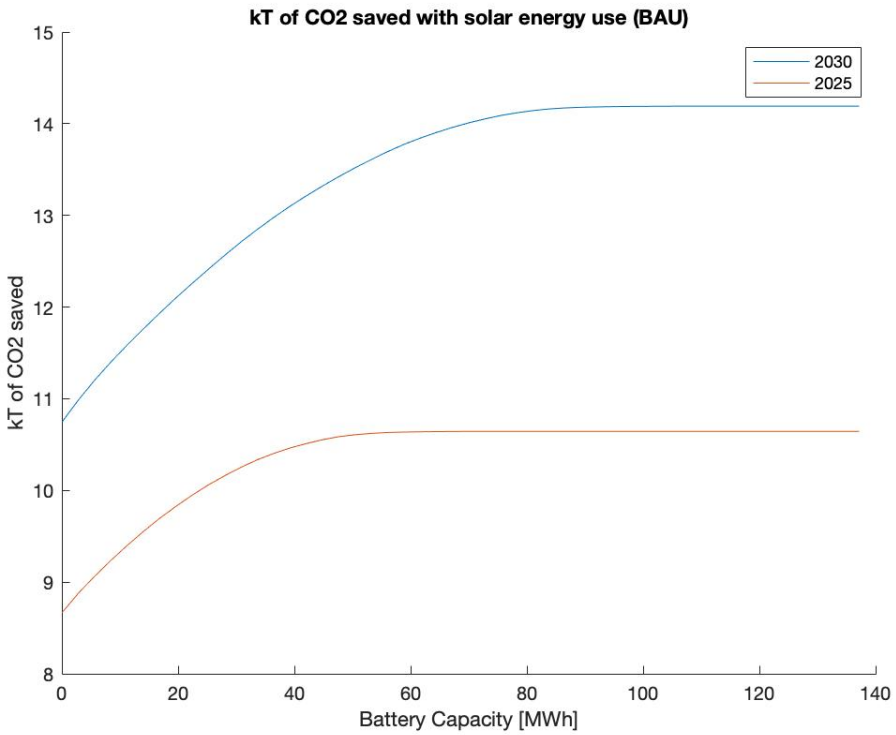

Figure 8.5: Absolute CO2 savings by the battery for different sizes, in kT. No flexibility is applied.

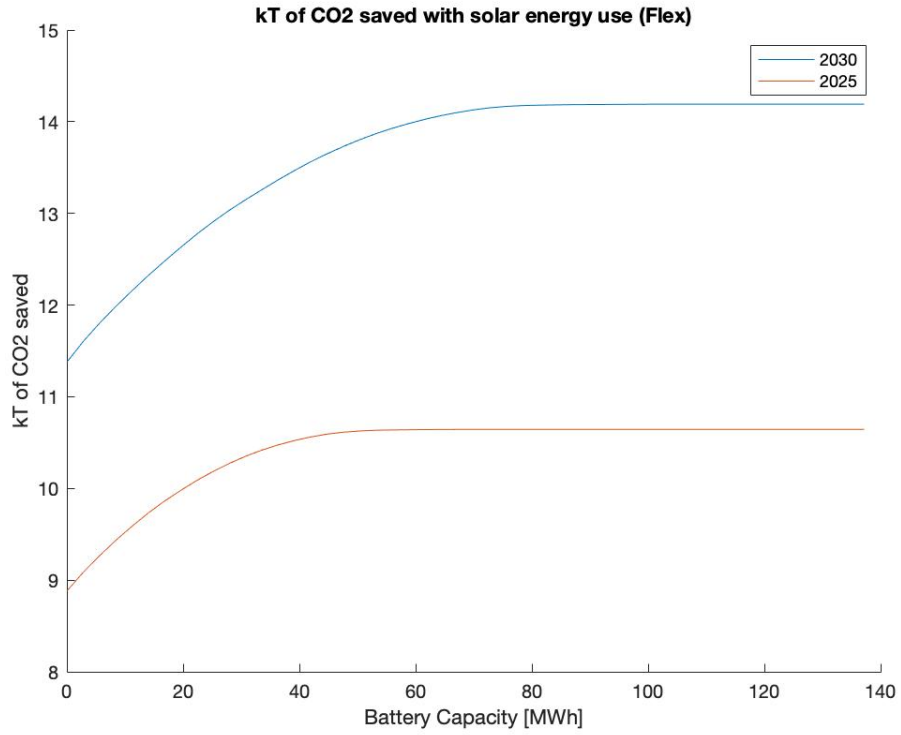

Figure 8.6: Absolute CO2 savings by the battery for different sizes, in kT. Flexibility is applied.

References

[1] Ministry of Economic Affairs and Climate Policy. "Klimaatakkoord". In: (2019), page 250. URL: https://www.klimaatakkoord.nl/binaries/klimaatakkoord/documenten/publicaties/2019/06/28/klimaatakkoord/klimaatakkoord.pdf.

[2] Gemeente Amsterdam. *Nieuw Amsterdams Klimaat*. Technical report. 2020.

[3] Gemeente Amsterdam. *Actieplan Schone Lucht*. Technical report. 2019.

[4] *Stroominfarct Amsterdam - Parool*. 2019. URL: https://www.parool.nl/amsterdam/netwerkbedrijf-alliander-stad-is-hard-op-weg-naar-een-stroominfarct%7B~%7Db74c497c/.

[5] Bovag. *Het effect van de elektrisch aangedreven (bedrijfs)auto op het aftersales businessmodel HIGHLIGHTS EV-ONDERZOEK*. Technical report. 2018.

[6] Jenny Love et al. "The addition of heat pump electricity load profiles to GB electricity demand: Evidence from a heat pump field trial". In: *Applied Energy* 204 (2017), pages 332–342. ISSN: 03062619. DOI: 10.1016/j.apenergy.2017.07.026. URL: http://dx.doi.org/10.1016/j.apenergy.2017.07.026.

[7] Dutch Heat Pump Association. "Positioning paper Heat pumps in domestic housing and demand management". 2015.

[8] Özge Okur et al. "Aggregator-mediated demand response: Minimizing imbalances caused by uncertainty of solar generation". In: *Applied Energy* 247.October 2018 (2019), pages 426–437. ISSN: 03062619. DOI: 10.1016/j.apenergy.2019.04.035. URL: https://doi.org/10.1016/j.apenergy.2019.04.035.

[9] Peter Bach Andersen, Junjie Hu, and Kai Heussen. "Coordination strategies for distribution grid congestion management in a multi-actor, multi-objective setting". In: *IEEE PES Innovative Smart Grid Technologies Conference Europe* (2012), pages 1–8. DOI: 10.1109/ISGTEurope.2012.6465853.

[10] Junjie Hu et al. "A multi-agent system for distribution grid congestion management with electric vehicles". In: *Engineering Applications of Artificial Intelligence* 38 (2015), pages 45–58. ISSN: 09521976. DOI: 10.1016/j.engappai.2014.10.017. URL: http://dx.doi.org/10.1016/j.engappai.2014.10.017.

[11] Samson Yemane Hadush and Leonardo Meeus. "DSO-TSO cooperation issues and solutions for distribution grid congestion management". In: *Energy Policy* 120.June (2018), pages 610–621. ISSN: 03014215. DOI: 10.1016/j.enpol.2018.05.065. URL: https://doi.org/10.1016/j.enpol.2018.05.065.

[12] G. Prettico et al. *JRC Science for Policy Report; Distribution System Operators Observatory 2018*. 2019. ISBN: 9789279987380. DOI: 10.2760/2690.

[13] Nina Voulis, Martijn Warnier, and Frances M.T. Brazier. "Storage coordination and peak-shaving operation in urban areas with high renewable penetration". In: *Proceedings of the 2017 IEEE 14th International Conference on Networking, Sensing and Control, ICNSC 2017* (2017), pages 531–536. DOI: 10.1109/ICNSC.2017.8000148.

[14] Thomas Bowen, Ilya Chernyakhovskiy, and Paul Denholm. "Grid-Scale Battery Storage: Frequently Asked Questions". In: *Nrel* 2013 (2018), pages 1–8. URL: www.greeningthegrid.org.

[15] *Projects – Resourcefully*. 2019. URL: https://resourcefully.nl/projects/.

[16] Energy Coin Foundation. *B-DER Project*. 2020. URL: https://www.energycoinfoundation.org/en/projects/b-der-project-university-utrecht/.

[17] Alle Cijfers. *Alle Cijfers - Data over het Oostelijk Havengebied*. 2020. URL: https://allecijfers.nl/wijk/oostelijk-havengebied-amsterdam/#adresgegevens.

[18] Tim van der Himst et al. *Realizing the Solar Energy Potential of the Eastern Docklands , Amsterdam*. Technical report. 2018.

[19] STEDIN et al. "IDCONS Product Specification GOPACS". In: (2019). URL: https://en.gopacs.eu/wpcms/wp-content/uploads/2019/10/20190827-IDCONS-product-specifications-v1.01_EN.pdf.

[20] CBS. *Kerncijfers Wijken en Buurten 2019*. Technical report. CBS, 2019. DOI: 10.1017/CBO9781107415324.004.

[21] Applied Sciences and Urban Technology. *Flexpower SEEV-4City*. Technical report July. 2019.

[22] Liander. *Liander Open Data*. 2014. URL: https://www.liander.nl/partners/datadiensten/open-data.

[23] Wikipedia. *Energieprestatiecoëfficiënt - Wikipedia*. 2015. URL: https://nl.wikipedia.org/wiki/Energieprestatieco%C3%ABffici%C3%ABnt.

[24] Tennet. "The Imbalance Pricing System". In: June (2015), pages 1–12. URL: https://www.tennet.eu/fileadmin/user_upload/Company/Publications/Technical_Publications/Dutch/imbalanceprice_3.6_clean_.doc.pdf.

[25] Carlos Varela Martín. *eflows*. 2018. URL: https://eflows.nl/#home.

[26] Liander. *Beschikbare data — Liander*. 2020. URL: https://www.liander.nl/partners/datadiensten/open-data/data.

[27] J.M. Sipma and M.D.A. Rietkerk. "Ontwikkeling energiekentallen utiliteitsgebouwen - Een analyse van 24 gebouwtypen in de dienstensector en 12 industriële sectoren". In: (2016), page 65. URL: https://repository.tudelft.nl/view/tno/uuid%3A6c43a6ac-1a4a-423b-b4ad-dcab9eae86d7.

[28] Netherlands Enterprise Agency RVO. "Statistics Electric Vehicles in the Netherlands". In: *Procedia Computer Science* 52.May (2020), pages 2–5. ISSN: 18770509. DOI: 10.1016/j.procs.2015.05.133.

[29] Dirk Warmerdam. *Inventarisatie Elektrificatie Oostelijk Havengebied*. Amsterdam, 2020.

[30] Nederland Elektrisch et al. *Nederland Elektrisch - Cijfers en statistieken EV's in Nederland*. URL: https://nederlandelektrisch.nl/actueel/verkoopcijfers.

[31] Aumacon and Business Insider. *Prediction EV-sales in 2020*. 2019. URL: https://www.businessinsider.nl/elektrische-auto-2020-aanbod-volkswagen-peugeot-tesla-opel/.

[32] Marco Sorrentino, Gianfranco Rizzo, and Luca Sorrentino. "A study aimed at assessing the potential impact of vehicle electrification on grid infrastructure and road-traffic green house emissions". In: *Applied Energy* 120 (2014), pages 31–40. ISSN: 03062619. DOI: 10.1016/j.apenergy.2014.01.040. URL: http://dx.doi.org/10.1016/j.apenergy.2014.01.040.

[33] Kotub Uddin, Matthieu Dubarry, and Mark B. Glick. "The viability of vehicle-to-grid operations from a battery technology and policy perspective". In: *Energy Policy* 113.August 2017 (2018), pages 342–347. ISSN: 03014215. DOI: 10.1016/j.enpol.2017.11.015. URL: https://doi.org/10.1016/j.enpol.2017.11.015.

[34] Liander. *Kosten elektriciteitsaansluiting - Liander*. 2020. URL: https://www.liander.nl/consument/aansluitingen/typen.

[35] CleanMobilEnergy. *CleanMobilEnergy*. Arnhem, 2020. URL: https://www.nweurope.eu/projects/project-search/cleanmobilenergy-clean-mobility-and-energy-for-cities/.

[36] Parool. *Rechtzaak warmtenet Amsterdam*. Amsterdam, 2020. URL: https://www.parool.nl/amsterdam/gemeente-in-hoger-beroep-na-verloren-rechtszaak-over-stadsverwarming-sluisbuurt~bd9e254e/.

[37] R de Smidt. *DemandProfiles_ECN*. 2015.

[38] M. Súri et al. *Photovoltaic Geographical Information System (PVGIS) — EU Science Hub*. 2020. URL: https://ec.europa.eu/jrc/en/pvgis.

[39] Iman Ghalehkhondabi et al. *An overview of energy demand forecasting methods published in 2005–2015*. Volume 8. 2. 2017, pages 411–447. ISBN: 7405930778. DOI: 10.1007/s12667-016-0203-y.

[40] Alfredo Nespoli et al. "Day-ahead photovoltaic forecasting: A comparison of the most effective techniques". In: *Energies* 12.9 (2019), pages 1–15. ISSN: 19961073. DOI: 10.3390/en12091621.

[41] Vincenzo Bonaiuto and Fausto Sargeni. "A Matlab Simulink model for the study of smart grid-Grid-integrated vehicles interactions". In: *RTSI 2017 - IEEE 3rd International Forum on Research and Technologies for Society and Industry, Conference Proceedings* (2017). DOI: 10.1109/RTSI.2017.8065953.

[42] Ali Mekkaoui, Mohammed Laouer, and Younes Mimoun. "Modeling and simulation for smart grid integration of solar / wind energy". In: 30 (2017), pages 31–46.

[43] Elpiniki Apostolaki-Iosifidou, Paul Codani, and Willett Kempton. "Measurement of power loss during electric vehicle charging and discharging". In: *Energy* 127 (2017), pages 730–742. ISSN: 03605442. DOI: 10.1016/j.energy.2017.03.015.

[44] Umweltbundesamt. "Ratgeber Batterien und Akkus". In: (2012). ISSN: 1098-6596.

[45] W. Schram et al. "MEP profiles". 2019.

[46] Michael Stadler et al. "Value streams in microgrids: A literature review". In: *Applied Energy* 162 (2016), pages 980–989. ISSN: 03062619. DOI: 10.1016/j.apenergy.2015.10.081. URL: http://dx.doi.org/10.1016/j.apenergy.2015.10.081.

[47] Eric Wiebes and Tweede Kamer Der Staten-generaal. "Antwoord op vragen van het lid Moorlag over de moeizame aansluiting van zonnepanelen op het elektriciteitsnetwerk". In: 2240 (2020), pages 2019–2021.

[48] Centraal Bureau voor de Statistiek (CBS). *Aandeel Hernieuwbare Energie in Nederland 2020*. 2020. URL: https://www.cbs.nl/nl-nl/nieuws/2020/22/verbruik-hernieuwbare-energie-met-16-procent-gegroeid.

[49] Wouter Schram et al. "On the use of average versus marginal emission factors". In: *SMART-GREENS 2019 - Proceedings of the 8th International Conference on Smart Cities and Green ICT Systems* (2019), pages 187–193. DOI: 10.5220/0007765701870193.

[50] ENTSOE Transparancy Platform. *dayaheadprices*. 2019. URL: https://transparency.entsoe.eu/transmission-domain/r2/dayAheadPrices/show?name=&defaultValue=true&viewType=TABLE&areaType=BZN&atch=false&dateTime.dateTime=01.01.2019+00:00%7CCET%7CDAY&biddingZone.values=CTY%7C10YNL----------L!BZN%7C10YNL----------L&dateTi.

[51] Maarten Afman, Sebastiaan Hers, and Thijs Scholten. "Energy and electricity price scenarios". In: *Power to Ammonia Project* (2017).

[52] Eric Wiebes and Menno Snel. *De voorzitter van de Tweede Kamer der Staten-Generaal Binnenhof 4 2513 AA DEN HAAG*. 2019.

[53] Francese Girbau-Llistuella et al. "Methodology for the sizing of a hybrid energy storage system in low voltage distribution grids". In: *Proceedings of 2019 8th International Conference on Modern Power Systems, MPS 2019* (2019). DOI: 10.1109/MPS.2019.8759696.

[54] Battery University. *Degradation of Li-Ion batteries*. 2020. URL: https://batteryuniversity.com/learn/article/how_to_prolong_lithium_based_batteries.

[55] Will Kenton and Julius Mansa. *Net Present Value*. 2020. URL: https://www.investopedia.com/terms/n/npv.asp.

[56] Marc Zenner et al. "The Most Important Number in Finance". In: *JP Morgan — Capital Structure Advisory & Solutions* May (2008). URL: http://www.morganmarkets.com..

[57] Florian Egli. "Renewable energy investment risk: An investigation of changes over time and the underlying drivers". In: *Energy Policy* 140.February (2020), page 111428. ISSN: 03014215. DOI: 10.1016/j.enpol.2020.111428. URL: https://doi.org/10.1016/j.enpol.2020.111428.

[58] Trading Economics. *Historical Inflation in the Netherlands*. 2020. URL: https://tradingeconomics.com/netherlands/inflation-cpi#:~:text=Inflation%20Rate%20in%20Netherlands%20averaged,percent%20in%20February%20of%201987..

[59] Melvin van Melzen. *Haalbaarheid en schaalbaarheid van de buurtbatterij*. Technical report. DNV-GL, 2018.

[60] ENTSO-E. *Frequency Containment Reserves (FCR)*. 2018. URL: https://www.entsoe.eu/network_codes/eb/fcr/.

[61] SENFAL (Vattenfall Flexibility Services). *What is Frequency Containment Reserve?* 2017. URL: http://whatis.techtarget.com/definition/frequency-jammer.

[62] Joeri Posma et al. "Provision of ancillary services from an aggregated portfolio of residential heat pumps on the Dutch Frequency Containment Reserve market". In: *Applied Sciences (Switzerland)* 9.3 (2019), pages 1–17. ISSN: 20763417. DOI: 10.3390/app9030590.

[63] Vattenfall. *Vattenfall hybrid solar/wind park*. 2020. URL: https://group.vattenfall.com/press-and-media/news--press-releases/newsroom/2020/vattenfalls-largest-hybrid-energy-park-is-taking-shape-in-the-netherlands.

[64] Niamh Oconnell et al. "Benefits and challenges of electrical demand response: A critical review". In: *Renewable and Sustainable Energy Reviews* 39 (2014), pages 686–699. ISSN: 13640321. DOI: 10.1016/j.rser.2014.07.098.

[65] CBS/KNMI. *CBS Average Temperature data*. 2017. URL: https://www.cbs.nl/en-gb/society/nature-and-environment/green-growth/environmental-quality-of-life/indicatoren/average-temperature.

[66] Cody A. Hill et al. "Battery energy storage for enabling integration of distributed solar power generation". In: *IEEE Transactions on Smart Grid* 3.2 (2012), pages 850–857. ISSN: 19493053. DOI: 10.1109/TSG.2012.2190113.

[67] Mihael Medved. "25 th International Conference on Electricity Distribution 25 th International Conference on Electricity Distribution Madrid , 3-6 June 2019". In: June (2019), pages 3–6.

[68] Centraal Bureau voor de Statistiek. *Windenergie; elektriciteitsproductie, capaciteit en windaanbod, 2002-2019*. 2019. URL: https://opendata.cbs.nl/statline/#/CBS/nl/dataset/70802ned/table?dl=1A48C.

[69] Hideharu Sugihara et al. "Economic and efficient voltage management using customer-owned energy storage systems in a distribution network with high penetration of photovoltaic systems". In: *IEEE Transactions on Power Systems* 28.1 (2013), pages 102–111. ISSN: 08858950. DOI: 10.1109/TPWRS.2012.2196529.